Functional interplay of two SWI/SNF chromatin remodeling accessory subunits during *C. elegans* development

Iris Elisabeth Ertl

TESI DOCTORAL UPF 2014

Thesis supervisor: Julián Cerón Madrigal

Department: Modeling Human Diseases in *C. elegans*
Cancer and Human Molecular Genetics Area
IDIBELL - Institut d'Investigació Biomèdica de Bellvitge

UNIVERSITAT POMPEU FABRA BARCELONA

Dedicated to my family……

“You are my shelter”…

…and always have been

Acknowledgements

A huge thank you to all those people that made the last four years one of the happiest and most exciting periods of my life:

Julián, who gave me all these great opportunities in the first place and quickly found out when to let me my peace and when to kick my butt.

Montse and Laura, who tried everything to make my start in Barcelona as pleasant as possible and gave me an inestimable amount of advice regarding "lab stuff".

Eric and Curro, who were my partners in crime throughout all this time and did not let me forget that there exists a life outside the lab.

Karinna, who went with me through thick and thin, sharing the best and the worst moments with me and Christina.

David, Silvia, Xabi with who I could unfortunately not spend as much time as I wanted, but who got very precious for me, nevertheless.

All the cool people working in "Genética molecular" and also those from "LRT1", especially the "Communidad".

Thanks to all, I gonna miss every single of you more than you maybe imagine!

Rock on!

Summary:

SWI/SNF complexes are ATP-dependent chromatin remodelers highly conserved through evolution. By altering the chromatin state, these complexes can regulate the accessibility of a given genomic region and thereby perform transcriptional regulation. Besides a central enzymatic subunit and various core proteins, SWI/SNF complexes incorporate accessory subunits that confer specificity to a given complex and vary depending on the cell type and developmental context.

The human accessory proteins BAF60a, BAF60b and BAF60c represent paralog proteins with specialized functions, and mutations in the BAF60 genes are involved in human disease (e.g. cancer). To get closer insight in the functions of SWI/SNF accessory subunits, we studied *C. elegans* homologs of the BAF60 proteins, encoded by the paralog gene pair *ham-3* and *swsn-2.2*.

We investigated *ham-3* and *swsn-2.2* functions in various tissues and developmental processes and observed that the two genes act redundantly in many contexts. However, as their human counterparts, HAM-3 and SWSN-2.2 have also acquired specialized functions.

Zusammenfassung:

SWI/SNF-Komplexe sind ATP-abhängige *chromatin remodeler* mit hoher evolutionärer Konservierung. Durch die Veränderung der Chromatin-Struktur können diese Multi-Protein-Komplexe die Zugänglichkeit einer bestimmten genomischen DNA-Region beeinflussen und dadurch transkriptionelle Regulation bewirken. Der Kern von SWI/SNF-Komplexen besteht aus einer zentralen katalytischen Untereinheit und mehreren Kern-Proteinen. Darüberhinaus beinhalten SWI/SNF-Komplexe Untereinheiten, die ihre Spezifität bestimmen und abhängig vom Entwicklungstadium und Zelltyp variieren. In humanen SWI/SNF-Komplexen übernehmen BAF60-Proteine eine solche Funktion. BAF60a, BAF60b und BAF60c sind paraloge Proteine, die während der Evolution spezialisierte Funktionen erworben haben. Mutationen von BAF60-Genen spielen erwiesenermaßen eine Rolle in der Entstehung verschiedener Krankheiten, z.B. Krebs. Um mehr Verständnis für die Funktion dieser SWI/SNF Untereinheiten zu entwickeln, nutzten wir den Modelorganismus *C. elegans* und untersuchten die Homologe der humanen BAF60-Gene, *ham-3* und *swsn-2.2*. Wir beleuchteten die Funktion der zwei paralogen Gene in verschiedenen Zelltypen und Entwicklungsprozessen und fanden neben etlichen gemeinsamen auch spezialisierte Funktionen.

Abstract:

SWI/SNF complexes are ATP-dependent chromatin remodelers highly conserved through evolution. By altering the chromatin state, these complexes can regulate the accessibility of a given genomic region for regulatory factors and thereby influence cellular processes like transcriptional regulation, cell differentiation and DNA repair.

SWI/SNF complexes consist of a central catalytic subunit associated with various core proteins. Besides the core subunits, there exist accessory proteins that confer specificity to a given complex and vary depending on the cell type and developmental stage. Amongst other human accessory subunits, the paralog proteins BAF60a, BAF60b and BAF60c have been shown to be involved in the pathogenesis of human diseases, including cancer. To shed light on the functions of SWI/SNF accessory subunits, we studied *C. elegans* homologs of the BAF60 genes, the paralog gene pair *ham-3* and *swsn-2.2*. Since the BAF60 proteins have developed specialized functions through evolution, we mainly concentrated on the question, whether HAM-3 and SWSN-2.2 act redundantly or in an independent manner in several developmental processes.

We had various mutant strains for both genes at our disposal and characterized their molecular nature and phenotypic effects. For *ham-3* we studied the putative null alleles *tm3309* and *n1654, as* well as *he159* that was isolated in our lab and encodes a truncated protein lacking the central SWIB/MDM2 domain.

Both *swsn-2.2* alleles used in this study give truncated proteins. While *ok3161* encodes a massively shortened product, *tm3395* gives a protein containing the SWIB/MDM2 domain.

We employed these mutant alleles as well as RNAi of *ham-3* and *swsn-2.2* to study the functions of the two genes in various cell types and developmental processes.
We found that *ham-3* and *swsn-2.2* are involved in germline proliferation as well as the development of the somatic gonad and act redundantly in these contexts. Beyond that, HAM-3 and SWSN-2.2 are required for correct development of the egg-lay apparatus and have redundant functions in the inhibition of the *let-60*/Ras pathway that drives the induction of vulval precursor cells.
We observed that *ham-3* and *swsn-2.2* have developed specialized functions in embryonic development, but also act redundantly at certain levels of embryogenesis. Further, we showed *ham-3* and *swsn-2.2* functions in the regulation of the intestinal cell cycle in embryonic and post-embryonic development.
RNA-seq revealed that *swsn-2.2* and *ham-3* are involved in the IIS pathway and have common and independent functions in this signaling cascade.
Last, but not least, we identified interaction partners of SWSN-2.2 by Co-Immunoprecipitation and Mass spectrometry, amongst them components of the nuclear envelope such as MEL-28 and NPP-9.

To summarize, we showed that *ham-3* and *swsn-2.2* act in several independent developmental processes. The two paralogs act redundantly in many contexts, but, as their human counterparts, they have also developed specialized functions.

Table of contents

Introduction

Results

Discussion

Material and Methods

Introduction

I. Introduction

I.1. The nematode *C. elegans* as model organism

The first article describing the genetics of *C. elegans* was published by Sydney Brenner in 1974 (Brenner, 1974). Since then this nematode has been established as one of the most popular and well studied model organisms in biological research. Jointly with Robert Horvitz and John Sulston, Sydney Brenner received the Nobel prize in Physiology/Medicine in 2002, underlining the impact of *C. elegans* for biomedical research. Since then, two additional Nobel prizes have been awarded for findings made in *C. elegans*. In 2006, Andrew Fire and Craig Mello received the Nobel prize in Physiology/Medicine for the discovery of RNA interference. Two years later, Martin Chalfie, Roger Tsien and Osamu Shimomura won the Nobel prize in Chemistry for the isolation and development of the green fluorescent protein (GFP).

I.1.1. *C. elegans*: A brief description of the model and its advantages

C. elegans has many features that make it an excellent model organism for biological research. As examples:

- *C. elegans* is a small nematode (approx. 1mm) that usually lives in the soil and feeds on microorganisms. Wild strains of *C. elegans* have been isolated all over the world. In the laboratory *C. elegans* feeds on *E. coli* and can be easily maintained. There exist techniques for freezing and thawing of living worms, which enables long term storage of many

different strains. Since *C. elegans* is non-parasitic, its handling does not bear risk for the researcher (Riddle et al., 1997).

- The life cycle is temperature-dependent and takes approximately 3 days at 22°C, what is short compared to many other model organisms. Between the embryonic stage and adulthood, four larval stages (L1-L4) exist, each of them ending with a molt. In response to unfavorable environmental conditions, late L1 larvae can enter dauer stage and arrest development up to several months (Fig.I.1) (Altun & Hall, 2009). The *C. elegans* body is transparent and allows the study of individual cells *in vivo* under usage of differential interference contrast (DIC) microscopy (Riddle et al., 1997).
- Two sexes exist in *C. elegans,* hermaphrodite and male. Males present only 0.1% of a wild type population and are not essentially required for reproduction, since the hermaphrodites are able to self-fertilize (Altun & Hall, 2009). The gender is determined by sex chromosomes (XX in hermaphrodite and XO in male), that exist besides the five pairs of autosomal chromosomes. The diploidy in combination with the ability to self-fertilize makes *C. elegans* a convenient tool for genetic analysis. Due to Mendelian segregation, the progeny resulting from self-fertilization of a heterozygote mother has three different genotypes. Thus, mutations can be maintained and their effects studied in homozygote animals, also when they affect essential genes. Additionally, males can be employed for the crossing of different mutants and thereby enable the combination of several genetic features in one strain.

- *C. elegans* development is highly invariant. Wild type adults have an exact number of somatic cells (hermaphrodites 959, males 1031) in constant positions that derive from stereotypical lineages (Sulston et al., 1983). The fate of each lineage can be traced from the zygote until hatching, what allows the comparison of development in the wild type and mutants.
- The *C. elegans* genome was the first metazoan genome to be sequenced and thereby the first multicellular organism, whose complete genetic information was available (The *C. elegans* Sequencing Consortium, 1998). Surprisingly, although the *C. elegans* genome is about 30 times smaller than the human, the number of coding genes is almost the same in the two organisms (20.541 vs. 20.389) (www.ensembl.org). This compactness might be explained with the absence of regulatory regions, less alternative splicing and less complex gene expression programs and facilitates the investigation of gene functions (Cerón, 2006).
- By RNA-mediated interference (RNAi) the function of any gene can be disrupted and the phenotypic effects of its inactivation studied. RNAi causes sequence specific degradation of mRNA and consequently the post-transcriptional silencing of the target gene. In *C. elegans* RNAi can be applied by feeding, soaking or injection, and the strength of the effect can be modulated. Two RNAi libraries exist for *C. elegans* that together cover 94% of the complete genome (Ahringer, 2006).

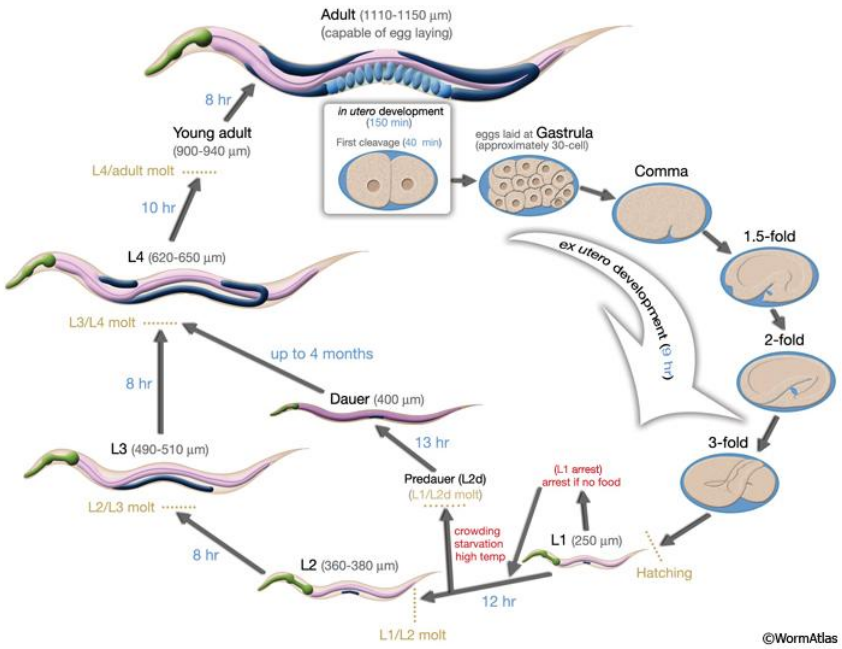

Fig.I.1: Life cycle of a *C. elegans* hermaphrodite at 22°C. The *C. elegans* life cycle is temperature-dependent and takes approximately 3 days at 22°C. The first steps of embryogenesis occur in the maternal uterus. At gastrulation, the eggs are disposed to the environment. Between hatching and adulthood four larva stages exist, each ending with a molt. In response to unfavorable environmental conditions, late L1 larvae can enter in dauer stage and arrest development for several months. Picture from: http://www.wormatlas.org

I.1.2. The *C. elegans* germline

The reproductive system of *C. elegans* hermaphrodites consists of two closely associated tissues, the germline and the somatic gonad.

All germ cells of an adult *C. elegans* derive from a single progenitor, the primordial gonadal cell P4, present in the early embryo. During gastrulation P4 divides, giving rise to Z2 and Z3, which remain quiescent until the end of embryogenesis. At hatching, the gonad is presented by a four-celled gonadal primordium, formed by Z2 and Z3 and the somatic gonad precursors (SGPs) Z1 and Z4 (Sulston et al., 1983; Hubbard & Greenstein, 2005).

The somatic gonad

Z1 and Z4 derive from the MS blastomere and give rise to all cell types of the somatic gonad, which are the sheath cells associated with the gonad arms, the cells forming the spermatheca and the uterus, the anchor cell and the two distal tip cells (DTCs) (Fig.I.2) (Hubbard & Greenstein, 2000).

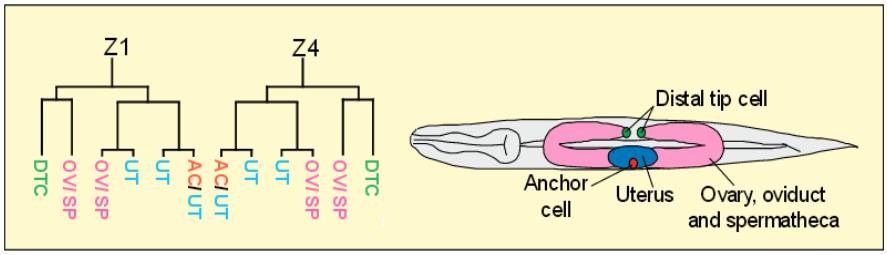

Fig.I.2: The somatic gonad precursors Z1 and Z4 give rise to all tissues of the somatic gonad. Z1 and Z4 divide three times to produce 12 cells with specified fates that will later give rise to all cell types of the adult somatic gonad. Picture modified from: Lambie, 1997

The distal tip cells are produced in L1 and lead the gonadal outgrowth during development. Thereby they determine the morphology of the adult gonad (Wong & Schwarzbauer, 2012). The two DTCs start migration at the ventral side of the animal, moving away from the gonad primordium in L2 (in anterior and posterior direction, respectively). After changing their direction in L3, the DTCs move back towards the center of the animal on the dorsal side in L4, thereby forming the two U-shaped arms of the adult gonad (Fig.I.3) (Wong & Schwarzbauer, 2012).

Beyond their leader function, the DTCs also shed proliferative signals inducing the mitosis of the germ cells in the growing gonad arms (Hubbard & Greenstein, 2000).

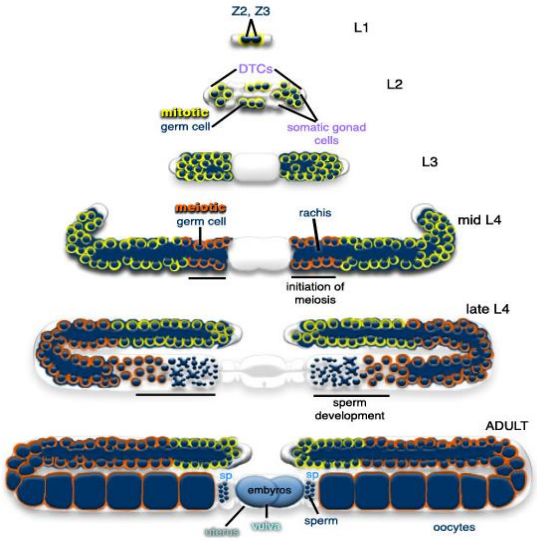

Fig.I.3: Germline development in *C. elegans.* The cells Z1 and Z4, which are present in the gonadal primordium, give rise to all cell types of the somatic gonad, including the distal tips cells (DTCs). The DTCs secrete proliferative signals and start to move away from the gonad primordium in L2 stage. During L3 and L4 they migrate through the body on a defined path, and thereby lead the elongation of the gonad arms. Picture from: http://www.wormatlas.org

The *C. elegans* germ cells

In contrast to sperm that is only generated in L4 stage, oocytes are produced all over the reproductive phase of a *C. elegans* hermaphrodite. For the maintenance of function of the adult gonad, the DTCs located on the tip of each gonad arm are required. As during gonad development, the DTCs secrete also in adult stage proliferative signals, such as the ligand LAG-2. The corresponding receptor in the germline is GLP-1, one of the two members of the LIN-12/Notch family of receptors in *C. elegans* (Hubbard, 2007). GLP-1 signaling activates positive downstream effectors (e.g. *lag-1*) and also inhibits factors required for the meiotic entry (e.g. *gld-1*, *gld-2*). Thereby it promotes mitotic division of germ cells in the most distal region of the gonad, the proliferative zone (Hubbard & Greenstein, 2000). With increasing distance to the DTCs, the influence of their proliferative signals decreases and the germ cells enter the transition zone, switching from mitotic to meiotic division (Hansen, Hubbard, & Schedl, 2004). After passing the transition zone, where the germ cells undergo the early phases of meiosis, they enter pachytene and grow in size. In response to signals from the gonad sheath, they move on to diplotene in the turn of the gonad arm (Church, Guan & Lambie, 1995). While passing the distal arm, the germ cells enter diakinesis and arrest until oocyte maturation, which takes place just before entering the spermatheca (Fig.I.4) (Lints & Hall, 2009).

Before oocyte formation, germ cells are not cellularized, but are nuclei in a syncytium without a proper membrane limiting the cytoplasm. Thus, DNA or any other substance that is injected into a germline is equally distributed into oocytes.

In response to induction by the major sperm protein (MSP), the oocyte enters the prometaphase and nuclear envelope breakdown occurs (Miller et al., 2001; Iwasaki et al., 1996).

Beyond oocyte maturation, the MSP is also required for ovulation. In *C. elegans*, the term ovulation stands for the expulsion of the oocytes from the gonad arm (Riddle, 1997; Hubbard & Greenstein, 2005). In concert with signals from the maturing germ cell, the MSP stimulates contractions of the sheath that push the oocytes into the spermatheca, where they are fertilized. The fertilized oocytes wander to the uterus, where they terminate meiosis and start embryogenesis (Miller et al., 2001; Iwasaki et al., 1996).

Due to the transparent body of *C. elegans,* the development of single germ cells can be monitored and processes like oogenesis, oocyte maturation and ovulation followed *in vivo*.

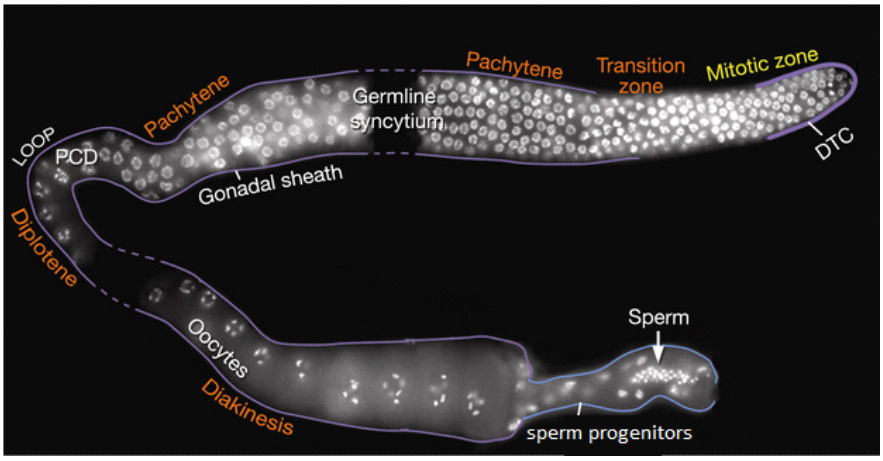

Fig.I.4: Dissected gonad arm of a wild type hermaphrodite during reproductive phase stained with DAPI. In wild type animals the gonad arms are characterized by defined regions of germ cells in different developmental stages. Picture from: http://www.wormatlas.org

I.1.3. *C. elegans* vulval development

I.1.3.1. Specification of vulval precursor cells

Vulval development occurs during postembryonic development and comprises a well coordinated series of steps starting in L1 (Sternberg, 2005).

At the ventral side of the animal, the six vulval precursor cells (VPCs), P3.p-P8.p, develop. Just after being produced, those cells arrest in G1 and do not proliferate until late L3 stage, when the cells of the adult vulva are generated (Sternberg, 2005). As a prerequisite, the anchor cell (AC) of the gonad must induce three of the six VPCs to acquire vulval fate in early L3 (Sundaram, 2004; Sternberg, 2005).

The AC secretes the EGF-like growth factor LIN-3 that stimulates a Receptor tyrosine kinase (RTK)/Ras/MAP kinase cascade in P5.p-P.7p. As a consequence, P6.p adopts the 1° vulval precursor cell (VPC) fate. The two cells flanking P6.p, P5.p and P7.p, receive lower levels of LIN-3 and are therefore induced as 2° fate VPCs. The three VPCs (P3.p, P4.p and P8.p) receiving the weakest signals from the anchor cell acquire non-vulval (3°) fate and fuse with the hypodermis (Schindler & Sherwood, 2013; Sternberg, 2005; Gupta, Hanna-Rose & Sternberg, 2012; Sundaram, 2004). Different classes of synMuv genes negatively regulate *lin-3* activity and thereby prevent inappropriate vulva induction. These genes are expressed in the hyp7 hypodermal syncytium and act in redundant pathways (Cui et al., 2006).

Besides LIN-3/EGF, LIN-12/Notch signaling is involved in the specification of 2° fate. Once induced, the 1° VPC up-regulates the expression of DSL, an inhibitory ligand of LIN-12/Notch, thereby promoting the 2° fate in its adjacent cells via lateral signaling

(Fig.I.5) (Schindler & Sherwood, 2013; Sternberg, 2005; Gupta, Hanna-Rose & Sternberg, 2012; Sundaram, 2004)

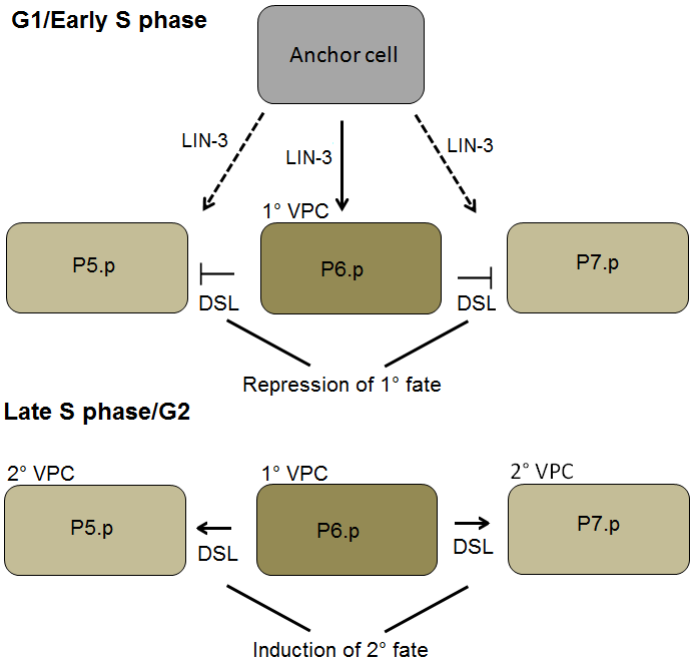

Fig.I.5: Two-step model for the induction of the VPCs by the anchor cell. During G1/early S phase P6.p acquires high levels of the EGF-like growth factor LIN-3 from the anchor cell and thereby adopts 1° VPC fate. By expression of the inhibitory Notch ligand DSL, P6.p represses the 1° VPC specification in the adjacent cells. In late S/G2 phase the 2° VPC fate is induced in P5.p and P7.p through the same ligand. Picture modified from: Kipreos, 2005

For the specification and maintenance of the VPC fate, the Hox gene *lin-39* is required. LIN-39 prevents on the one hand fusion of the VPCs with the main hypodermal body syncytium (hyp7) and on the other stimulates cell division. *lin-39* expression in the VPCs is maintained by a Wnt pathway. Thus, at least three major signaling cascades, Notch, Ras and Wnt, are involved in the development of the VPCs (Sternberg, 2005).

I.1.3.2. Vulva formation

In late L3, the 1° fate VPC enters proliferation and divides three times giving rise to eight cells of two different cell types (VulE and VulF). Also the two 2° fate VPCs start division and each produces seven progenitor cells of five different types (VulA, VulB1, VulB2, VulC and VulD) (Schindler & Sherwood, 2013). Thus, the vulva of an adult *C. elegans* hermaphrodite consists of a total of 22 cells of seven different types that vary in their expression profiles. (Sternberg, 2005; Gupta, Hanna-Rose & Sternberg, 2012) (Fig.I.6A).

In parallel to these rounds of division, AC invasion occurs. Induced by signals from the 1° VPC, the AC moves dorsally, penetrates the membrane separating uterus and vulva thereby establishing a connection between the two tissues (Schindler & Sherwood, 2013). The AC invasion is followed by the first event of morphogenesis, the invagination (Fig.I.6B).

Starting with the VulF cells, all the newly produced vulval cell types move dorsally towards the AC in a highly organized manner. Once in their final position, cells of one given type make contacts between each other and thereby form rings around a lumen that connects the epithelium of the uterus with the external epithelium (Schindler & Sherwood, 2013; Gupta, Hanna-Rose & Sternberg, 2012).

The last step of vulva morphogenesis is the eversion of the whole structure during the final molt between L4 and young adult stage (Fig.I.6B) (Sharma-Kishore et al., 1999).

In order to provide the ability to lay eggs, the vulva has to associate with muscle and nerve cells. Sixteen specialized smooth muscle

cells that are regulated by two different kinds of motor neurons have been shown to be involved in the expulsion of the embryos. Besides a pair of hermaphrodite-specific neurons (HSN), six ventral cord neurons (VCs) induce on the one hand the constriction of the uterus, on the other the opening of the vulva and thereby the disposal of the eggs (Schafer, 2005; White et al., 1986) The HSNs and two subclasses of the VCs (VC5 and VC6) use, besides other neurotransmitters, also serotonin to stimulate the muscle cells (Weinberg et al., 2013; White el al., 1986).

In response to mutations of genes that are involved in vulval development various phenotypes can develop. For instance, inactivation of components involved in the induction of the VPCs causes the Vulvaless (Vul) phenotype, while excess of induction results in Multivulva (Muv) (Ferguson & Horvitz, 1985). Failures in the signaling between nerves and vulva musculature can cause Egg-laying-defects (Egl) (Trent, Tsuing & Horvitz, 1983). Beyond these phenotypes, morphological phenotypes, such as protruding Vulva (Pvl) and abnormal Eversion of the vulva (Evl) exist (Eisenmann & Kim, 2000; Seydoux, Savage & Greenwald, 1993).

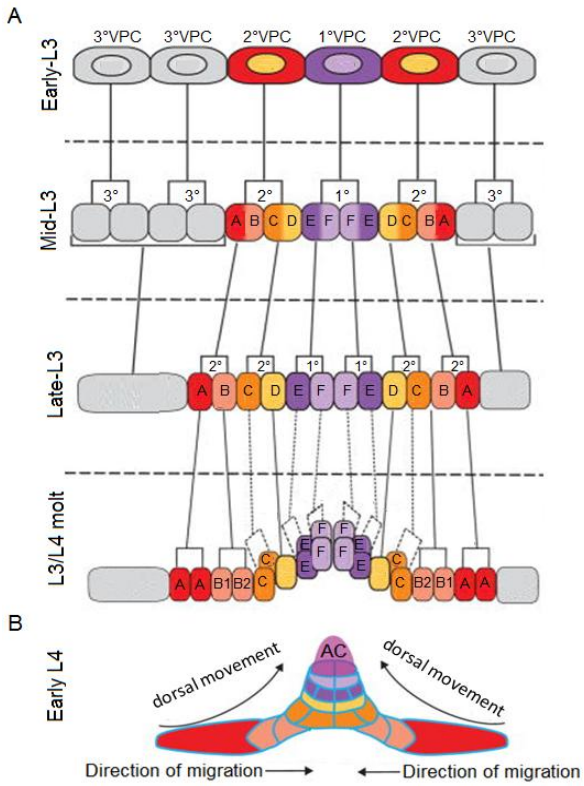

Fig.I.6: Vulval development during L3 and L4 stage. (A) During L3 stage, the three VPCs give rise to the 22 cells of 7 different types present in the adult vulva. (B) A prerequisite for correct vulval development is the invagination led by the anchor cell of the somatic gonad. During early L4, the anchor cells moves dorsally and is followed by the newly produced vulval cells in a highly ordered fashion. Picture modified from: http://www.wormatlas.org

I.1.4. *C. elegans* embryonic development

The embryonic development of *C. elegans* is invariant and the fate of the embryonic lineages can be traced from zygote to L1 stage due to the transparence of the eggs (Sulston et al., 1983; Zipperlen et al., 2001). These features and the large numbers of embryos that can be easily obtained under laboratory conditions, make *C. elegans* an excellent model for embryogenesis.

Embryonic development is divided in two stages, proliferation and morphogenesis (Sulston et al., 1983).

The proliferative stage lasts 330-350min. at 22°C and is further subdivided into two phases. The first phase consists of several rounds of cell divisions in the maternal uterus, giving rise to the embryonic founder cells. 150min. after fertilization, when the embryo has reached approximately 30-cell stage and gastrulation has just started, it is expelled from the maternal body. During the second phase of the proliferative stage, gastrulation is completed and multiple rounds of cell division occur. All the 558 cells present at hatching are produced during the proliferative stage (Altun & Hall, 2009; Sulston et al., 1983).

In order to get a closer insight into these initial steps of embryonic development, a large number of mutations causing early embryonic lethality have been isolated. Many of them affect genes that are involved in essential mechanisms like meiosis, mitosis, cell polarity or cytokinesis (Zipperlen et al., 2001).

The second stage of embryogenesis, the morphogenesis, lasts from 5.5-6h to 12-14h after fertilization at 22°C. At the beginning of this stage, the embryo is organized into three germ layers, ectoderm, mesoderm and endoderm. During morphogenesis terminal differentiation occurs, the embryo elongates and a larva

with functional tissues is formed (Fig.I.7) (Altun & Hall, 2009; Sulston et al., 1983).

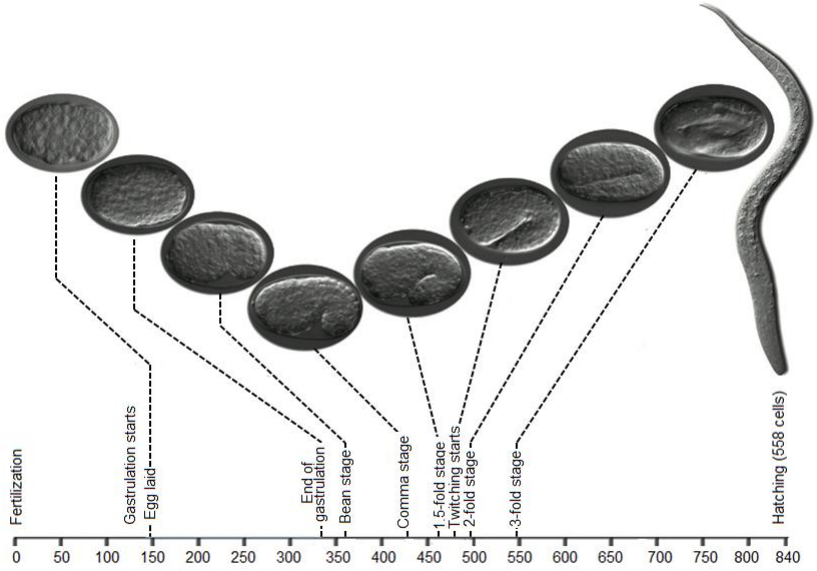

Fig.I.7: Schematic view of *C. elegans* embryogenesis at 22°C. The first steps of embryogenesis occur in the maternal uterus. At gastrulation the eggs are laid. Picture modified from: http://www.wormatlas.org

In order to provide the development of different tissues and organs, embryonic cells have to acquire their respective fates. In *C. elegans* the cell fate specification is provided by two classes of events. Just after fertilization six founder cells (AB, MS, E, C, D, and P4) are produced by several rounds of asymmetric cleavages of the zygote (Fig.I.8) (Maduro, 2010; Priess, 2005)

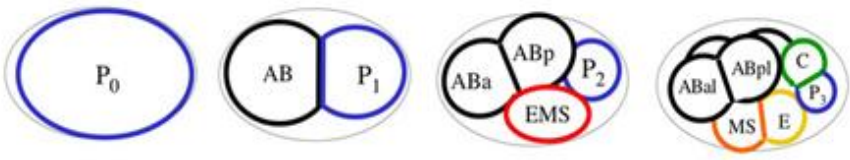

Fig.I.8: Generation of founder cells in the early *C. elegans* embryo. After fertilization, the zygote undergoes several rounds of asymmetric cleavages to give rise to the six founder cells of the adult tissues. Picture modified from: http://www.wormatlas.org

Each of these blastomeres has a characteristic expression program which determines the fate of its descendants. A prerequisite for these differentiation events are cell-cell interactions mediated by the *lin-12*/Notch pathway (Priess, 2005).

The second class of specification event is the synthesis of tissue-specific factors that regulate the formation of different tissue types. These factors act independently from the lineage and can induce the development of a certain tissue in the descendents of different founder cells. This independent mode of action is necessary, since, apart from germline and intestine, all tissues arise from more than one embryonic lineage (Maduro, 2011).

Besides *lin-12*/Notch signaling, different Wnt pathways are crucial for correct embryonic development. Asymmetric cell divisions require the correct orientation of the mitotic spindle that is partially regulated by Wnt (Walston & Hardin, 2006). Beyond that, Wnt pathways are involved in the regulation of gastrulation, which is characterized by the movement of the founder cells of germline, pharynx and body wall muscles towards the inside of the embryo (Hardin & King, 2008; Altun & Hall, 2009). Also other processes like cell migration and the engulfment of apoptotic bodies are mediated by Wnt (Gómez-Orte et al., 2013).

I.1.5. The *C. elegans* intestine as a model for cell cycle regulation

I.1.5.1. Intestinal development

All cells of an adult *C. elegans* intestine derive from a single progenitor cell, the E blastomere of the 8-cell embryo (McGhee, 2013; Sulston et al, 1983).

During embryonic development four rounds of divisions occur, in whose course sixteen descendants of the E blastomere are generated (Leung, Hermann & Priess, 1999). Four of these cells undergo one additional round of division, so that the intestine consists of twenty mononucleate cells at the time of hatching (Sulston et al., 1983). At the beginning of the first larval molt, a variable number (10-14) of the nuclei of these twenty cells divide. As a consequence, the intestine still consists of 20 cells, but has 30-34 nuclei.

Before every molt at the end of the four larval stages, a round of endoreplication occurs in all intestinal nuclei. The adult intestine is consequently formed by 20 cells with 30-34 large nuclei containing 32 chromosomes each (Fig.I.9) (Hedgecock & White, 1985).

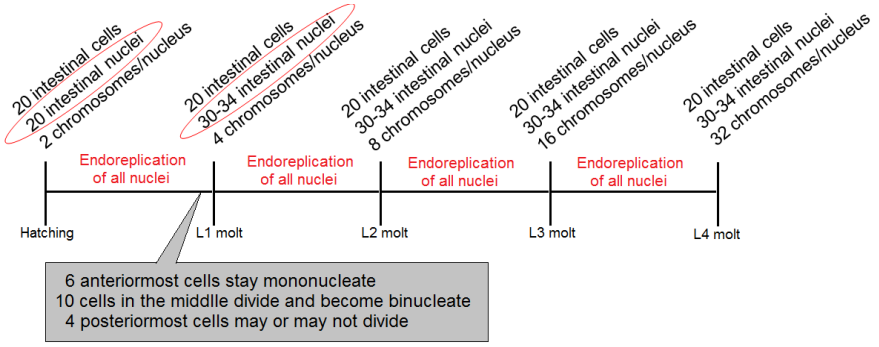

Fig.I.9: Schematic view of intestinal development in *C. elegans*. At hatching, the *C. elegans* intestine consists of 20 mononucleate cells. During L1 stage, the nuclei of 10-14 cells divide, giving rise to the 30-34 nuclei present in late L1 stage and in adults. After each larval stage endomitotic replication of all nuclei occurs resulting in nuclei with 32 chromosomes each. Picture modified from: http://www.wormatlas.org

I.1.5.2. Regulation of the intestinal cell number

To provide a coordinated series of events during intestinal development, a complex network of regulatory mechanisms is required. As in other eukaryotes, the cell cycle in *C. elegans* is controlled by complexes of cyclins and cyclin dependent kinases (cdks). When bound to their respective partner cyclines, cdks are active and phosphorylate their targets, thereby promoting entry in the next phase of the cell cycle. While cdks are continuously expressed, the synthesis of cyclines is stage-specific, what provides the timely coordinated formation of cyclin/cdk complexes. Their activity is modulated by inhibiting and activating regulators, such as kinases and phosphatase (van den Heuvel, 2005).

In *C. elegans,* many families of essential cell cycle regulators are presented by one homolog only and, as described above, the E lineage is well characterized. Due to these features, the intestine of the nematode represents an excellent model for the study of

fundamental mechanisms in cell cycle regulation (Koreth & van den Heuvel, 2005).

Two different pathways have been shown to regulate the number of intestinal cells upon hatching. Both, the *lin-35* and the *cki-1* pathway, act inhibiting on G1/S transition and thereby negatively regulate proliferation. The only *C .elegans* homolog of cyclin D, CYD-1, forms complexes with CDK-4 and inhibits the signaling of the *lin-35* and the *cki-1* pathway, consequently promoting entry into the S phase (Boxem & van den Heuvel, 2001).

Besides *lin-35* and *cki-1* that are global cell cycle regulators, also an organ-specific factor has been shown to control G1/S transition. CDC25.1, a homolog of the human family of CDC25 phosphatases, acts in an independent pathway in the control of the intestinal cell cycle, but does not have known function in other tissues (Fig.I.10) (Kostić & Roy, 2002).

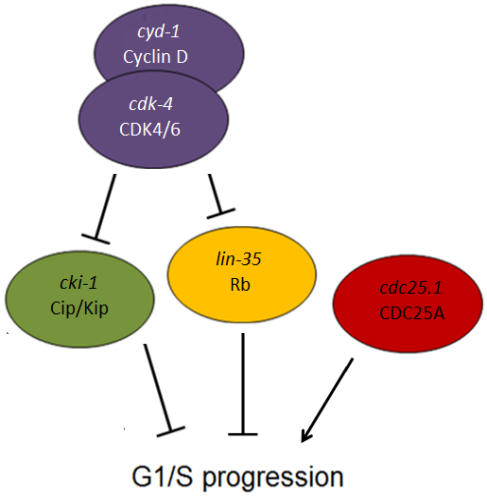

Fig.I.10: Schematic view of pathways involved in cell cycle regulation in the E lineage of *C. elegans*. Three independent pathways have been shown to regulate the G1/S transition. The *lin-35* and the *cki-1* pathways act redundantly. [Rb: Retinoblastoma protein; Cip/Kip: CDK interacting protein/Kinase inhibitory protein]

I.1.6. *C. elegans* as model for stress response pathways and aging

The Insulin/IGF-1 signaling (IIS) pathway is conserved over the eukaryotic lineage from yeast to human. In *C. elegans* it is involved in the control of various processes, such as life span, fat storage, reproduction, stress response and innate immunity. (Baugh & Sternberg, 2006; Kurz & Tan, 2004; Oh et al., 2006).

Also L1 arrest and dauer stage, which are both induced by lack of nutrients and other unfavorable environmental factors, are regulated by the IIS pathway. Larvae that hatch in the absence of food halt postembryonic development and undergo L1 arrest until development is induced by the uptake of nutrients. L1 arrested animals have increased stress resistance compared to developing larvae, but do not show morphologic changes (Baugh, 2013).

Starvation, but also other stress factors, like high temperatures, can also induce dauer stage. In contrast to L1 arrest, animals enter in dauer stage in late L1 and show morphological differences to developing larvae. Dauer animals generate a special cuticle, are slimmer and do not perform pharyngeal pumping for food uptake. To shield them even more from harmful environmental factors, their orifices are plugged and their pharynxes constricted. As arrested L1 larvae, dauer animals show a higher resistance to stress (Hu, 2007).

The gene *daf-2* encodes the only *C. elegans* homolog of the family of insulin-like growth factor receptors (IGFs) (Baugh & Sternberg, 2006). In the presence of food, DAF-2 induces a PL3-Kinase/Akt signaling cascade that results in the phosphorylation of the FOXO transcription factor DAF-16. As a consequence, DAF-16 is inactive and located in the cytoplasm. In response to starvation and

consequently absence of signals from DAF-2, DAF-16 is dephosphorylated, thereby activated and translocates to the nucleus, where it induces the transcription of a large number of target genes (Fig.I.11) (Barbieri et al., 2003; Baugh & Sternberg, 2006, Pinkston-Gosse & Kenyon, 2007).

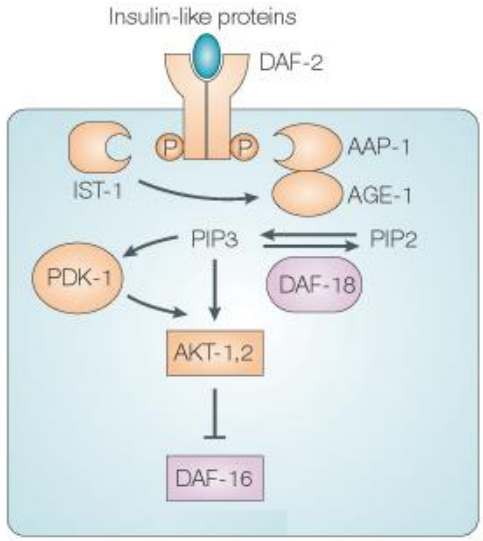

Fig.I.11: Schematic view of the Insulin/IGF signaling (IIS) pathway in *C. elegans*. Once activated, the receptor DAF-2 initiates a PL3-Kinase/Akt signaling cascade, thereby inhibiting the FOXO transcription factor DAF-16.

Unsurprisingly, many genes that are involved in stress response, encode antimicrobial factors or are required for fat and steroid hormone synthesis are amongst the transcriptional targets of DAF-16 (Murphy & Hu, 2013). To provide the cessation of cell proliferation during developmental arrest, also the expression of cell cycle regulators is regulated by *daf-16*. For instance, the expression levels of the cyclin-dependent kinase inhibitor *cki-1* are significantly up-regulated upon activation of DAF-16 (Baugh & Sternberg, 2006).

Loss-of-function mutants for *daf-2*, *daf-16* and other components of the IIS pathway have been isolated. Animals lacking functional *daf-2* are, despite the presence of food, constitutively in L1 arrest and show a significantly enhanced life span compared to wild type animals. In contrast, mutations causing inactivation of *daf-16* result in a failure of the animals to undergo development arrest and in a decreased life span.

As many other major signaling pathways, also the IIS pathway is highly conserved, yet comparably simple in *C. elegans* (Baugh & Sternberg, 2006). Thus, the nematode represents an excellent model for the study of stress response, the aging process and the impact of external factors on life and health span.

I.2. Chromatin remodeling

I.2.1. Chromatin structure and function

In eukaryotic cells, the DNA is tightly packed through the action of proteins to form chromatin (Das, Tyler & Churchill, 2010). This form of organization enables the storage of large amounts of genetic material in the limited space of the eukaryotic nucleus (Narlikar, Sundaramoorthy & Owen-Hughes, 2013). Beyond that, it confers stability to the genome and provides protection from DNA damage (Ljungman & Hanawalt, 1992).

The compact packaging of the DNA is achieved by various levels of organization with nucleosomes as basic element. Nucleosomes consist of a histone octamer (formed by two copies of each of the core histones H3, H4, H2A and H2B) that is enwrapped by approximately 147bp of DNA (Rivera et al., 2014; Das, Tyler & Churchill, 2010). Single nucleosome core particles are separated by linker DNA that can be associated with another type of histone, the linker histone H1 (Cooper, 2000; Bustin, Catez & Lim, 2005).

In complex with histone H1, nucleosomes are called chromatosomes and form a chromatin fiber with a diameter of 10nm, the so-called beads on the string structure (Cooper, 2000). Further compactation is achieved by interactions of the H1 histones that cause coiling to a 30nm fiber (Cooper, 2000).

The extent of chromatin condensation varies and depends on the stage of the cell cycle. The highest level of compactation is reached during metaphase of mitosis, when the chromosomes are distributed to the daughter cells (Fig.I.12) (Cooper, 2000; Anunnziato, 2008).

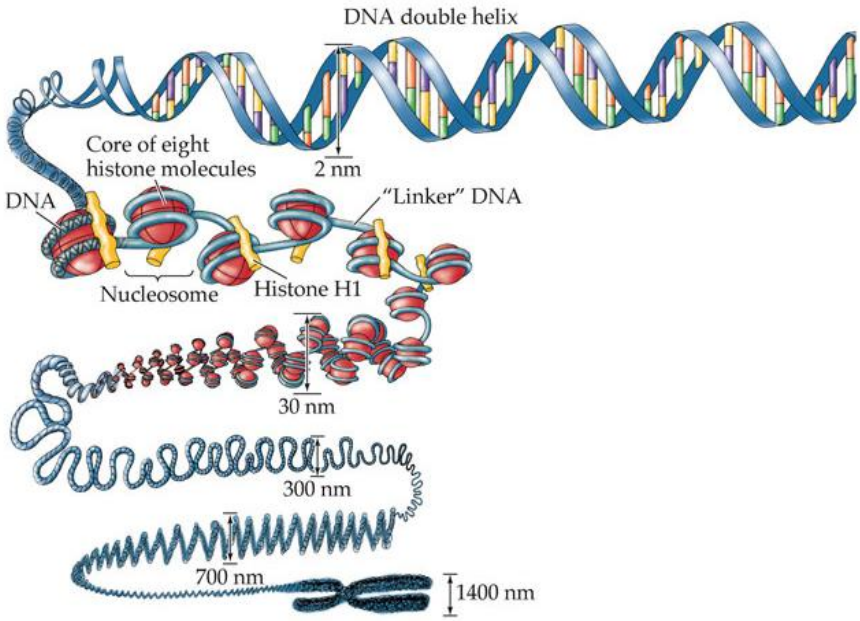

Fig.I.12: Organization levels of DNA in chromatin. Due to various levels of packaging the complete DNA of an eukaryotic cell can be stored in the nucleus in a highly ordered manner. Picture modified from: http://www.http://course1.winona.edu

Since chromatin is a dynamic molecule, it has not only structural, but also regulatory functions. By alterations of the chromatin state, the accessibility of a given genomic region by proteins can be controlled and thereby influence processes such as transcription, replication or DNA repair (Das & Tyler, 2012; Ho & Crabtree, 2010; Shibata et al., 2012).

There are two main classes of enzymes known to induce alterations of the chromatin state, I) histone modifying enzymes and II) ATP-dependent chromatin remodelers.

The histone modifying enzymes perform post-translational modifications of the N-terminal tails of histones. Thereby they can alter the interactions between nucleosomes and DNA and consequently the chromatin state. Beyond that, histone

modifications can enable the recruitment of regulatory proteins, since they provide binding sides. (Hargreaves & Crabtree, 2011; Petty & Pillus, 2013; Wang, Allis & Chi, 2007).

ATP dependent chromatin remodelers in contrast, change the position of nucleosomes under usage of ATP by sliding them along the DNA or catalyzing their ejection or insertion (Fig.I.13) (Hargreaves & Crabtree, 2011; Euskirchen, Auerbach & Snyder, 2012)

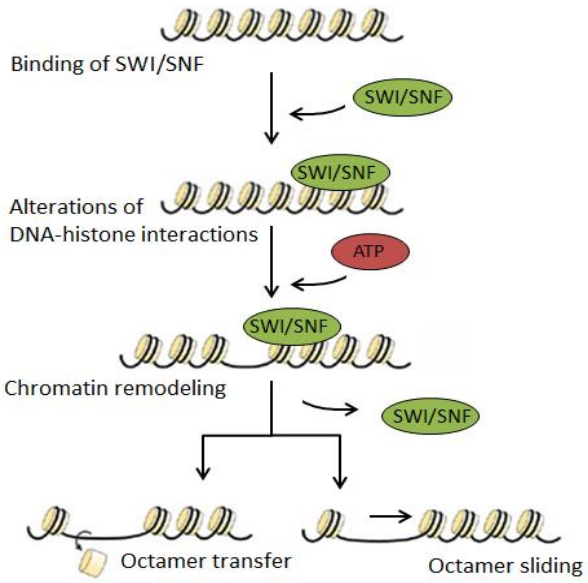

Fig.I.13: Putative mechanism of chromatin remodeling by a SWI/SNF complex. By ejecting, inserting or moving nucleosomes, ATP-dependent SWI/SNF complexes are able to control the accessibility of a given DNA region. Picture modified from: Roberts & Orkin, 2004

I.2.2. SWI/SNF complexes

The first ATP-dependent chromatin remodeling complex discovered was SWI/SNF in yeast. Components of this complex were identified in two independent screens for mutations affecting the mating type switching or the ability to grow on sucrose, hence the names SWI (SWItching defective) and SNF (sucrose non-fermenting) (Stern, Jensen & Herskowitz, 1984; Neigeborn & Carlson, 1984) Later studies in diverse organisms showed that SWI/SNF complexes are well conserved (Hargreaves & Crabtree, 2011).

The composition of SWI/SNF complexes is similar in all species, even when they have acquired complexity during evolution (Hargreaves & Crabtree, 2011). A central ATPse subunit associates with a group of core proteins and a variety of accessory subunits. While all SWI/SNF complexes of an organism share the same core subunits, the accessory subunits vary depending on the tissue and the cellular state, thereby conferring specificity to a given complex (Weissman & Knudsen, 2009; Euskirchen, Auerbach & Snyder, 2012).

Besides SWI/SNF, a second ATP-dependent chromatin remodeling complex exists in yeast, called RSC (Cairns et al., 1996).

SWI/SNF and RSC complexes differ in the number and composition of their subunits. SWI/SNF consists of 12 proteins and contains the enzymatic subunit Swi2/Snf2 (Monahan et al., 2008). RSC is composed by a total of 17 proteins and its ATPase subunit is Sht1, a paralog of Snf2 (Monahan et al., 2008; Roberts & Orkin, 2004). Beyond the enzymatic subunit, several proteins incorporated in SWI/SNF have paralogs in RSC, amongst them the core subunits (Snf5 and Swi3 in SWI/SNF, Sfh1 and Rsc8 in RSC).

Some subunits, Arp 7 and Arp 9 for instance, are shared between the SWI/SNF and RSC complexes (Monahan et al., 2008).

In *Drosophila* and mammals, two subclasses of SWI/SNF complexes have been classified that are distinguished by specific signature subunits.

One subclass is called BAF (or SWI/SNF-α) in humans and BAP in *Drosophila.* BAF/BAP complexes are characterized by signature subunits (BAF250/ARID1 in human, Osa in *Drosophila*) that contain AT-rich interaction (ARID) domains. This motif is conserved in the Swi1 subunit of the yeast SWI/SNF complex (Collins et al., 1999; Nie et al., 2000).

The second subclass of SWI/SNF complexes is called PBAF (or SWI/SNF-β) in humans and PBAP in *Drosophila*. PBAF/PBAP complexes incorporate the signature subunits BAF180 and BAF200 or Polybromo and BAP170 (Mohrmann et al., 2004; Yan et al., 2005).

BAF180 and Polybromo are homolog to three components of the yeast RSC complex, Rsc1, Rsc2 and Rsc4, while BAF200 and BAP170 are related to Rsc9 (Tang, Nogales, & Ciferri, 2010; Mohrmann et al., 2004)

Thus, the PBAF complex is closer to the yeast RSC complex, while BAF has a higher similarity to the yeast SWI/SNF complex.

Drosophila and *C. elegans* SWI/SNF complexes contain only one enzymatic subunit, Brahma (BRM) and SWSN-4, respectively. In contrast, two ATPase subunits, hBRM and BRG-1, exist in the human. hBRM is a paralog of Swi2, the enzymatic subunit of yeast SWI/SNF. BRG-1 is related to Shf1, the ATPse of the RSC complex (Mohrmann et al., 2004; Roberts & Orkin, 2004). The human BAF complex can either have hBRM or BRG-1 as enzymatic subunit.

The PBAF complex in contrast, can only contain BRG-1. The two subclasses of human SWI/SNF complexes have been shown to have partially overlapping, but also specialized functions (Wang et al., 2004).

SWI/SNF complexes are involved in transcriptional regulation and thereby control cellular key processes, such as proliferation and differentiation (Lans et al., 2010).
Mutations of SWI/SNF components play a role in the pathogenesis of human diseases and disorders, including cancer, viral infections, intellectual disability and muscular dystrophy. The broad spectrum of defects that can arise due to alterations of SWI/SNF complexes reflects their importance for a variety of biological processes (Wilson & Roberts, 2011; Shain & Pollack, 2013; Santen, Kriek & van Attikum, 2012; Zhang et al., 2006)

I.2.3. Human BAF60 proteins

Amongst the accessory subunits that are incorporated in both subclasses of human SWI/SNF complexes are the paralog proteins BAF60a, -b and –c (also known as SMARCD1, SMARCD2 and SMARCD3, respectively). The three BAF60 genes are well conserved and have one single homolog in yeast (Swp73/Snf12) and two in *C. elegans* (*ham-3* and *swsn-2.2*) (Euskirchen, Auerbach & Snyder, 2012; Roberts & Orkin, 2004; Large & Mathies, 2014). BAF60a, -b and –c are mutually exclusive in a given complex and have acquired specialized gene functions, reflected by their different expression patterns (Puri & Mercola, 2012).

BAF60a, for instance, is ubiquitously expressed (Bennett-Lovsey et al., 2002). The BAF60a protein directly interacts with tumor suppressor p53 and is thereby involved in the regulation of apoptosis and cell cycle arrest (Oh et al., 2008). BAF60a was also shown to be required for steroid receptor function (Hsiao et al., 2003)

BAF60b is predominantly expressed in the muscles (Bennett-Lovsey et al., 2002; Wang et al., 1996). In contrast to the other two members of the protein family, BAF60b contains a central domain termed SWIB (for SWI/SNF complex B). This SWIB domain presents homology with the p53-binding domain of the human MDM2 oncoprotein, a negative regulator of the tumor suppressors p53 and pRb. MDM2 can bind and block the transactivation domain of tumor suppressor p53 through the SWIB domain, thereby inhibiting its capacity to activate transcription (Bennett-Lovsey et al., 2002).

BAF60c is highly expressed in the pancreas and in the developing heart and somites during murine embryonic development (Wang et al., 1996; Puri & Mercola, 2012). It has been shown to be required for normal skeletal and cardiac myogenesis (Puri & Mercola, 2012; Lickert et al., 2004). BAF60c has also been proposed to be involved in transcriptional regulation via the Notch pathway (Takeuchi et al., 2007).

All members of the BAF60 family have been related with different kinds of human tumors. For example, reduced expression of BAF60a is associated with an increased risk of lung cancer and loss-of-function mutations were found in breast cancers (Reisman, Glaros & Thompson, 2009; Stephens et al., 2012). BAF60b overexpression was observed in human breast cancers (Sgroi et al., 1999). BAF60c shows reduced expression in neuroblastoma (Weissman & Knudsen, 2009).

Subunit	Association with human tumors
BAF60a	reduced expression associated with increased lung cancer risk
BAF60b	overexpressed in breast cancers
BAF60c	reduced expression in neuroblastoma

Table R.1: The BAF60 proteins and tumorigenesis. All members of the BAF60 family have been related to different kinds of human tumors.

For the sake of simplicity, we can summarize this information as follows:

I) BAF60a and BAF60c may function as tumor suppressors whereas BAF60b seems to act as oncogene.

II) BAF60a is related to proliferative processes, while BAF60c is involved in cell differentiation.

Still, mutations in other SWI/SNF components could mask or modify mutations in BAF60 proteins.

I.2.4. SWI/SNF complexes in *C. elegans*

The first SWI/SNF genes described in *C. elegans, swsn-1* and *swsn-4* (formerly *psa-1* and *psa-4*), were identified due to the Psa (phasmid sock absent) phenotype, which arises as a consequence of mutations in these genes (Sawa, Kouike & Okano, 2000).

In absence of functional *swsn-1* or *swsn-4*, failures in the asymmetric cell division of the tail hypodermal cell occur; instead of giving rise to hypodermal and neural cells (from the anterior and posterior daughter cell, respectively), the T cell produces hypodermal cells only (Sawa, Kouike & Okano, 2000).

swsn-4 encodes the only ATPase subunit of SWI/SNF in *C. elegans.* SWSN-4 associates with the non-enzymatic components SWSN-1 and SWSN-5, forming the core of the *C. elegans* SWI/SNF complex. According to the tissue and developmental context, this core can associate with a number of accessory proteins (e.g. HAM-3 or SWSN-2.2) in different combinations.

All human SWI/SNF subunits have *C. elegans* homologs (Table 1 and Fig.I.14). Similarly to their human counterparts, *C. elegans* SWI/SNF complexes seem to be involved in a variety of cellular processes. Mutations of SWI/SNF components have been associated with various phenotypes such as abnormal gonad and vulval development, alterations in the stress response, and neurological abnormalities (Large & Mathies, 2014; Hayes, Riedel, & Ruvkun, 2011; Weinberg et al., 2013; Kuzmanov et al., 2014).

As in other species, SWI/SNF complexes can be classified in two subclasses.

The BAF complex is characterized by the specific subunit LET-256, a homolog of BAF250/ARID1. The PBAF complex can incorporate two different signature subunits, SWSN-7 and PBRM-1. SWSN-7 is a homolog of BAF200/ARID2, while PBRM-1 is the counterpart of BAF180 (Large & Mathies, 2014; Mohrmann et al., 2004).

BAF and PBAF complexes in *C. elegans* have partly overlapping functions, but also act independently, each regulating the expression of a specific set of target genes (Shibata et al., 2012)

	Human	***C. elegans***
Enzymatic subunit	BRG1 or BRM	SWSN-4
Core subunit	BAF155 and BAF170	SWSN-1
	BAF47	SWSN-5/ SNFC-5
Accessory subunits	BAF60 a or BAF60b or BAF60c	HAM-3
		SWSN-2.2
	BAF57	SWSN-3
	BAF53a or BAF53b	SWSN-6
	BAF45a	PHF-10
	BAF45b or BAF45c or BAF45d	DPFF-1
	BRD7/BRD9	SWSN-9
Accessory subunits BAF	BAF250a/ARID1a BAF250b/ARID1b	LET-526
Accessory subunits PBAF	BAF200/ARID2	SWSN-7
	BAF180	PBRM-1

Table R.2.: Subunits of human SWI/SNF complexes and their respective homologs in *C. elegans*. All SWI/SNF subunits in *C. elegans* present one or more homologs in human.

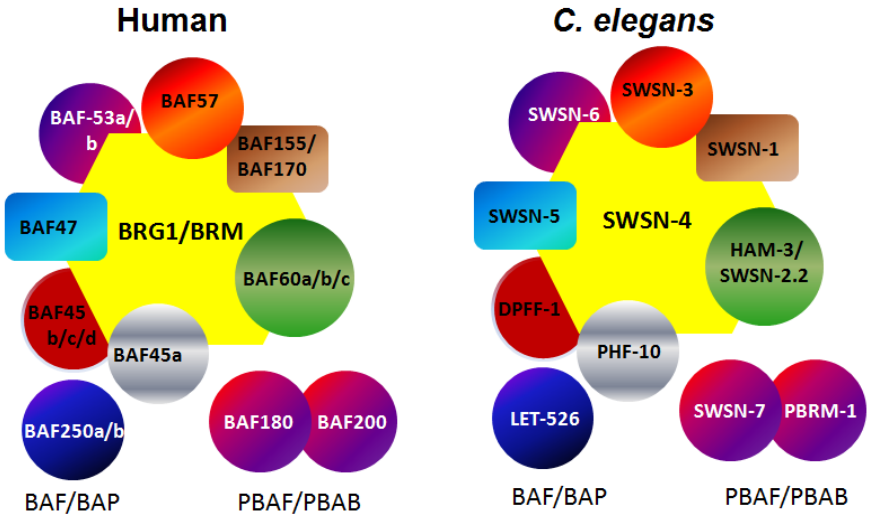

Fig.I.14: Schematic presentation of SWI/SNF complexes in human and *C. elegans*. SWI/SNF complexes are well conserved throughout evolution. All *C. elegans* subunits have one or more human homologs.

I.2.5. The *C. elegans* accessory subunits HAM-3 and SWSN-2.2

The *C. elegans* SWI/SNF accessory subunits HAM-3 and SWSM-2.2 are encoded by the paralog gene pair *ham-3* (formerly ZK1128.5 or *swsn-2.1*) and *swsn-2.2* (formerly C18E3.2) on chromosome III and I, respectively. HAM-3 and SWSN-2.2 are not specific for either the BAF or the PBAF complex, but can be incorporated in both subclasses of the *C. elegans S*WI/SNF complex (Large & Mathies, 2014; Riedel et al., 2013).

Both proteins contain a central SWIB domain highly similar to their human counterpart BAF60b. However, also when they share the SWIB domain with BAF60b, *ham-3* and *swsn-2.2* are not clear orthologs of one of the three human BAF60 proteins only, but share equal similarity with all of them (Weinberg et al., 2013; Large and Mathies, 2014).

The two *C. elegans* paralogs and their human counterparts come from the same evolutionary ancestor (Fig.I.15). The similarity of *ham-3* and *swsn-2.2* (66.8%) is comparable with the similarity amongst the BAF60 proteins (BAF60a and -b: 59.8%; BAF60b and –c: 60.4%; Fig.I.16) (Weinberg et al., 2013).

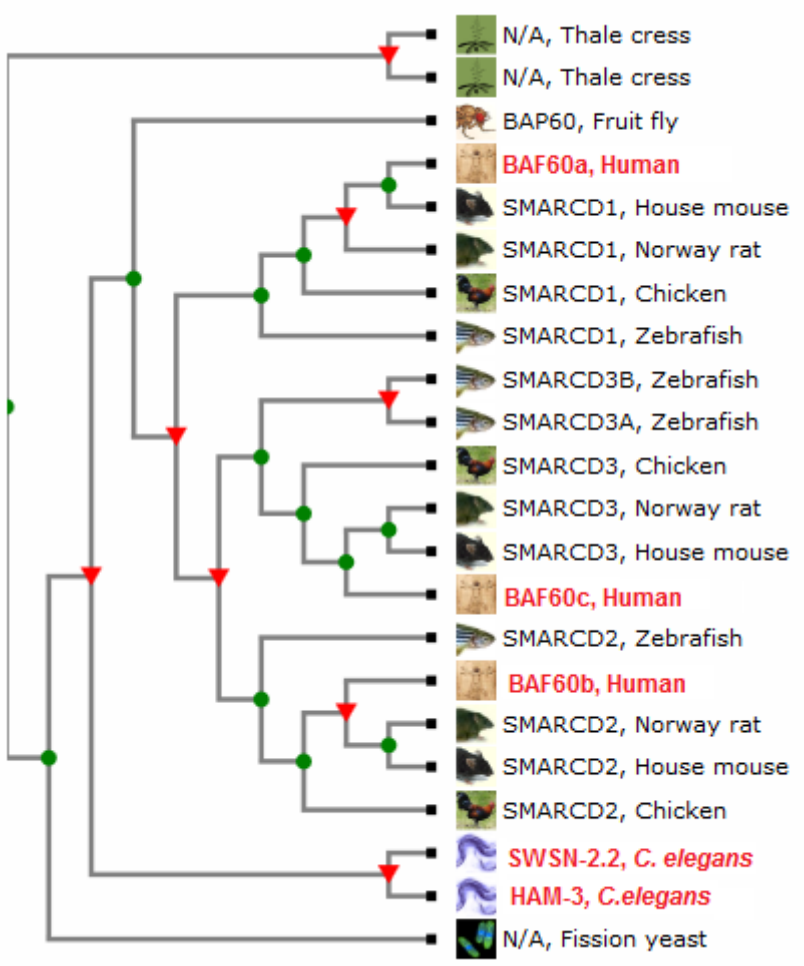

Fig.I.15: Phylogenetic tree of the BAF60 family. The two *C. elegans* paralogs *ham-3* and *swsn-2.2* and their human counterparts BAF60a, -b and -c have the same evolutionary ancestor.

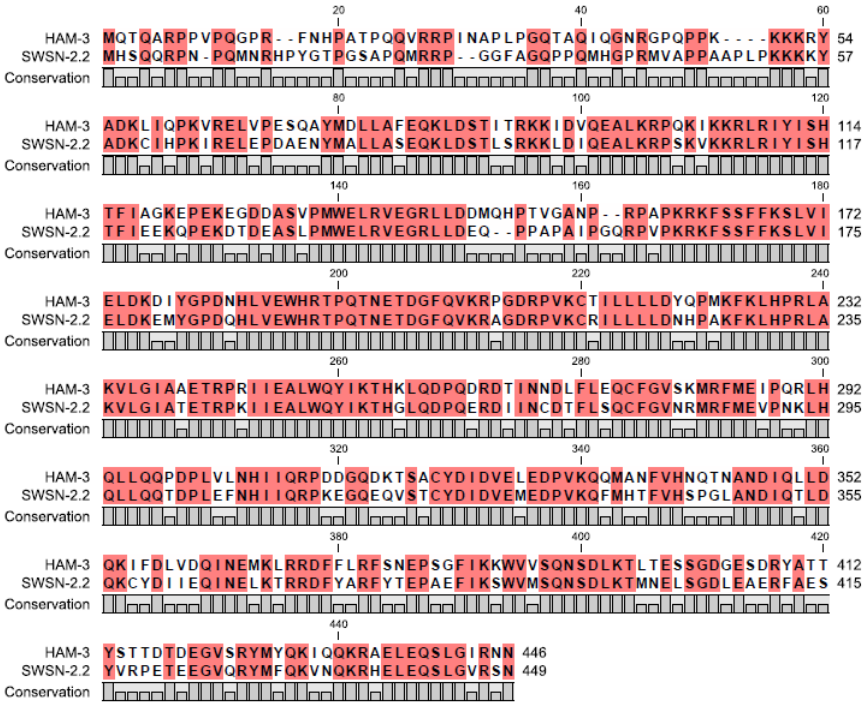

Fig.I.16: Alignment of HAM-3 and SWSN-2.2 protein sequences. The protein sequences of the two paralogs share a similarity of 66.8%.

I.2.6. Previously characterized functions of *ham-3* and *swsn-2.2*

The gene *ham-3* was initially identified in a screen for mutations affecting the development of the hermaphroditic-specific neurons (HSN), hence the name (*ham* for HSN abnormal migration) (Desai & Horvitz, 1989). More recently it was demonstrated that this specific neuronal phenotype is probably caused due to changes in the expression of the two Zinc-finger transcription factors *ham-2* and *sem-4* (Weinberg et al., 2013). Apart from its function in HSN, *ham-3* was shown to play a role in various developmental processes.

ham-3 was found to be a genetic interactor of *lin-35*/Rb and to be involved in vulval development and processes required for fertility (Cui, Fay & Han, 2004; Cerón et al., 2007). Moreover, it has been shown that *ham-3* is involved in the development of the somatic gonad. The *hunchback* and Ikaros-like (HIL) gene *ehn-3* acts as transcriptional regulator and is required for the differentiation of the somatic gonad precursors and thereby the generation of the distal tip cells. *ham-3* was identified as a genetic enhancer of a weak allele of *ehn-3* (Large & Mathies, 2014).

The Zinc-finger protein SOMI-1 regulates the differentiation of the hypodermis. SOMI-1 binds the promoters of genes causing their inactivation, probably by mediating their silencing by miRNAs (Hayes, Riedel & Ruvkun, 2011). *somi-1* loss-of-function causes a failure in the exit from the molting cycle and it was shown that SWI/SNF complexes containing the accessory subunit HAM-3 interact with SOMI-1 in this developmental context (Hayes, Riedel & Ruvkun, 2011).

swsn-2.2 functions are less characterized than those of its paralog *ham-3.* However, in the course of the same RNAi screens as *ham-3*, also *swsn-2.2* was identified as a genetic interactor of *lin-35*/Rb (Cerón, 2007; Cui, Fay & Han, 2004). Further, it was shown that *swsn-2.2* is, similarly to *ham-3,* a genetic enhancer of *ehn-3* and is involved in processes like gonad and vulval development (Large & Mathies, 2014; Cui, Fay & Han, 2004). Also in terms of impaired fertility, *swsn-2.2* loss-of-function phenocopies lack of functional HAM-3 (Sawa, Kouike & Okano, 2000; Cui, Fay & Han, 2004; Large & Mathies, 2014).

Also when the two genes have similar functions in many contexts, they seem to have acquired specialized functions during evolution. In contrast to *ham-3*, *swsn-2.2* has been reported to be an

essential gene (Weinberg et al., 2013). Beyond that, HAM-3 is required for correct development of the hermaphrodite-specific neurons, while SWSN-2.2 is not (Weinberg et al., 2013).

Results

R.1. *ham-3* and *swsn-2.2* mutants

A total of five mutant alleles exist for *ham-3* and *swsn-2.2*. Four of them are available at the *Caenorhabditis* Genetics Center (CGC), while one was isolated by us. Although some of them have been partially studied, here we describe a comprehensive molecular and phenotypic characterization of these mutant alleles.

R.1.1. Molecular characterization of *ham-3* mutant alleles

The *ham-3* alleles *tm3309* and *n1654* have been used in previous studies (Weinberg et al., 2013; Large & Mathies, 2014).

tm3309 combines a deletion of 243 base pairs with an insertion of 4 base pairs (Fig.R.1A; Fig.R.4.A; Annex 1). *In silico* analysis suggests that the mutation causes the retention of the second intron (Annex 2) and results in premature stop codons (PTC) (Fig.R.2B). Thus, the gene product encoded by *tm3309* is expected to be degraded by the nonsense mediated decay (NDM) system.

n1654 presents a point mutation (Fig.R.1A; Annex 1). Similarly to *tm3309*, the mutation causes a PTC (Fig.R.2C), probably resulting in the degradation of the encoded transcript.
We validated these assumptions by performing Reverse-Transcription PCR of *ham-3* with cDNA from *tm3309* and *n1654* animals, and indeed did not detect gene products (Fig.R.5A,B). Thus, we assume that both mutations represent null alleles.

By screening a deletion library, we isolated ***he159***, which is the third *ham-3* allele included in this study. Sequencing showed that *he159* presents a deletion of 1211 base pairs (Fig.R.1A; Fig.R.4.B; Annex 1).

The mutation probably causes the retention of the last intron (Annex 2) and results in a frameshift (Fig.R.2D), but does not produce premature stop codons (Fig.R.2D). Thus, it is expected to encode a truncated protein (189 instead of 446 amino acids). By Reverse-Transcription PCR we verified that the *he159* allele produces a shorter transcript (Fig.R.5C). The predicted protein lacks a region of 257 amino acids including the SWIB/MDM2 domain and, due to a frameshift, only the first 154 amino acids are identical to the wild type protein (Fig.R.2D). Since the central domain is missing and we observed a high similarity of the phenotypes caused by *ham-3(he159)* and those displayed by the *ham-3* null alleles *tm3309* and *n1654*, we conclude that *he159* presents a loss-of-function allele.

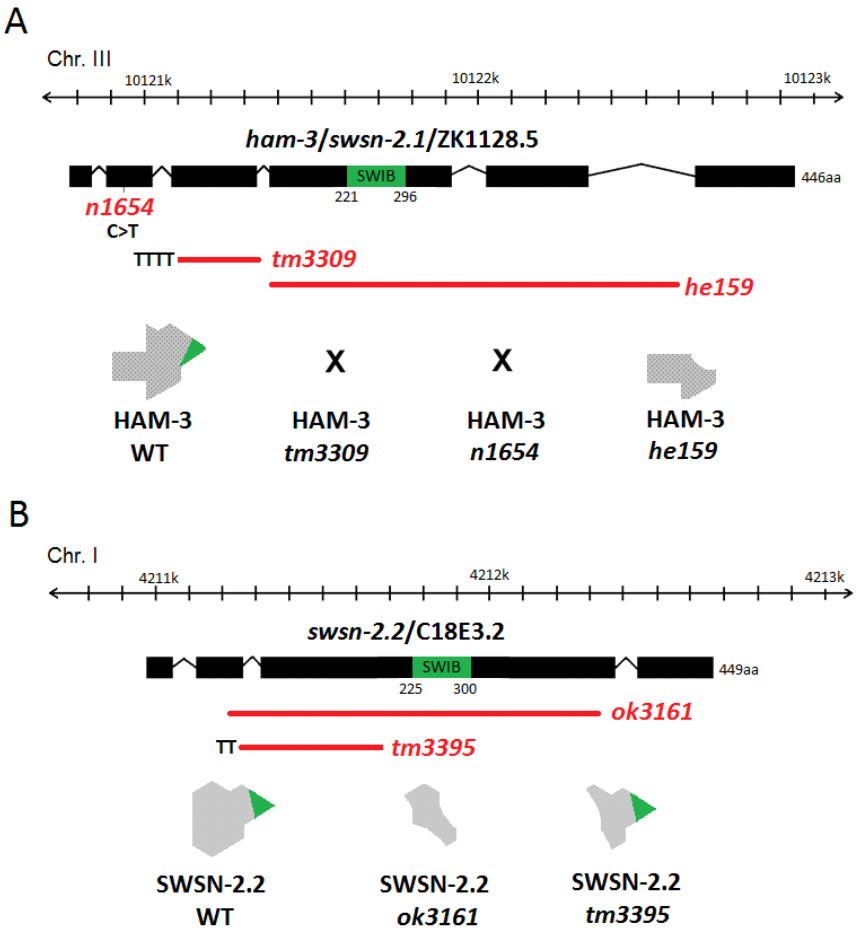

Fig.R.1: ***ham-3* and *swsn-2.2* mutant alleles and their expected gene products.** The SWIB/MDM2 domain is labeled in green. The red bars represent deletions of the respective allele. The letters indicate insertions or transitions. (A) *ham-3(n1654)* and *ham-3(tm3309)* are null alleles, since their products are expected to be degraded by the NMD pathway. *ham-3(he159)* encodes a truncated protein lacking the central domain. (B) Both *swsn-2.2* mutant alleles give truncated proteins. While the product encoded by *swsn-2.2(ok3161)* lacks the central domain, *swsn-2.2(tm3395)* gives a protein containing the SWIB/MDM2 motif.

A) Wild type

Met Q T Q A R P P V P Q G P R F N H P A T P Q Q V R R P I N A P L P G Q T A Q I Q G N R G P Q P P K K K K R Y A D K L I Q P K V R E L V P E S Q A Y Met D L L A F E Q K L D S T I T R K K I D V Q E A L K R P Q K I K K R L R I Y I S H T F I A G K E P E K E G D D A S V P Met W E L R V E G R L L D D Met Q H P T V G A N P R P A P K R K F S S F F K S L V I E L D K D I Y G P D N H L V E W H R T P Q T N E T D G F Q V K R P G D R P V K C T I L L L L D Y Q P Met K F K L H P R L A K V L G I A A E T R P R I I E A L W Q Y I K T H K L Q D P Q D R D T I N N D L F L E Q C F G V S K Met R F Met E I P Q R L H Q L L Q Q P D P L V L N H I I Q R P D D G Q D K T S A C Y D I D V E L E D P V K Q Q Met A N F V H N Q T N A N D I Q L L D Q K I F D L V D Q I N E Met K L R R D F F L R F S N E P S G F I K K W V V S Q N S D L K T L T E S S G D G E S D R Y A T T Y S T T D T D E G V S R Y Met Y Q K I Q Q K R A E L E Q S L G I R N N Stop

B) *tm3309*

Met Q T Q A R P P V P Q G P R F N H P A T P Q Q V R R P I N A P L P G Q T A Q I Q G N R G P Q P P K K K K R Y A D K L I Q P K V R E L V F T Y Stop V N T L K L I G F F C Y S N I P Q L E Q I P V Q L Q N G N S V H F S K A Stop L L S W I K I Y Met A Q T T I S L S G T V L H K P Met K L T D F K Stop S A P E I V P L N A Q S F F Y S I I S Q Stop S L N F I R D L Q K F S E L L Q K L V R E L L K P C G S T S K L T S F K I H R I V I Q S I Met I F S W S N V L V Stop A R Stop D L W R F L K D F I N S C N S L I L Stop S Stop I I L F S G L Met Met V K I K L L L V Met I L Met S S S R I Q S N N K W Q I S F T I K Q Met R T T F N Y L I K K Y S T W Stop I K Stop T R Stop S C V V I S S F V S R T S P V D S S R N G L Stop A R I L T Stop R L Stop Q N Q V V Met E N P I V Met R Q R T V Q L I Q Met K V Y H G T C I R K S N K N E P S W S K V S E S A T I

C) *n1654*

Met Q T Q A R P P V P Q G P R F N H P A T P Stop Q V R R P I N A P L P G Q T A Q I Q G N R G P Q P P K K K K R Y A D K L I Q P K V R E L V P E S Q A Y Met D L L A F E Q K L D S T I T R K K I D V Q E A L K R P Q K I K K R L R I Y I S H T F I A G K E P E K E G D D A S V P Met W E L R V E G R L L D D Met Q H P T V G A N P R P A P K R K F S S F F K S L V I E L D K D I Y G P D N H L V E W H R T P Q T N E T D G F Q V K R P G D R P V K C T I L L L L D Y Q P Met K F K L H P R L A K V L G I A A E T R P R I I E A L W Q Y I K T H K L Q D P Q D R D T I N N D L F L E Q C F G V S K Met R F Met E I P Q R L H Q L L Q Q P D P L V L N H I I Q R P D D G Q D K T S A C Y D I D V E L E D P V K Q Q Met A N F V H N Q T N A N D I Q L L D Q K I F D L V D Q I N E Met K L R R D F F L R F S N E P S G F I K K W V V S Q N S D L K T L T E S S G D G E S D R Y A T T Y S T T D T D E G V S R Y Met Y Q K I Q Q K R A E L E Q S L G I R N N Stop

D) *he159*

Met Q T Q A R P P V P Q G P R F N H P A T P Q Q V R R P I N A P L P G Q T A Q I Q G N R G P Q P P K K K K R Y A D K L I Q P K V R E L V P E S Q A Y Met D L L A F E Q K L D S T I T R K K I D V Q E A L K R P Q K I K K R L R I Y I S H T F I A G K E P E K E G D D A S V P Met W E L R V E G R L L D D Met Q H P T V G A N L I I F I S K I L Y F P G T C I R K S N K N E P S W S K V S E S A T I

Fig.R.2: Predicted protein sequences encoded by *ham-3* and the mutant alleles *tm3309*, *n1654* and *he159*. (A) The WT protein encoded by *ham-3* contains a central SWIB/MDM2 domain indicated in green. (B) *tm3309* results in a frameshift causing premature stop codons. The encoded protein is therefore expected to be degraded by NDM. Sequences that are identical to the wild type protein are indicated in yellow, amino acids arising due to a frameshift in red. (C) *n1654* causes replacement of a single base pair resulting in a premature stop codon and probably the degradation of the product by NMD. (D) The truncated protein (189 instead of 446 amino acids) encoded by *he159* does not contain the central SWIB/MDM2 domain and shows a frameshift after 154 amino acids. Amino acids that are identical to the WT protein are highlighted in yellow, amino acids arising due to a frame-shift in red.

R.1.2. Molecular characterization of *swsn-2.2* alleles

The *swsn-2.2* mutant alleles employed for this study were *ok3161* and *tm3395*. Both alleles have been partially characterized previously (Weinberg et al., 2013; Large & Mathies, 2014).

ok3161 presents a deletion of 1122 base pairs (Fig.R.1B; Fig.R.4C; Annex 3). The remaining sequence does not present PTCs and the allele might therefore produce a massively truncated product (91 instead of 449 amino acids) (Fig.R.3A; Annex 4). *In silico* analysis suggests that the encoded protein lacks the central SWIB/MDM2 domain (Fig.R.3A), but since no frameshift is introduced, the remaining parts of the sequence are identical to the wild type protein (Fig.R.3A; Annex 4). Reverse-Transcription PCR of *swsn-2.2* with cDNA from *ok3161* animals confirmed the presence of a truncated transcript (Fig.R.5D). However, because of the extended loss of the core of the protein including the central SWIB/MDM2 domain, *ok3161* probably presents a null allele.

The second *swsn-2.2* mutant allele*,* ***tm3395***, combines a deletion of 421 base pairs with an insertion of 2 base pairs (Fig.R.1B; Fig.R.4D; Annex 3). *In silico* analysis predicts a partial retention of the second intron (Annex 4) and a truncated protein (Fig.R.3B). The putative protein lacks a region of 127 amino acids that is replaced by three amino acids arising due to a frameshift, but, in contrast to *ok3161*, the central SWIB/MDM2 domain is conserved (Fig.R.3B). Indeed, we detected a truncated transcript upon performing Reverse-Transcription PCR (Fig.R.5E). As will be shown later in the text, the phenotypes caused by *tm3395* are similar to those of *ok3161* animals, but less penetrant. As result of the milder phenotypic effects, it is possible to maintain a homozygote *tm3395* population, while *ok3161* homozygotes are

not viable. We therefore suggest that *tm3395* presents a partial loss-of-function mutation and is not a null allele like *ok3161*.

To summarize, all studied alleles are loss-of-function mutations. While the two *ham-3* alleles *tm3309* and *n1654* do not give gene products, *he159* encodes a truncated protein. However, since the central domain is absent, this shorter protein is probably not functional.
Both *swsn-2.2* alleles give truncated proteins, but in contrast to *ok3161*, the *tm3395* sequence encodes the SWID/MDM2 domain and may conserve certain functions.

A)

Wild type

Met H S Q Q R P N P Q Met N R H P Y G T P G S A P Q Met R R P G G F A G Q P P Q Met H G P R Met V A P P A A P L P
K K K K Y A D K C I H P K I R E L E P D A E N Y Met A L L A S E Q K L D S T L S R K K L D I Q E A L K R P S K V K K R L R I Y I
S H T F I E E K Q P E K D T D E A S L P Met W E L R V E G R L L D E Q P P A P A I P G Q R P V P K R K F S S F F K S L V I E L
D K E Met Y G P D Q H L V E W H R T P Q T N E T D G F Q V K R A G D R P V K C R I L L L L L D N H P A K F K L H P R L A K
V L G I A T E T R P K I I E A L W Q Y I K T H G L Q D P Q E R D I I N C D T F L S Q C F G V N R Met R F Met E V P N K L H
Q L L Q Q T D P L E F N H I I Q R P K E G Q E Q V S T C Y D I D V E Met E D P V K Q F Met H T F V H S P G L A N D I Q T L
D Q K C Y D I I E Q I N E L K T R R D F Y A R F Y T E P A E F I K S W V Met S Q N S D L K T Met N E L S G D L E A E R F A E
S Y V R P E T E E G V Q R Y Met F Q K V N Q K R H E L E Q S L G V R S N Stop

ok3161

Met H S Q Q R P N P Q Met N R H P Y G T P G S A P Q Met R R P G G F A G Q P P Q Met H G P R Met V A P P A A P L P
K K K K Y A D K C I H E E G V Q R Y Met F Q K V N Q K R H E L E Q S L G V R S N Stop

B)

Wild type

Met H S Q Q R P N P Q Met N R H P Y G T P G S A P Q Met R R P G G F A G Q P P Q Met H G P R Met V A P P A A P L P
K K K K Y A D K C I H P K I R E L E P D A E N Y Met A L L A S E Q K L D S T L S R K K L D I Q E A L K R P S K V K K R L R I Y
I S H T F I E E K Q P E K D T D E A S L P Met W E L R V E G R L L D E Q P P A P A I P G Q R P V P K R K F S S F F K S L V I
E L D K E Met Y G P D Q H L V E W H R T P Q T N E T D G F Q V K R A G D R P V K C R I L L L L L D N H P A K F K L H P R L
A K V L G I A T E T R P K I I E A L W Q Y I K T H G L Q D P Q E R D I I N C D T F L S Q C F G V N R Met R F Met E V P N K L
H Q L L Q Q T D P L E F N H I I Q R P K E G Q E Q V S T C Y D I D V E Met E D P V K Q F Met H T F V H S P G L A N D I Q T
L D Q K C Y D I I E Q I N E L K T R R D F Y A R F Y T E P A E F I K S W V Met S Q N S D L K T Met N E L S G D L E A E R F A
E S Y V R P E T E E G V Q R Y Met F Q K V N Q K R H E L E Q S L G V R S N Stop

tm3395

Met H S Q Q R P N P Q Met N R H P Y G T P G S A P Q Met R R P G G F A G Q P P Q Met H G P R Met V A P P A A P L P
K K K K Y A D K C I H P K V L F R T P Q T N E T D G F Q V K R A G D R P V K C R I L L L L L D N H P A K F K L H P R L A K V L
G I A T E T R P K I I E A L W Q Y I K T H G L Q D P Q E R D I I N C D T F L S Q C F G V N R Met R F Met E V P N K L H Q L L
Q Q T D P L E F N H I I Q R P K E G Q E Q V S T C Y D I D V E Met E D P V K Q F Met H T F V H S P G L A N D I Q T L D Q
K C Y D I I E Q I N E L K T R R D F Y A R F Y T E P A E F I K S W V Met S Q N S D L K T Met N E L S G D L E A E R F A E S Y
V R P E T E E G V Q R Y Met F Q K V N Q K R H E L E Q S L G V R S N Stop

Fig.R.3: Predicted protein sequences encoded by *swsn-2.2* and the mutant alleles *ok3161* and *tm3395*. (A) The truncated protein (91 instead of 449 amino acids) encoded by *ok3161* does not contain the central SWIB/MDM2 domain. Amino acids absent in the mutant protein are indicated in red. Sequences present in the wild type and the mutant protein are marked in yellow. (B) The truncated protein (325 instead of 449 amino acids) encoded by *tm3395* lacks a region of 127 amino acids and instead contains a short sequence (3 amino acids, marked in red) that is not present in the wild type protein. However, since no frameshift occurs, *tm3395* encodes a product containing the central SWIB/MDM2 domain.

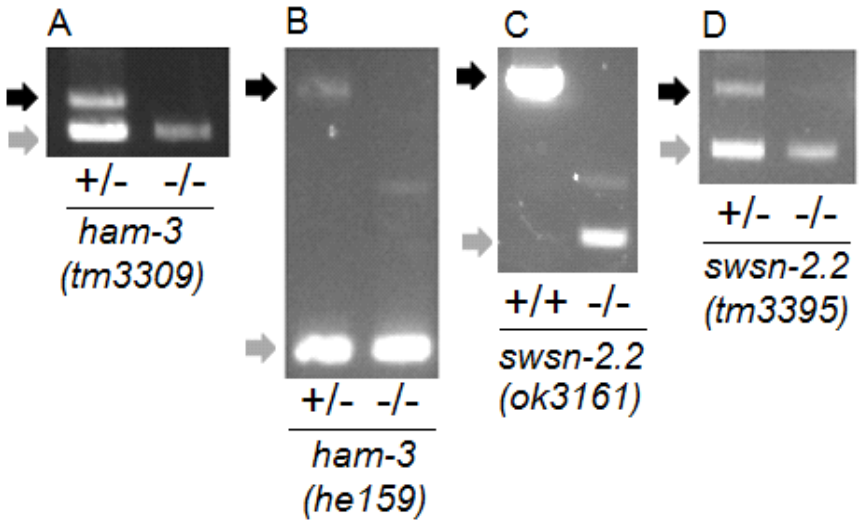

Fig.R.4: Genotyping of the *ham-3* and *swsn-2.2* mutant alleles *tm3309*, *he159*, *ok3161* and *tm3395* (A, B, C and D, respectively). Black arrows indicate bands corresponding to wild type genes, grey arrows the PCR products of mutant alleles.

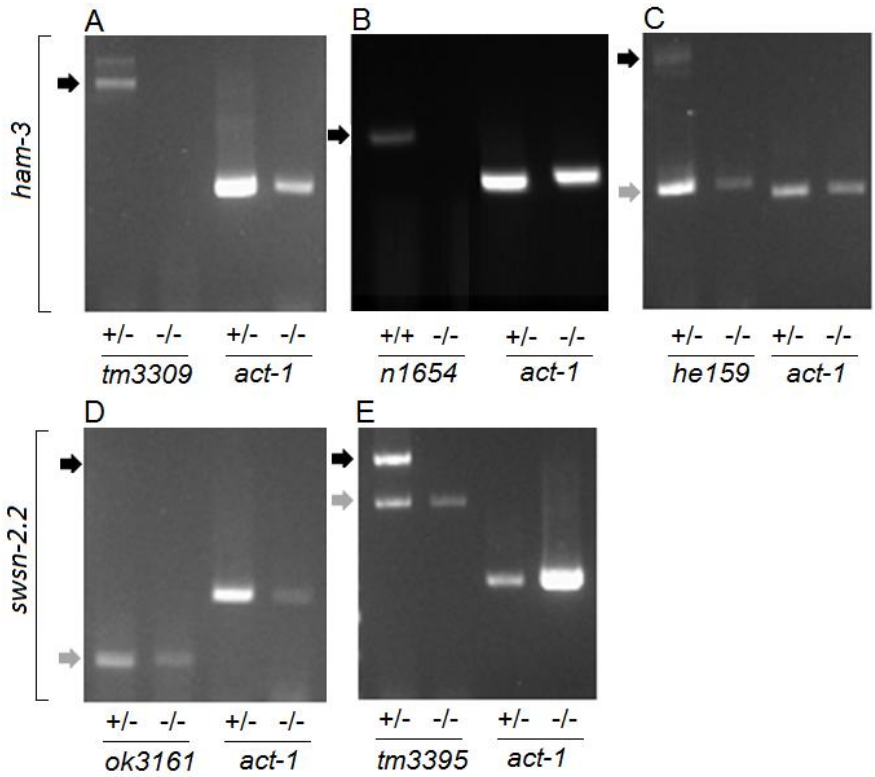

Fig.R.5: cDNA analysis of *ham-3* and *swsn-2.2* mutants. Total RNA isolated from *ham-3* and *swsn-2.2* mutants was reversely transcribed and used for analysis of the respective alleles by PCR. (A,B) *n1654* and *tm3309* give rise to premature stop codons that apparently cause the degradation of the encoded mRNA by the NMD pathway. The bands of the wild type alleles are on different levels, since different reverse primers were used. (C) *he159* encodes a truncated form of HAM-3. (D,E) Both mutant alleles of *swsn-2.2, ok3161* and *tm3395*, give truncated forms of SWSN-2.2. Black arrows indicate wild type bands, grey arrows mutant bands.

R.1.3. Expression of *ham-3* in adult animals

To determine the expression patterns of HAM-3, we generated the transgenic strain CER12 bearing an extrachromosomal array encoding HAM-3::GFP. The red fluorescence protein mCherry was used as transformation marker expressed in muscles and neurons due to the usage of *myo-3* and *rab-3* promoters. Performing confocal microscopy we observed the presence of HAM-3::GFP in the nuclei of various cell types, such as neurons and muscle cells (Fig.R.6). Although HAM-3 is expected to be ubiquitous, we did not find expression in all cells, because of the mosaicism produced by the extrachromosomal array.

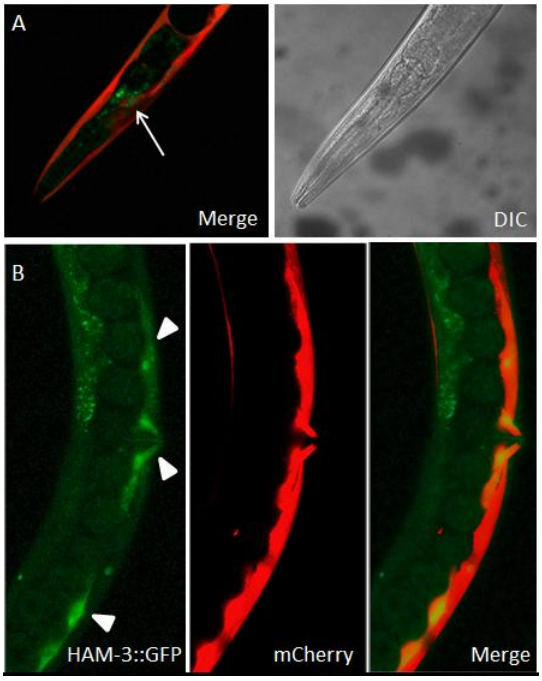

Fig.R.6: HAM-3:GFP localization is observed in the nuclei of various cell types in adult animals. The strain CER12 bearing an extrachromosomal array expressing HAM-3::GFP shows nuclear localization in distinct cell types, such as (A) neurons (arrow) and (B) muscle cells (arrow heads). P*myo-3*::mCherry and P*rab-3*::Cherry were used as transformation markers.

R.1.4. General phenotypic description of *ham-3* and *swsn-2.2* mutant alleles

We observed that *ham-3* and *swsn-2.2* mutants exhibit several obvious phenotypes. All *ham-3* and *swsn-2.2* alleles analyzed in this study cause short body lengths and protrusions of the vulva (Pvl), whereby the penetrance of this phenotype is enhanced with increasing temperature (Fig.R.7; Table R.1). Beyond that, except of *swsn-2.2*(*tm3395),* all studied alleles result in Egg-laying-defects (Egl) (Table R.1). This observation suggests that the truncated SWSN-2.2 protein encoded by the *tm3395* allele conserves at least certain functions.

Mainly, but not only due to the Egl phenotype, *ham-3* and *swsn-2.2* mutants suffer adult lethality at high penetrances (Table R.1). The comparably low ratios of adult lethality of *swsn-2.2*(*tm3395)* animals are therefore explainable by the low penetrance of the Egg-laying-defects.

The only obvious phenotype that is caused by *swsn-2.2*, but not *ham-3* mutant alleles is embryonic lethality (Emb). While the *ham-3* alleles *he159*, *tm3309* and *n1654* show this phenotype at low incidence*, swsn-2.2(ok3161)* homozygotes exhibit embryonic lethality at high penetrances (Fig.R.19). Also in the embryonic context, the effect of *swsn-2.2(tm3395)* is milder than that of the null allele *swsn-2.2(ok3161)*, what is further supporting that the protein encoded by *swsn-2.2(tm3395)* is at least partially functional (Fig.R.19).

To summarize, inferred from the mutant phenotypes we conclude that both genes function in vulva formation, but *ham-3* has a higher impact on processes related to egg-laying. Correlating with the higher penetrance of Egl in *ham-3* mutants, the rates of adult

lethality are higher than in response to *swsn-2.2* loss-of-function. Finally, *swsn-2.2* has a major and distinct role in embryonic development. All these conclusions will be detailed below, in addition to a distinct functional relation with the IIS pathway.

Phenotype	**Pvl (%)**		**Egl (%)**		**Adl (%)**	
Temperature	**15°C**	**25°C**	**15°C**	**25°C**	**15°C**	**25°C**
ham-3(tm3309)* [m+, z-]	100	72,5	100	n.d. (Ste)	87,2	52
***ham-3(n1654)* [m-, z-]**	62,2	80,7	100	100	91,7	100
***ham-3(he159)* [m-, z-]**	59,9	100	100	100	80	90
swsn-2.2(ok3161)* [m+, z-]	89,3	91,6	37,5	45,8	11,1	50
***swsn-2.2(tm3395)* [m-, z-]**	58,7	95	0	6,25	35	35

Table R.1: The penetrances of *ham-3* and *swsn-2.2* mutant phenotypes are temperature-dependent. To determine the penetrance of the Protruding vulva (Pvl) phenotype, homozygote animals were grown at 15°C, gravid mothers dissected and the progeny incubated at the respective temperatures until reaching young adult stage (n≥122). To investigate Egg-laying-defects (Egl), homozygote animals were grown at 15°C until reaching L4 stage, singled out and incubated at the indicated temperatures. Mothers that accumulated embryos and/or died due to the Bag of worms (Bag) or Rupturing vulva (Rup) phenotypes were regarded as Egl (n≥30). Animals that died within 72h or 96h (at 25°C or 15°C, respectively) were scored as adult lethal (Adl).
* Apart from *swsn-2.2(ok3161)* and *ham-3(tm3309),* all animals derived from homozygote mothers. [m+ or m−] indicates maternal, [z+ or z−] zygotic contribution of the respective wild type protein.

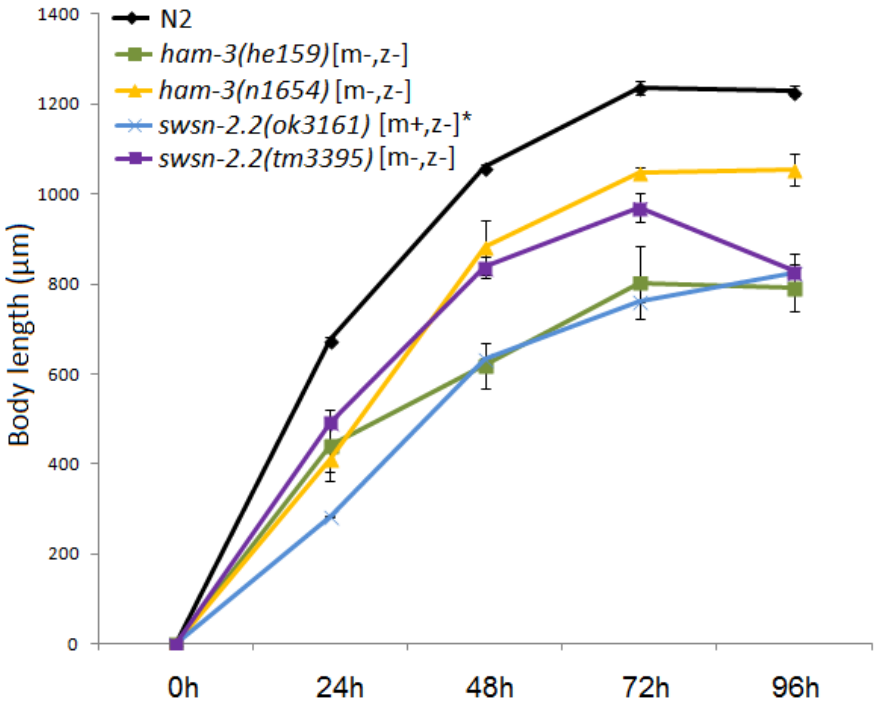

Fig.R.7: *ham-3* and *swsn-2.2* mutants are smaller than wild type worms. Synchronized wild type (N2) and mutant populations were seeded on NGM plates, incubated at 25°C and their body length measured every 24h using the NIS Elements D3.2 software (n≥100).
* Apart from *swsn-2.2(ok3161)*, all animals derived from homozygote mothers. Error bars indicate the standard deviations of the body length between individuals.

R.2. *ham-3* and *swsn-2.2* function in germline development

R.2.1. *ham-3* and *swsn-2.2* mutant alleles reduce the size of the gonad and affect the brood size

In order to investigate the effects of *ham-3* and *swsn-2.2* loss-of-function mutations on fertility, we quantified brood sizes at various temperatures.

We observed that the progeny of all mutants was significantly reduced in a temperature-dependent manner (Fig.R.8). However, since all these alleles, especially the *ham-3* loss-of-function mutations, cause Egg-laying-defects, the animals die before ending their reproductive phase (Table R.1). The small number of larvae produced by *swsn-2.2* mutants is mainly caused by high rates of embryonic lethality (Fig.R.19). Thus, the number of the F1 animals of the studied mutant alleles does not accurately reflect the fertility of the worms in terms of the capacity to produce oocytes/embryos. Still, the negative impact of these mutations on fertility is evident.

To investigate the effects of *ham-3* and *swsn-2.2* loss-of-function mutations on the germline, we performed gonad dissections and DAPI staining. We observed that the gonads of the mutant animals were smaller than in wild types, but that all types of germ cells were present (Fig.R.9).

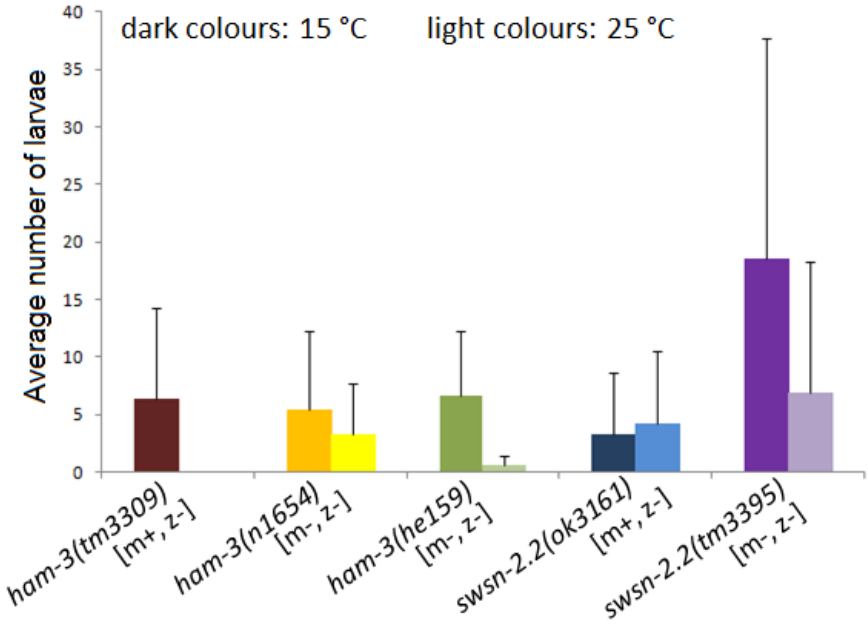

Fig.R.8: *ham-3* and *swsn-2.2* mutants show reduced brood sizes. Homozygote animals (F1) coming from homozygote mothers (P0) [except of homozygote *swsn-2.2(ok3161)* and *ham-3(tm3309)* mutants (F1) coming from heterozygote mothers (P0)] were grown at 15°C until reaching L4 stage, singled out and incubated at 15°C or 25°C (n≥24). Until the end of their reproductive phase, the animals were transferred to new NGM plates every 24h and the number of larvae (F2) determined. In the case of animals dying due to Egl, the number of larvae coming out of the mother's corpse was counted. Normally, wild type (N2) hermaphrodites produce 300-350 larvae (Riddle et al., 1997).
Error bars indicate the standard deviation in the brood sizes of individuals determined in two individual experiments.

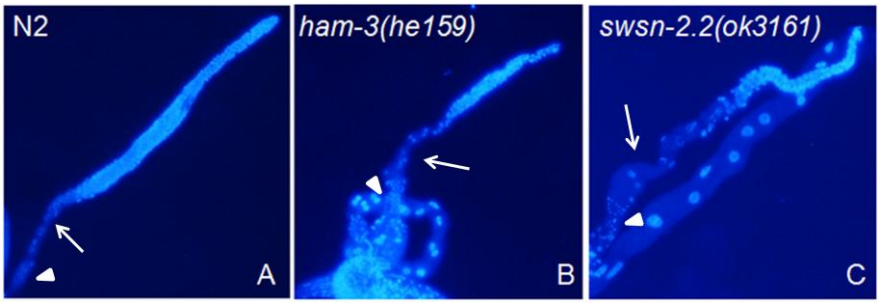

Fig.R.9: The gonads of *ham-3* and *swsn-2.2* mutants are smaller than wild type gonads. Synchronized populations of wild type (N2) or mutant animals were seeded on NGM plates and incubated at 20°C. After 60h (approximately 1 day after reaching adult stage) the germlines were dissected. (A) Wild type (N2) gonad. (B,C) *ham-3* and *swsn-2.2* loss-of-function mutants show smaller gonads, but all types of germ cells are present. Arrows mark oocytes, arrow heads indicate sperm. *swsn-2.2(ok3161)* animals came from heterozygote mothers.

R.2.2. Double RNAi of *ham-3* and *swsn-2.2* results in sterility

To investigate whether *ham-3* and *swsn-2.2* act redundantly in germline development, we performed individual and double RNAi of the two genes in a wild type background. The efficiency and specificity of the RNAi was confirmed by Reverse-Transcription PCR using cDNA of animals fed with the respective RNAi clones as template (Fig.R.10).

Concurrent with the phenotype of the mutants, we observed reduced brood sizes in response to *ham-3(RNAi)* or *swsn-2.2(RNAi)* compared to the control (Fig.R.11).

However, similar to the *ham-3* mutant alleles, *ham-3(RNAi)* causes Egg-laying-defects (Egl) resulting in lethality during the reproductive phase due to larvae that hatch inside the maternal body (Bag) at high penetrances (Table R.1; Fig.R.12). Thus, the reduced brood size reflects the effect of *ham-3(RNAi)* on vulva functionality in addition to their impact on fertility.

Interestingly, double RNAi of *ham-3* and *swsn-2.2* caused complete sterility due the incapacity of the animals to produce eggs (Fig.R.11). We performed DAPI staining of whole worms and dissected gonads and observed that the germlines of these animals were reduced in size (Fig.R.13A). Despite of these effects, each studied gonad arm showed the characteristic regions found in wild type germlines and produced oocytes. However, instead of being fertilized, the oocytes were found to undergo endomitotic replication in the gonad arm (Emo), causing the sterility of the animals (Fig.R.13).

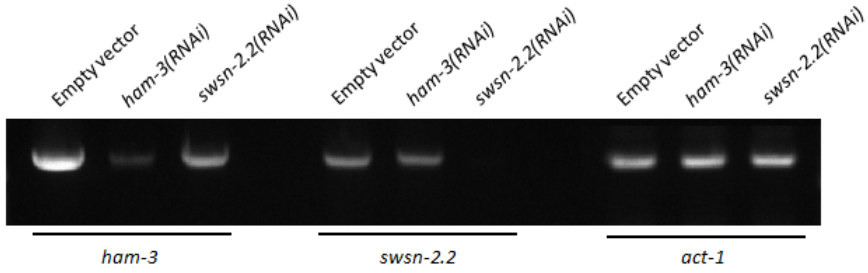

Fig.R.10: Reverse-Transcription PCR confirming specificity of *ham-3(RNAi)* and *swsn-2.2(RNAi)*. Feeding with *ham-3(RNAi)* or *swsn-2.2 (RNAi)* causes reduced levels of the respective transcript, while not affecting the levels of the corresponding paralog.

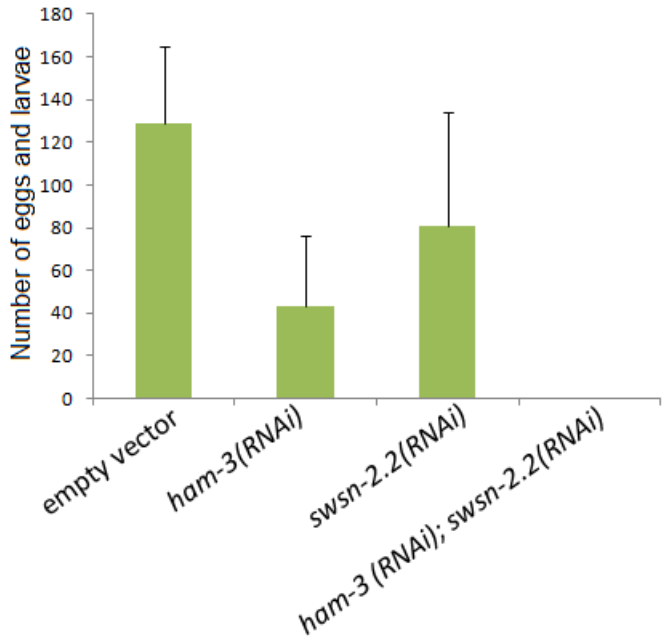

Fig.R.11: RNAi of *ham-3* or *swsn-2.2* causes reduced brood sizes, while double RNAi results in sterility. Animals were grown on the respective RNAi clones or a control at 25°C until reaching L4 stage, singled out and incubated at 25°C. Until the end of their reproductive phase, the animals were transferred to new NGM plates every 24h and the number of larvae determined (n≥24). In the case of animals dying due to Egl, the number of larvae coming out of the mother's corpse was counted. Error bars indicate the standard deviations in the brood sizes of individuals determined in two independent experiments.

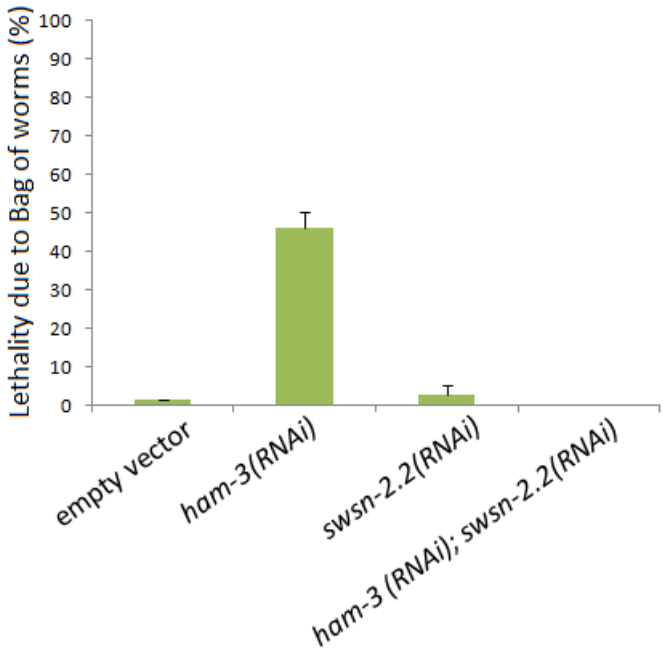

Fig.R.12: RNAi of *ham-3* and *swsn-2.2* causes lethality due to Egg-laying-defects. N2 were fed with the respective RNAi clones for 72h after L1 stage at 25°C. The numbers of animals that had died due to formation of Bag of worms (Bag) were determined under the dissection microscope (n≥337). The penetrance of the Bag phenotype is higher in response to *ham-3(RNAi)* compared to *swsn-2.2(RNAi).* Due to their incapacity to produce embryos, animals treated with *ham-3(RNAi)* and *swsn-2.2(RNAi)* in parallel do not exhibit the Bag phenotype. Error bars indicate the standard deviation between three independent experiments.

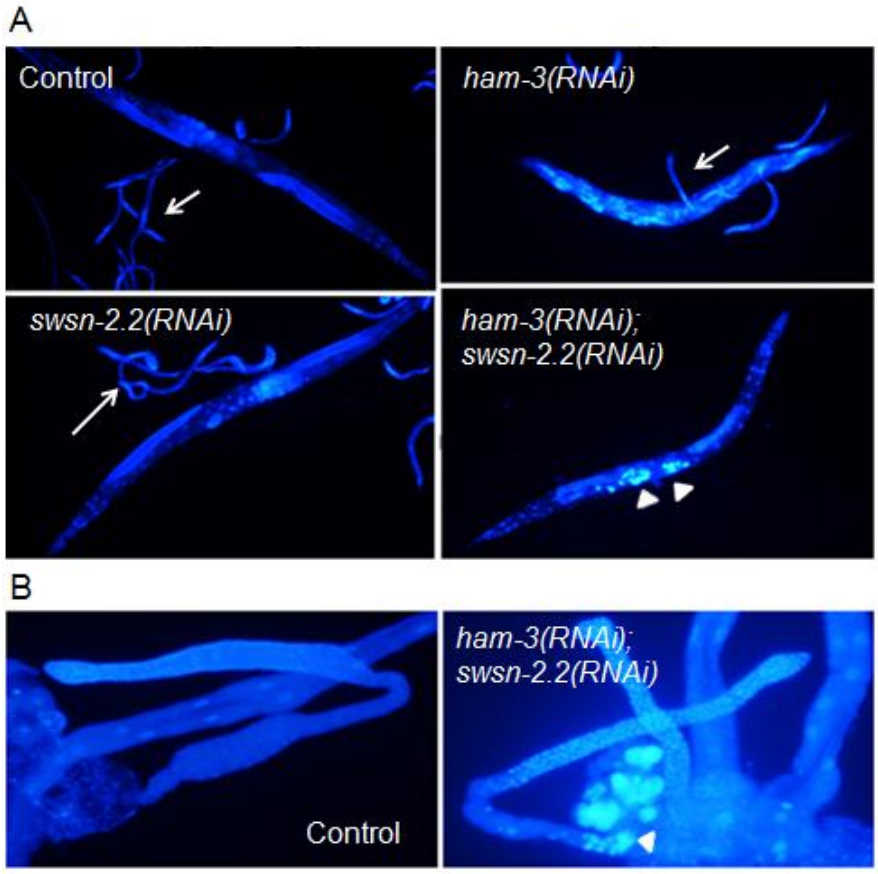

Fig.R.13: Double RNAi of *ham-3* and *swsn-2.2* causes synthetic sterility. Synchronized wild type (N2) animals were grown on the respective RNAi clones or a control at 25°C. (A) Whole worms. (B) Dissected gonads. In contrast to single RNAi of *ham-3* and *swsn-2.2*, double RNAi results in sterility due to the incapacity of the animals to produce embryos. Endomitotic oocytes accumulate in the gonad arms. F1 larvae are indicated by arrows, endomitotic oocytes by arrow heads.

R.2.3. *ham-3* and *swsn-2.2* are involved in germline proliferation

As mentioned above, the size of the gonads was reduced in *ham-3* and *swsn-2.2* mutants, as well as in animals treated with double RNAi of *ham-3* and *swsn-2.2*.

To investigate, whether HAM-3 and SWSN-2.2 might be involved in germ cell proliferation, we performed single and double RNAi in a *glp-1* gain-of-function background.

Germline proliferation is controlled by an inductive signal from the distal tip cells (DTCs) that is transduced by a member of the Notch family of transmembrane receptors, GLP-1 (Hubbard, 2007). With increasing distance to the DTCs, the influence of their proliferative signals decreases and the germ cells enter meiosis (Hansen, Hubbard & Schedl, 2004). Animals bearing strong *glp-1* gain-of-function alleles, e.g. *glp-1(oz264)*, develop a tumorous germline consisting of proliferative cells only, since the germ cells fail to exit mitosis.

To avoid a distortion of the results by effects of the RNAi on somatic tissues, we employed a strain combining the *glp-1(oz264)* gain-of-function mutation with the *rrf-1(pk1417)* loss-of-function allele. Due to this mutation RNAi is inefficient in somatic tissues (Kumsta & Hansen, 2012).

We observed that single, and especially double RNAi of *ham-3* and *swsn-2.2* in the *glp-1*(gf) background caused a reduction of the gonad size (Fig.R.14). However, in none of the studied animals we found meiotic cells or even functional germlines (Fig.R.14).

Regarding the negative effect of RNAi of *ham-3*, *swsn-2.2* and especially double RNAi on proliferation, we must conclude that the two genes have a direct effect on the cell cycle of germ cells and act redundantly.

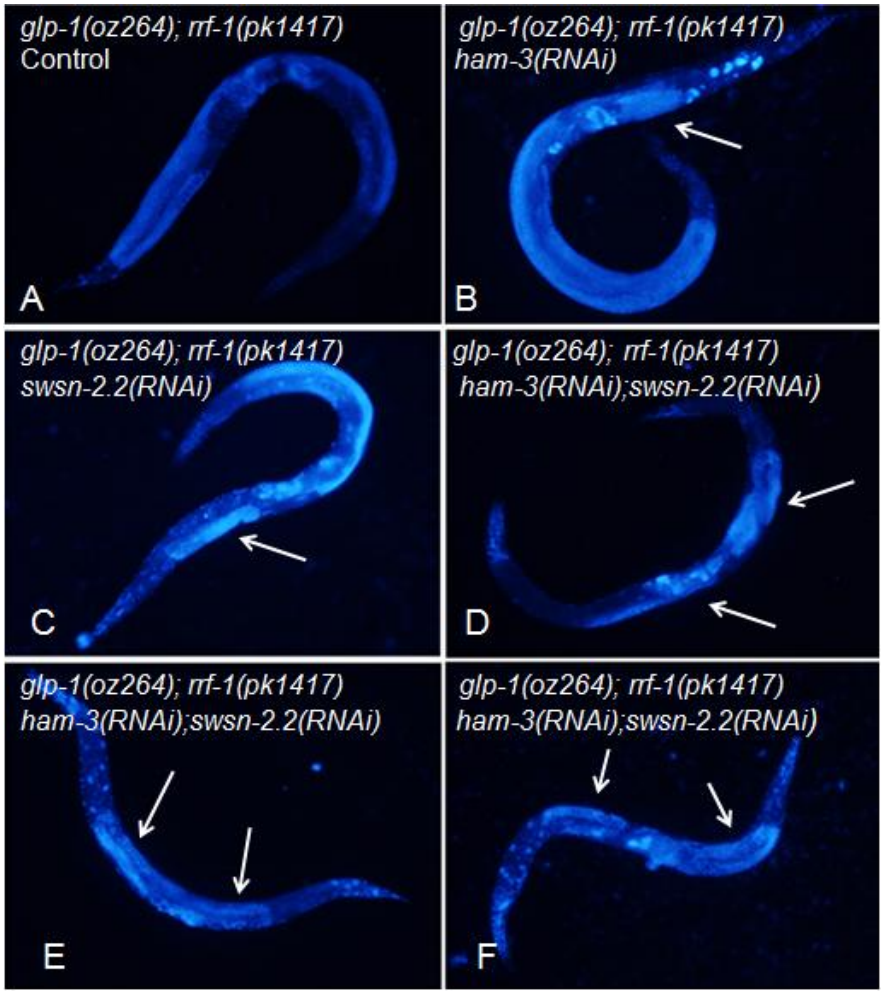

Fig.R.14: RNAi of *ham-3*, *swsn-2.2* or both genes affects the gonad size of *glp-1* gain-of-function mutants. Synchronized populations of *glp-1(oz264)* animals were seeded on the respective RNAi plates or a control and incubated at 25°C. After 72h the germlines were observed (n≥40). (A) Control. (B-F) Individual or double RNAi of *ham-3* and *swsn-2.2* causes a reduction of the gonad size. Arrows indicate reduced germlines.

R.2.4. *ham-3* and *swsn-2.2* control redundantly the number of the distal tip cells

ham-3 and *swsn-2.2* loss-of-function results in gonadogenesis defects that are related to abnormalities in the development of the somatic gonad (Large & Mathies, 2014).

The morphology of the gonad is determined by the distal tip cells leading gonad arm elongation during germline development (Wong & Schwarzbauer, 2012). We therefore wondered whether the two genes may be involved in the development of the DTCs. To address this question, we employed a strain bearing a *lag-2::gfp* reporter that fluorescently marks the distal tips cells.

We observed that simultaneous RNAi of *ham-3* and *swsn-2.2* resulted in the loss of one DTC at high penetrances, while single RNAi did not have any effect (Fig.R.15)

Thus, we conclude that *ham-3* and *swsn-2.2* redundantly control the development of the DTCs.

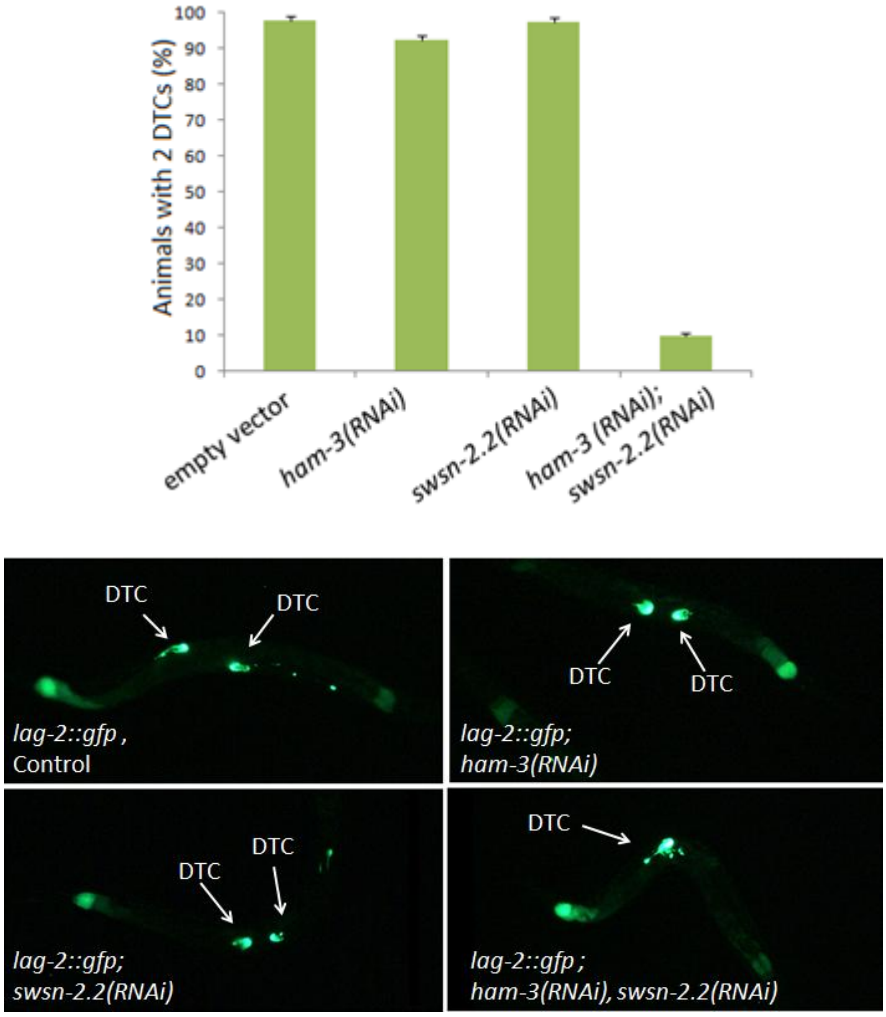

Fig.R.15: Double inactivation of *ham-3* and *swsn-2.2* by RNAi affects the development of the distal tip cells. Synchronized populations of animals expressing LAG-2::GFP were seeded on the respective RNAi plates or a control and incubated at 25°C. After 36h the number of DTCs was determined (n≥50). While *ham-3(RNAi)* and *swsn-2.2(RNAi)* did not show an effect, double RNAi of both genes causes loss of one DTC.

R.3. *ham-3* and *swsn-2.2* are involved in vulval development

R.3.1. *ham-3* and *swsn-2.2* act redundantly in vulval development

The development of the six vulval precursor cells to make an adult vulva requires a complex regulatory network including distinct signaling cascades, such as Notch, Wnt and *let-60*/Ras pathways. Deregulation of components of these pathways results in vulva phenotypes like Egg-laying-defects (Egl), Protruding vulva (Pvl), Vulvaless (Vul) or Multivulva (Muv) (Ferguson & Horvitz, 1985; Trent, Tsuing & Horvitz, 1983; Eisenmann & Kim, 2000; Seydoux, Savage & Greenwald, 1993).

As described in section R.1.4., all studied *ham-3* and *swsn-2.2* alleles cause the Protruding vulva phenotype (Pvl) (Table R.1).

ham-3(RNAi) and *swsn-2.2(RNAi)* in the wild type background phenocopy the Pvl phenotype of *ham-3* and *swsn-2.2* loss-of-function alleles, whereby at low penetrances (Fig.R.16).

Interestingly, simultaneous RNAi of *ham-3* and *swsn-2.2* results in a synthetic interaction that produces the Pvl phenotype in almost 100% of the animals, implicating redundant functions of the two proteins in this context (Fig.R.16).

To support this hypothesis, we performed *ham-3(RNAi)* in a *swsn-2.2* loss-of-function background and *swsn-2.2(RNAi)* in *ham-3* mutants (Fig.16). In all approaches we observed an enhancement of the effect, further supporting the redundancy of *ham-3* and *swsn-2.2* in vulval development.

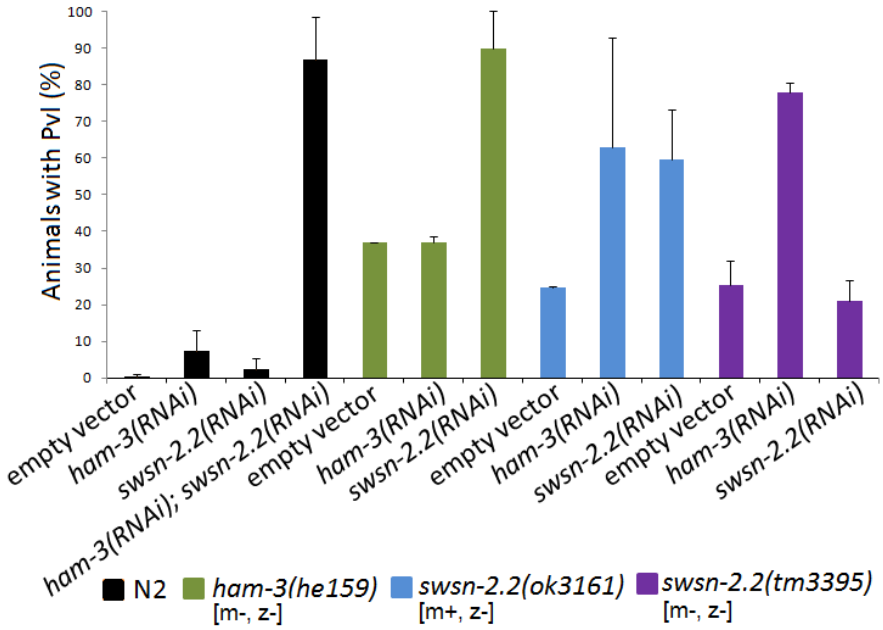

Fig.R.16: *ham-3* and *swsn-2.2* act redundantly in vulval development.
Synchronized population of wild type (N2) or mutant animals were seeded on the respective RNAi plates or a control and incubated at 25°C or 20°C. The numbers of animals showing Pvl was determined in young adult stage (n≥86).
ham-3(RNAi) and *swsn-2.2(RNAi)* caused Pvl at low penetrances in the wild type background. The phenotype was significantly enhanced upon double RNAi of both genes. *ham-3(RNAi)* in a *swsn-2.2* mutant background or *swsn-2.2(RNAi)* in *ham-3* mutants also showed a synergistic effect.
Except of *swsn-2.2(ok3161)*, all studied mutant animals (F1) derived from homozygote mothers (P0). Experiments with wild type animals were performed at 25°C, the experiments with *ham-3* or *swsn-2.2* mutants at 20°C (n≥58). Error bars indicate the standard deviation between two or three independent experiments.

R.3.2. *ham-3* and *swsn-2.2* are involved in the induction of the vulval precursor cells

The Pvl phenotype can be caused by diverse defects in vulval development, e.g. it was observed in mutants with problems in the vulva-uterine connection (Sternberg, 2005).

To test whether *ham-3* and *swsn-2.2* are involved particularly in the induction of the vulval precursor cells, we used a sensor strain with loss-of-function mutations in two genes of different synMuv classes. The synMuv (synthetic multivulva) genes encode proteins that negatively regulate the induction of vulval precursor cell fates by the *let-60*/Ras pathway. While mutation of one synMuv gene only does not cause a phenotype, simultaneous mutations in genes of different synMuv classes result in Muv (Ceol et al., 2006; Fay & Yochem, 2007).

ham-3(RNAi) or *swsn-2.2(RNAi)* in the *lin-61(n3447); lin-8(n2731)* background caused an enhancement of the phenotype (Fig.R.17A) Not only the number of animals showing the Muv phenotype was increased, but also the average number of protrusions per animal (Fig.R.17B).

To further support that *ham-3* and *swsn-2.2* inhibit vulva induction, we repeated the experiment in a strain with a *let-60*/Ras gain-of-function mutation resulting in a mild Muv phenotype. As positive control we performed RNAi of *somi-1* and *lin-15A*, which are genes that have previously been shown to be involved in the negative regulation of the *let-60*/Ras pathway (Ceol et al., 2006; Hayes, Riedel & Ruvkun, 2011).

We observed an enhancement of the Muv phenotype in response to *ham-3(RNAi)* and *swsn-2.2(RNAi)*. This enhancement was increased in response to RNAi of both genes (Fig.R.18A). Also in

this case, the average number of protrusions per animals was enhanced (Fig.18B).

Taken together, the results let conclude that *ham-3* and *swsn-2.2* negatively regulate the induction of the vulval precursor cell fates via the *let-60*/Ras pathway, and act redundantly in this task.

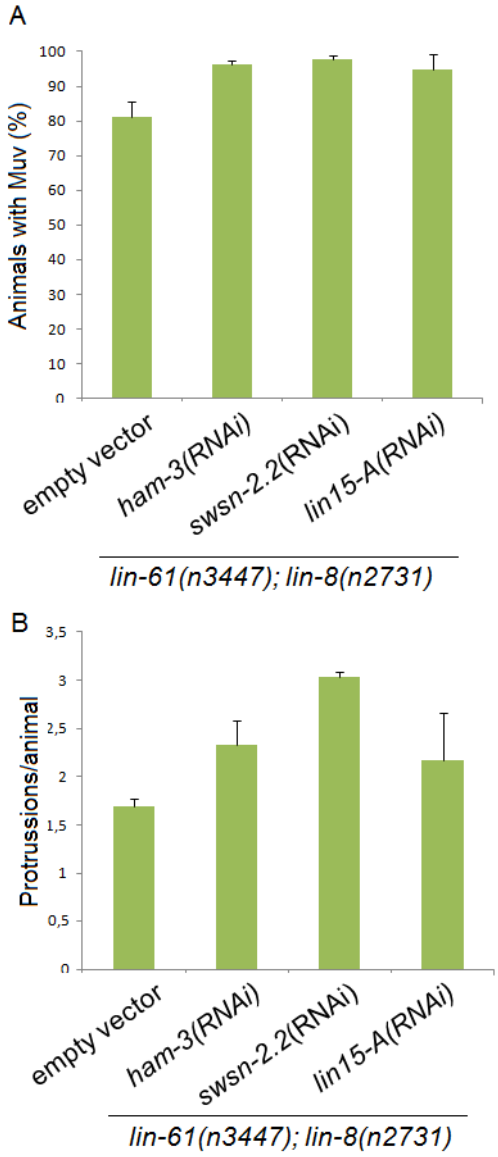

Fig.R.17: *ham-3(RNAi)* and *swsn-2.2(RNAi)* enhance the Muv phenotype of *lin-61(n3447); lin-8(n2731)* mutants. Synchronized L1 larvae were fed with the respective RNAi clones for 48h after L1 stage at 25°C. The vulva phenotype was determined under the dissection microscope (n≥243). *lin-15A(RNAi)* was used as control (Ceol et al., 2006). (A) *ham-3(RNAi)* and *swsn-2.2(RNAi)* enhanced the penetrance of the Muv phenotype. (B) Besides the enhancement of the penetrance, also the average number of protrusions was increased. Error bars indicate the standard deviation between three independent experiments.

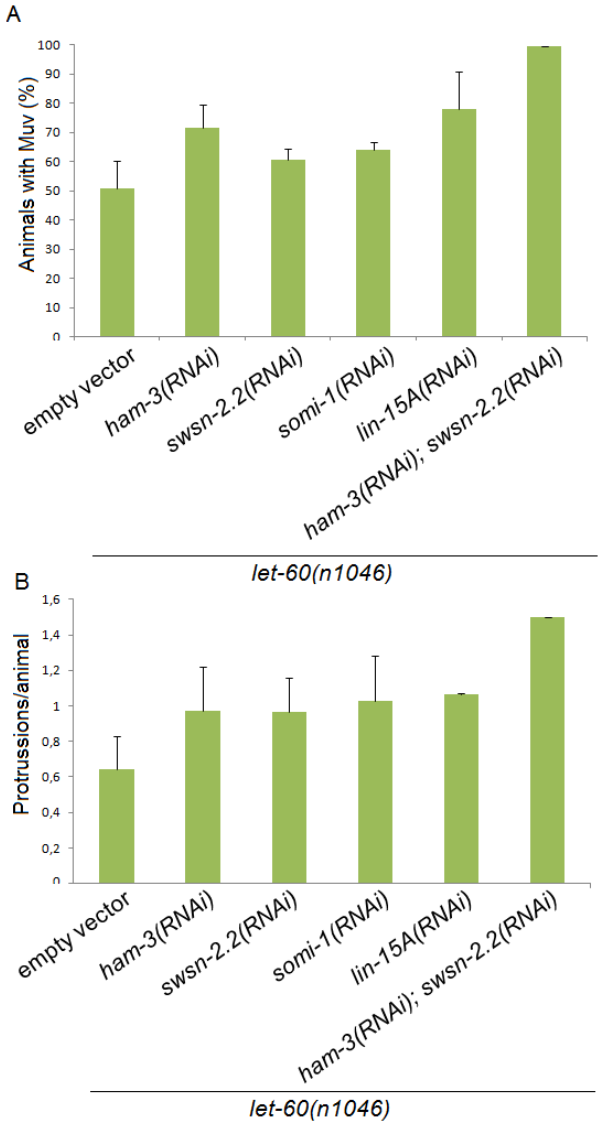

Fig.R.18: *ham-3* and *swsn-2.2* act redundantly in the Ras/*let-60* pathway. Synchronized L1 larvae were fed with the respective RNAi clones for 48h after L1 stage at 25°C. The vulva phenotype was determined under the dissection microscope (n≥169). (A) *ham-3(RNAi)*, *swsn-2.2(RNAi)* and especially double RNAi enhanced the penetrance of the Muv phenotype. (B) Besides the enhancement of the penetrance, also the average number of protrusions was increased. Error bars indicate the standard deviation between two independent experiments. *somi-1(RNAi)* and *lin-15A(RNAi)* served as positive controls (Ceol et al., 2006; Hayes, Riedel & Ruvkun, 2011).

R.4. *ham-3* and *swsn-2.2* have independent and common functions during embryonic development

R.4.1. *swsn-2.2* and *ham-3* mutations have a distinct impact on embryogenesis

All studied *ham-3* mutant alleles cause embryonic lethality at low penetrances (Fig.R.19). *swsn-2.2* loss-of-function in contrast, results in severe defects in embryonic development.

The progeny of animals homozygote for *ok3161,* the putative *swsn-2.2* null allele, suffers embryonic lethality at high penetrances (Fig.R.19). The few escapers die during larval development, what means that without maternal product *swsn-2.2(ok3161)* mutants are not able to reach the adulthood.

The truncated protein encoded by *swsn-2.2(tm3395)* seems to conserve some functions also in this context, since the mutants can be maintained as homozygote population, although the levels of embryonic lethality are high (Fig.R.19).

RNAi of *ham-3* and *swsn-2.2* by feeding has a much lower effect on embryogenesis than the loss-of-function mutations. However, also RNAi approaches revealed a greater impact of loss of *swsn-2.2* than of *ham-3* on embryonic development (Fig.R.20). Thus, the two genes seem to play different roles in embryonic development, whereby the inactivation *of swsn-2.2* causes much more severe effects than loss of *ham-3*.

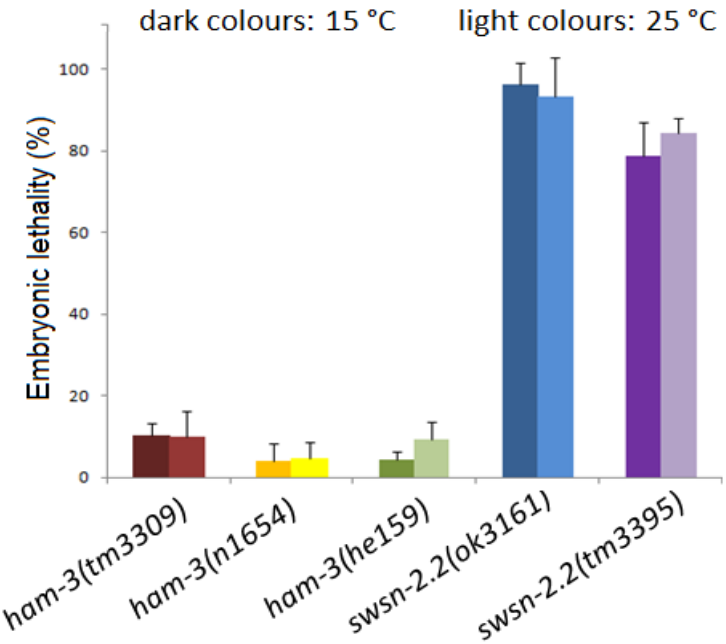

Fig.R.19: In contrast to *ham-3* mutants, *swsn-2.2* mutants show embryonic lethality at high penetrances. Homozygote *ham-3* or *swsn-2.2* mutants were grown at 15°C until reaching adult stage, dissected and the embryos incubated at the indicated temperatures. 24h after dissection, the numbers of eggs unable to hatch were determined (n≥371).
Except of *swsn-2.2(ok3161)* and *ham-3(tm3309)*, the dissected animals derive from homozygote mothers. Error bars indicate the standard deviations between three independent experiments.

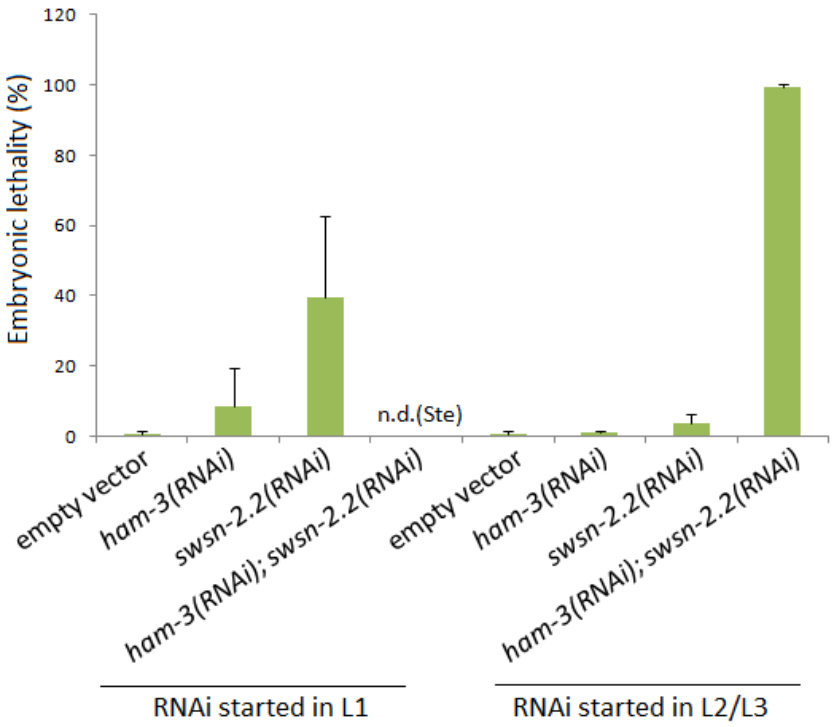

Fig.R.20: RNAi assays uncover functional redundancy of *ham-3* and *swsn-2.2* in embryonic development. *ham-3(RNAi)* and *swsn-2.2(RNAi)* performed according to the standard protocol caused Emb at low penetrances. The effect of simultaneous RNAi of both genes was not determinable, because the animals lose the capacity to produce eggs. When *ham-3(RNAi)* and *swsn-2.2(RNAi)* was started at later developmental stages, animals remained able to generate embryos. Double RNAi of *ham-3* and *swsn-2.2* resulted in Emb at complete penetrance. Error bars indicate the standard deviation between two independent experiments.

R.4.2. *ham-3* and *swsn-2.2* cooperate during processes in embryonic development

In order to study whether *ham-3* and *swsn-2.2* have redundant functions in embryogenesis, both genes in parallel were knocked down by RNAi. Since simultaneous RNAi of *ham-3* and *swsn-2.2* started in L1 stage causes sterility, the protocol had to be modified (Fig.R.20). Feeding was started in later developmental stages

(L2/L3) and the animals indeed remained the capacity to produce embryos. However, the eggs showed embryonic lethality at complete penetrance. These observations strongly implicate that *ham-3* and *swsn-2.2* might cooperate in embryonic development.

R.4.3. *swsn-2.2* is required for early embryonic cell divisions

As mentioned above, *tm3395* encodes a truncated form of SWSN-2.2 that seems to conserve some functions required for embryogenesis (Fig.R.19). In contrast, *ok3161* is a putative *swsn-2.2* null allele that causes Emb at almost complete penetrance (Fig.R.19). Therefore, we chose *ok3161* to further study *swsn-2.2* functions in embryogenesis.

Microscopy showed that *ok3161* embryos present cell division defects in early stages (Fig.R.21). This observation was confirmed by 4-D videorecording and lineage analysis. The studied *ok3161* embryos (n=2) showed severe defects in early embryonic cell divisions causing embryonic lethality (Fig.R.21).

Immunostaining showed the presence of SWSN-2.2 in developing oocytes and early embryos (Fig.R.22).

These observations indicate that *swsn-2.2* functions in the first steps of embryonic development.

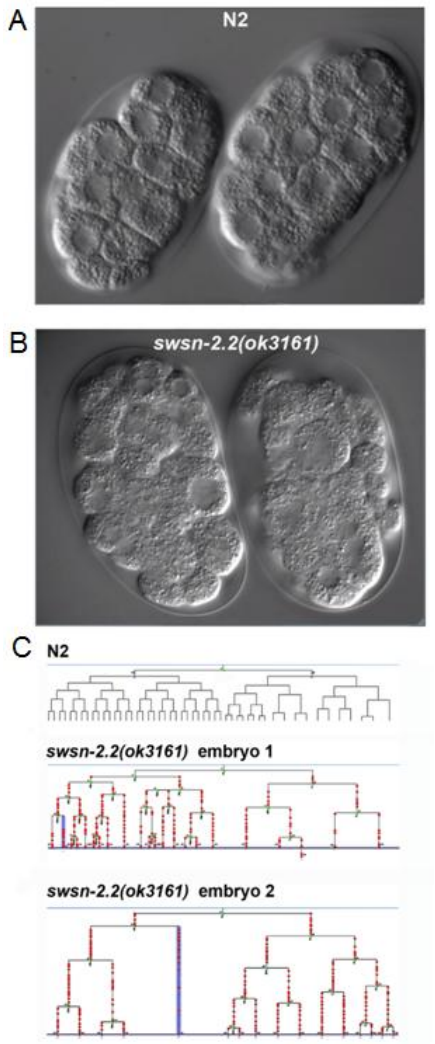

Fig.R.21: *swsn-2.2* mutants present cell division defects in the early embryo. (A) N2 wild type embryos after few rounds of cell division. The size of nuclei in each embryo is uniform (B) Early *swsn-2.2(ok3161)* embryos show nuclei of different sizes, which is indicative of defective cell divisions. (C) Cell lineage analyses for the first cell divisions of N2 wild type and *swsn-2.2(ok3161)* embryos. Green and red spots indicate cell divisions and points of lineage scoring, respectively. The aberrant cell division pattern in *swsn-2.2(ok3161)* embryos hampers the lineage analysis after few divisions and causes the death of the embryos before comma stage.

A

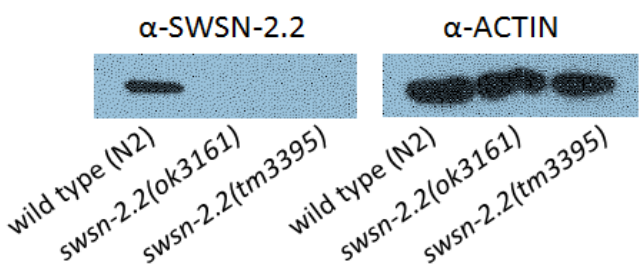

Met H S Q Q R P N P Q **Met** N R H P Y G T P G S A P Q **Met** R R P G G F A G Q P P Q **Met** H G P R **Met** V A P P A A P L P
K K K K Y A D K C I H P K I R E L E P D A E N Y **Met** A L L A S E Q K L D S T L S R K K L D I Q E A L K R P S K V K K R L R I Y I
S H T F I E E K Q P E K D T D E A S L P **Met** W E L R V E G R L L D E Q P P A P A I P G Q R P V P K R K F S S F F K S L V I E L
D K E **Met** Y G P D Q H L V E W H R T P Q T N E T D G F Q V K R A G D R P V K C R I L L L L D N H P A K F K L H P R L A K
V L G I A T E T R P K I I E A L W Q Y I K T H G L Q D P Q E R D I I N C D T F L S Q C F G V N R **Met** R F **Met** E V P N K L H
Q L L Q Q T D P L E F N H I I Q R P K E G Q E Q V S T C Y D I D V E **Met** E D P V K Q F **Met** H T F V H S P G L A N D I Q T L
D Q K C Y D I I E Q I N E L K T R R D F Y A R F Y T E P A E F I K S W V **Met** S Q N S D L K T **Met** N E L S G D L E A E R F A E
S Y V R P E T E E G V Q R Y **Met** F Q K V N Q K R H E L E Q S L G V R S N

B

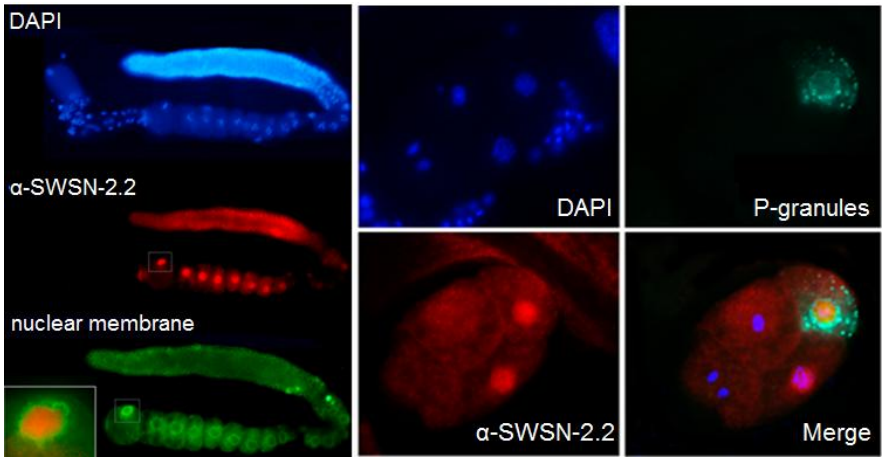

Fig.R.22: Immunostaining of SWSN-2.2 in the germline and early embryos. (A) Test on specificity of the α-SWSN-2.2 antibody by Western blotting. The sequence that is recognized by the antibody (amino acids 1-89; marked in yellow) is (partially) absent in the truncated proteins encoded by *swsn-2.2(ok3161)* and *swsn-2.2(tm3395)*. Protein extracts of both mutant strains were therefore used as control. (B) Immunostaining using the α-SWSN-2.2 antibody showed the presence of SWSN-2.2 in the nuclei of developing oocytes and early embryos. As control, the antibodies KT23 or OICD14 (markers for the nuclear membrane or P-granules, respectively) were used. In both cases the nature of the antigen is unknown. These samples were studied under a conventional fluorescence microscope and not by confocal microscopy.

R.4.4. *ham-3* regulates the cell number in the E lineage and processes driven by the Wnt pathway

Similarly to *swsn-2.2(ok3161)*, *ham-3(he159)* encodes a truncated form of the wild type protein lacking the central SWIB domain. In that sense, the two alleles are comparable and therefore lineage analysis was performed with *ham-3(he159)* embryos.

The most penetrant effect of *ham-3* loss-of-function is the overproliferation of the embryonic intestinal cells (Fig.R.23A). This phenotype was validated in *ham-3(n1654)* mutants and will be described more detailed in section R.5.1.

Moreover, we observed defects in the orientation of the mitotic spindle in one of the studied embryos (n=12) (Fig.R.23B). In wild-type embryos in 8-cell stage four descendents of the AB blastomere are present (Draper et al., 1996). While the spindles of three of these cells (ABal, ABpl and BApr) are aligned in parallel, the spindle of the fourth cell (ABar) is orientated perpendicular to the others (Rocheleau et al., 1997). In the *ham-3(he159)* embryo this perpendicular orientation was not given, but all four spindles found to be orientated in parallel (Fig.R.23B).

We also found that the engulfment of the apoptotic bodies in *ham(he159)* mutants was retarded, resembling a phenotype observed in mutants of the Wnt signaling pathway (Fig.R.23C) (Cabello et al., 2010). Interestingly, also the correct polarization of the ABar blastomere is regulated by Wnt signaling (Walston et al., 2004; Goméz-Orte et al., 2013).

Thus, we conclude that *ham-3* is required for the control of the number of intestinal cells and the regulation of developmental processes driven by the Wnt pathway.

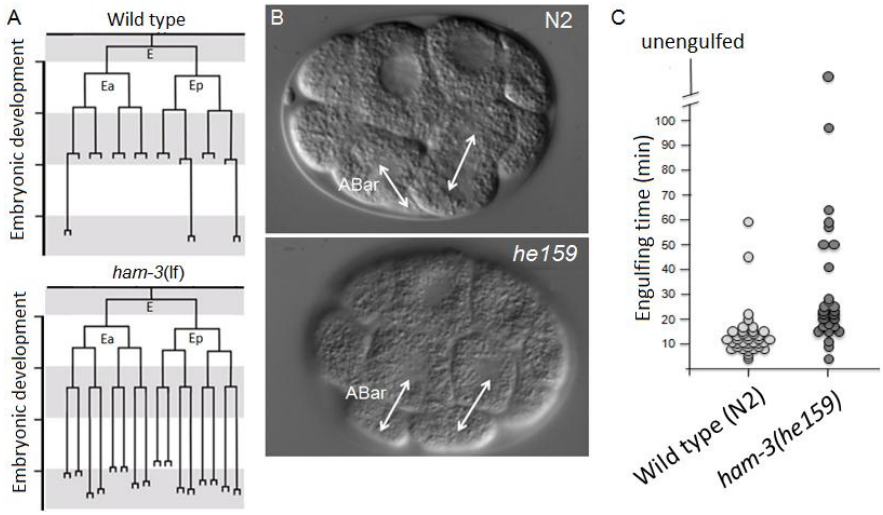

Fig.R.23: *ham-3* loss-of-function causes various embryonic phenotypes. (A) *ham-3(he159)* and *ham-3(n1654)* cause additional cell divisions in the E lineage. (B) *ham-3(he159)* embryos exhibit defects in the orientation of the mitotic spindle. (C) *ham-3(he159)* embryos show retarded engulfment of apoptotic bodies.

R.5. *ham-3* and *swsn-2.2* control intestinal cell proliferation

R.5.1. Lineage analysis of *ham-3* mutants

As mentioned above, lineage analysis of *ham-3(he159)* embryos showed that *ham-3* loss-of-function causes intestinal hyperplasia. All recorded embryos (n=12) showed extra cell division in the E lineage, whereby the intestinal cell number upon hatching varied between different mutants (Fig.R.24B-D).

To conform that this phenotype is caused due to *ham-3* loss-of-function and not to an altered function of the truncated protein encoded by *ham-3*(*he159)*, lineage analysis was repeated with *ham-3(n1654)* embryos. Similar to *ham-3(he159),* also the putative *ham-3* null allele *n1654* caused extra divisions of various cells of the E lineage at full penetrance (n=3) (Fig.R.24E-F).

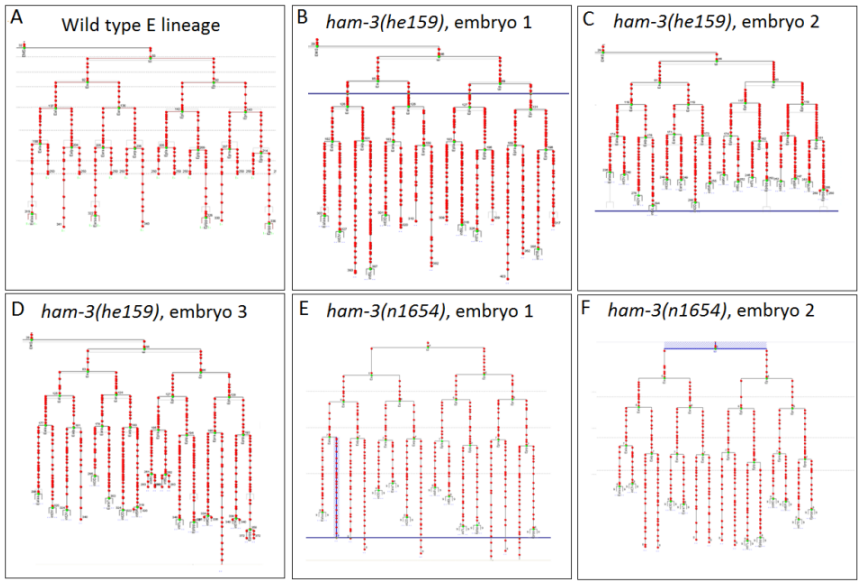

Fig.R.24: Embryonic E lineage of *ham-3* mutants. (A) E lineage of a wild type embryo. (B-D) E lineage of three different *ham-3(he159)* embryos showing extra cell divisions. (E-F) E lineage of two different *n1654* embryos with additional intestinal nuclei. Green and red spots indicate cell divisions and points of lineage scoring, respectively.

R.5.2. *ham-3 and swsn-2.2* loss-of-function mutations have a similar effect on the number of intestinal nuclei

In order to determine the influence of *swsn-2.2* on the number of intestinal nuclei, the strain CER31 combining the *swsn-2.2(ok3161)* allele and an *elt-2::gfp* reporter was created. The *elt-2* promoter provides GFP expression in the intestinal nuclei only and enables to count their number accurately. Homozygote *swsn-2.2(ok3161)* larvae from heterozygote mothers showed upon hatching an increased number of intestinal nuclei compared to wild type animals with the *elt-2::gfp* construct (Fig.R.25).

To confirm the results of the lineage analysis regarding *ham-3* function on intestinal cell cycle regulation, the strain CER30

bearing the *ham-3(he159)* allele and an *elt-2::gfp* reporter was created. Homozygote animals coming from heterozygote mothers showed a significant increase of the number of intestinal nuclei compared to control animals (Fig.R.25).

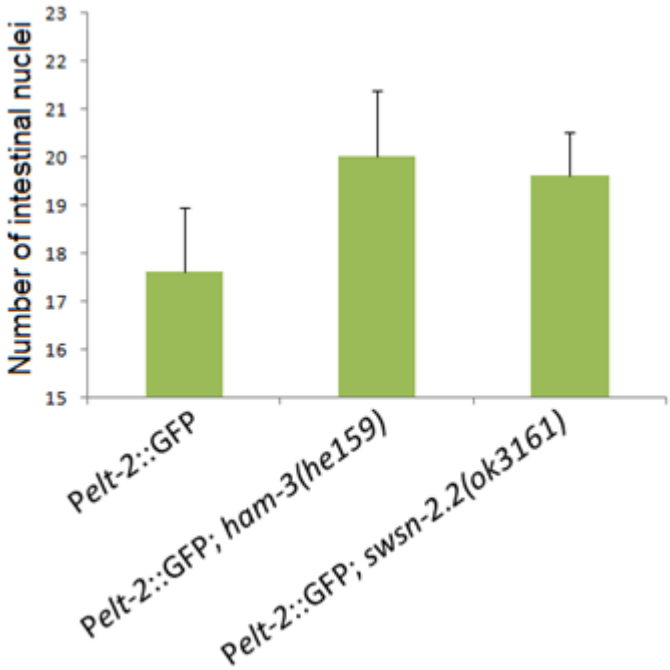

Fig.R.25: Number of intestinal nuclei of *ham-3* and *swsn-2.2* mutants at hatching. The number of intestinal nuclei of homozygote *ham-3(he159)* and *swsn-2.2(ok3161)* mutants bearing an *elt-2::gfp* construct was determined under the fluorescence microscope in L1 larvae (n≥45). In both cases the animals came from heterozygote mothers. An increase of the number of intestinal nuclei in response to loss-of-function of *ham-3* and *swsn-2.2* was observed. Error bars indicate the standard deviations between three independent experiments.

R.5.3. *ham-3* and *swsn-2.2* function in the regulation of the intestinal cell cycle in postembryonic stages

In order to examine whether *ham-3* and *swsn-2.2* have functions in the regulation of the intestinal cell cycle in postembryonic stages, RNAi of *ham-3*, *swsn-2.2* and both genes in parallel was performed in wild type worms carrying the *elt-2::gfp* reporter. Individual knock-down of the two genes caused a significant increase of the number of intestinal nuclei (Fig.R.26). Simultaneous inactivation of *ham-3* and *swsn-2.2* caused an enhancement of the effect (Fig.R.26). This result lets suggest that the two proteins cooperate in this context.
To further confirm this, *swsn-2.2(RNAi)* was performed in *ham-3(he159)* mutants. Also in this approach an increase of the number of intestinal nuclei was observed upon simultaneous inactivation of both genes (Fig.R.26).

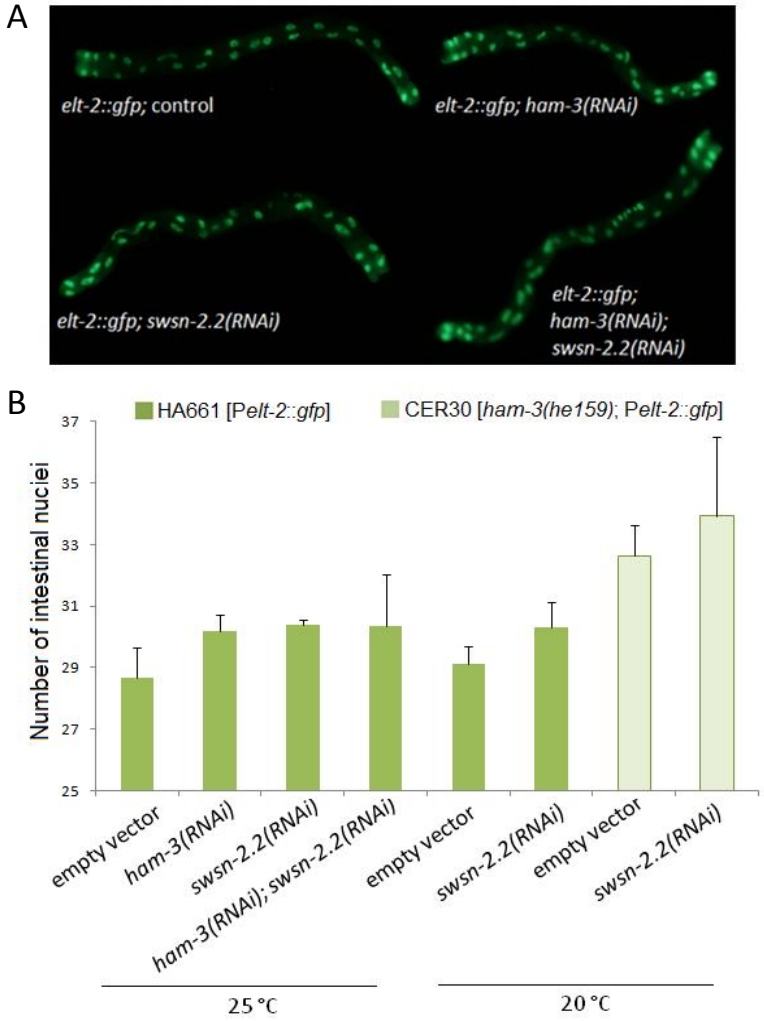

Fig.R.26: *ham-3* and *swsn-2.2* have redundant functions in intestinal cell cycle regulation. RNAi of *ham-3, swsn-2.2* and both genes was performed in wild type animals bearing an *elt-2::gfp* construct at 25 °C. (A) The number of GFP-marked intestinal nuclei was determined in L4 stage under a fluorescence microscope (n<50). (B) *ham-3(RNAi)* and *swns-2.2(RNAi)* caused an increase of the average number of intestinal nuclei and the effect was enhanced upon RNAi of both genes in parallel. To confirm this result, RNAi of *swsn-2.2* was performed in the *ham-3(he159)* mutant background. Due to the sickness of the mutants on high temperatures, the experiment was performed at 20°C. In late L4 stage the number of GFP-marked intestinal nuclei was determined (n<43). Error bars indicate the standard deviation between two independent experiments performed in biological triplicates.

R.5.4. *ham-3* acts downstream *cyd-1* in cell cycle control

The intestinal cell number has shown to be regulated by two distinct signaling cascades, the *cki-1* and the *lin-35* pathways. In both cases the inhibitory signals are repressed by CYD-1/CDK4 complexes, thereby providing proliferation (Boxem & van den Heuvel, 2001).

To further study *ham-3* functions, RNAi by injection was employed. The *cyd-1(he116)* loss-of-function allele results in a reduced number of intestinal cells. Loss of components acting downstream *cyd-1* should rescue this phenotype. Indeed, *ham-3(RNAi)* caused an increase of the intestinal nuclei compared to untreated *cyd-1(he116)* mutants (Fig.R.27)

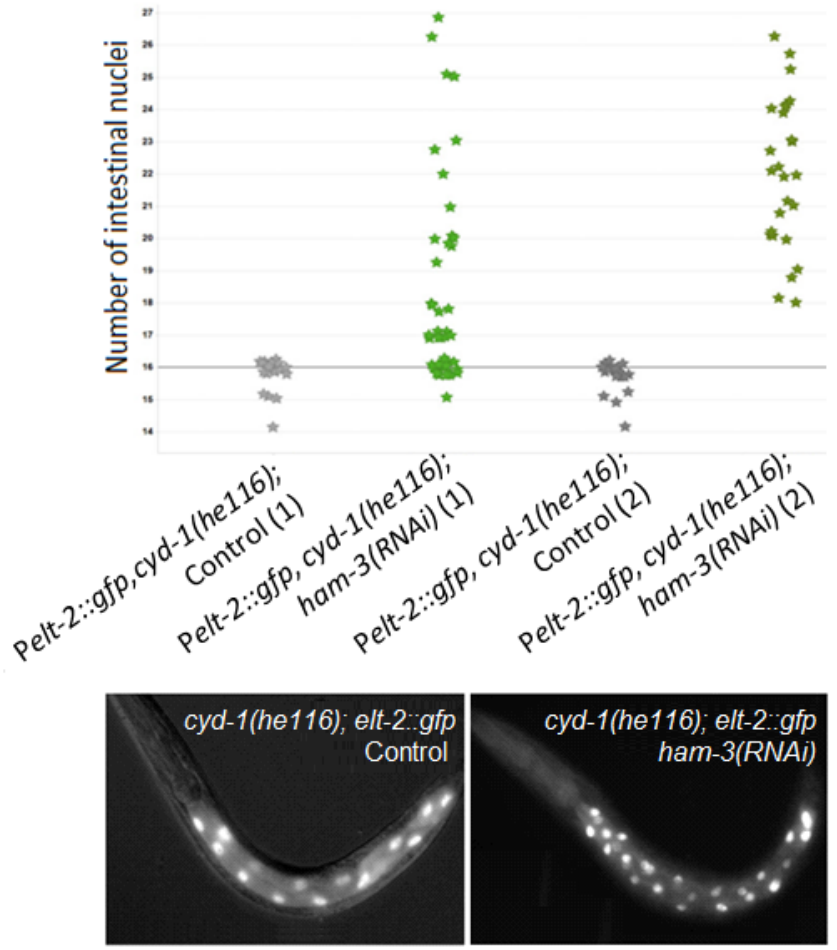

Fig.R.27: *ham-3(RNAi)* partially rescues the intestinal phenotype caused by a *cyd-1* loss-of-function mutation. *cyd-1(he116)* mutants were injected with *ham-3* dsRNA in two independent experiments. Inactivation of *ham-3* resulted in a partial rescue of the intestinal phenotype of F1 animals.

R.6. *swsn-2.2* and *ham-3* are involved in the IIS pathway

R.6.1. Expression of *ham-3* and *swsn-2.2* throughout development

In order to study the expression of *ham-3* and *swsn-2.2* throughout development, we synchronized populations of wild type animals and harvested fractions in all larval stages. Reverse-Transcription PCR was performed with cDNA from these populations and we observed that both genes are expressed in all developmental stages, but not in arrested L1 (Fig.R.28A,B). To verify this, qPCR was performed with cDNA of L1 that had either been starved or fed after hatching, and we observed downregulation of *ham-3* and *swsn-2.2* in response to starvation (Fig.R.28C). Interestingly, *ham-3* and *swsn-2.2* expression was also found to be significantly down-regulated in dauer animals (Fig.R.29A).

L1 arrest and dauer stage are regulated by the FOXO transcription factor DAF-16 that is activated in response to stress conditions, e.g. starvation. Lack of food causes the inactivation of the insulin receptor DAF-2 and thereby the activation of DAF-16, which consequently translocates to the nucleus, where it induces the expression of its target genes (Barbieri et al., 2003; Baugh & Sternberg, 2006).

We performed Reverse-Transcription PCR and qPCR with cDNA coming from temperature-sensitive *daf-2(e1370)* mutants grown under permissive (15°C) and non-permissive (25°C) conditions. Due to loss-of-function of *daf-2* on high temperatures, DAF-16 is active and the animals consequently in dauer stage (Baugh & Sternberg, 2006). We observed in both, Reverse-Transcription PCR and qPCR, that in the mutants grown under non-permissive

conditions *ham-3* and *swsn-2.2* expression was significantly down-regulated (Fig.R.29B,C).

In summary, these results show that *ham-3* and *swsn-2.2* are expressed throughout all developmental stages, but are down-regulated in response to low insulin/IGF-1 signaling.

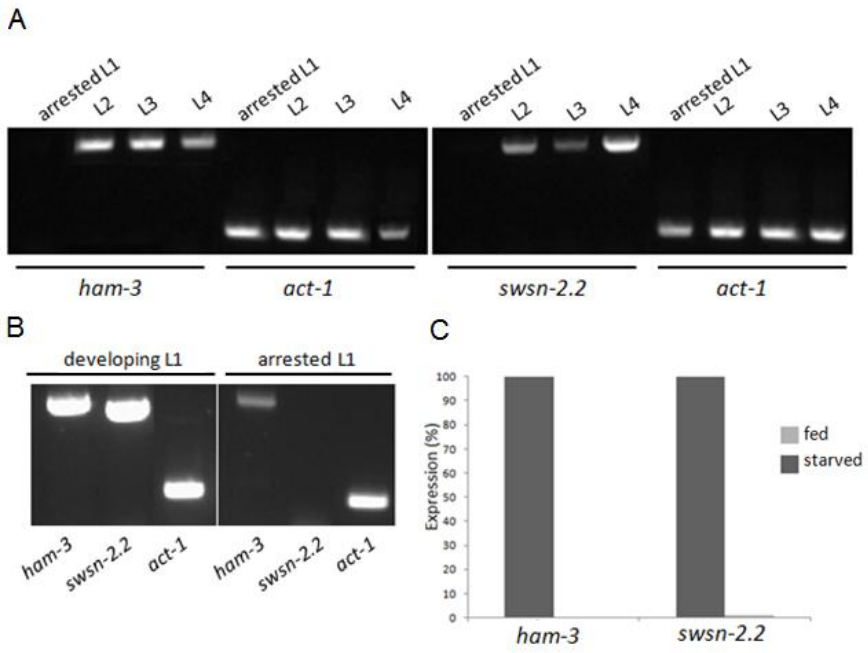

Fig.R.28: Expression of *ham-3* and *swsn-2.2* throughout development. (A,B) Reverse-Transcription PCR with cDNA from N2 shows that *ham-3* and *swsn-2.2* are expressed throughout all developmental stages, but not in starved L1. (C) qPCR confirms that both genes are down-regulated in arrested (starved) L1 animals. Expression data of all samples were normalized to transcript levels of *act-1.*

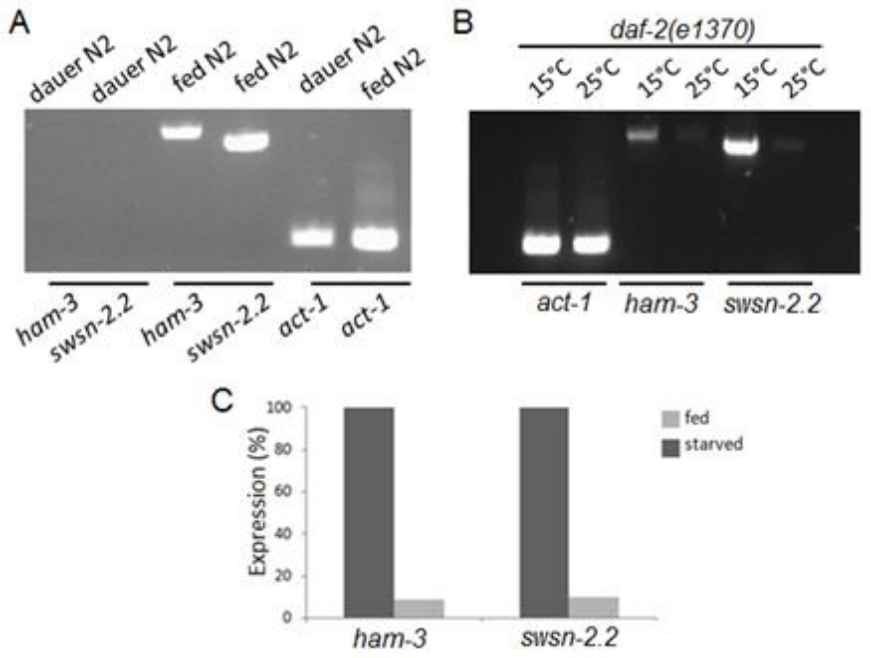

Fig.R.29: Expression of *ham-3* and *swsn-2.2* in response to low insulin signaling. (A) Reverse-Transcription PCR with cDNA from starved N2 shows that neither *ham-3* nor *swsn-2.2* are expressed in dauer stage. (B,C) Reverse-Transcription PCR and qPCR show that *ham-3* and *swsn-2.2* are down-regulated in *daf-2* mutants grown on non-permissive conditions. Expression data of all samples were normalized to transcript levels of *act-1.*

R.6.2. *swsn-2.2* and *ham-3* affect the expression of *daf-16* regulated genes

RNA-seq was performed with cDNA coming from synchronized L4 populations of wild type (N2) animals fed with *ham-3(RNAi)*, *swsn-2.2(RNAi)* or *gfp(RNAi)* as a control. According to the functional redundancies previously observed, a total of 183 genes was found to be regulated by both, HAM-3 and SWSN-2.2 (69 activated and 114 repressed) (Fig.R.30). This observation suggests that the SWI/SNF complexes regulating the expression of these genes can incorporate either of the two proteins.

Beyond that, we found genes whose expression is apparently regulated by either HAM-3 or SWSN-2.2. The number of targets that are up- or downregulated by the two proteins implicates that HAM-3 plays a major role in the activation of gene expression, while SWSN-2.2 seems rather be related to repression (Fig.R.30)

Interestingly, we also found 31 genes to be antagonistically regulated by HAM-3 and SWSN-2.2. This could mean that a given complex can induce the expression of a certain gene when one of the two paralogs is incorporated, while repressing the same target upon presence of the other paralog. Alternatively, the antagonistic regulation could be explained by an indirect effect.

To further explore this opposite gene regulation, a second RNA-seq was performed and the transcriptomes of *ham-3(RNAi)* and *swsn-2.2(RNAi)* worms compared. The differential regulation of 18 genes was confirmed (Table.R.2). Remarkably, the most of these targets have previously been related with DAF-16 (Table.R.2). We chose five of those genes to be validated by qPCR and could confirm the upregulation of the target in response to *swsn-*

2.2(RNAi) (Fig.R.31). However, the downregulation due to *ham-3(RNAi)* was not shown in this approach (Fig.R.31).

In summary, RNA-seq revealed that *ham-3* and *swsn-2.2* have common, but also independent transcriptional targets. According to the results of the RNA-seq, there exist also genes that are antagonistically regulated by the two genes. However, validation by qPCR did not confirm this, and we therefore believe that HAM-3 and SWSN-2.2 have an indirect effect on the IIS pathway.

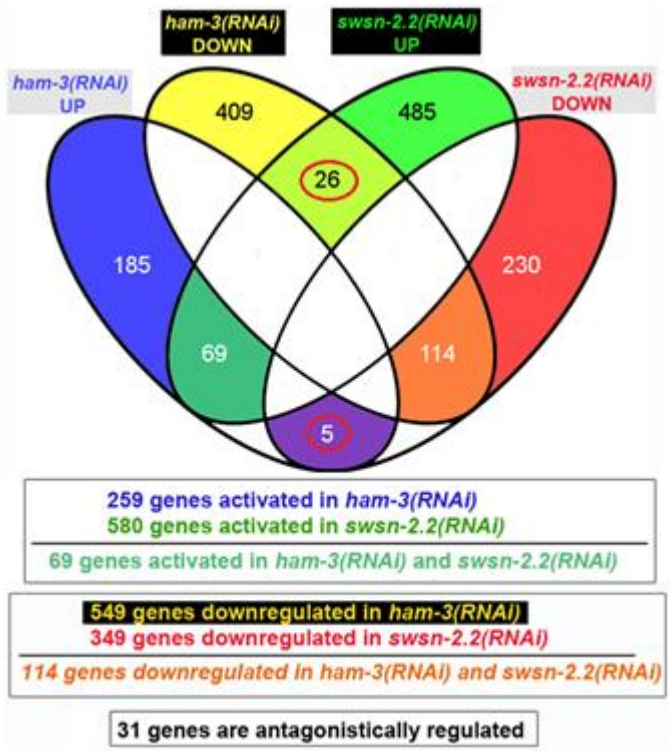

Fig.R.30: Genes differentially regulated in response to *ham-3(RNAi)* or *swsn-2.2(RNAi).* RNA-seq was performed with cDNA from synchronized wild type (N2) populations in L4 stage that were fed for 36h at 25°C with *ham-3(RNAi)*, *swsn-2.2(RNAi)* or *gfp(RNAi)* as a control. Besides co-regulated targets, genes regulated by either *ham-3* or *swsn-2.2* were identified. A small fraction of genes (marked with red circles) was found to be regulated in an antagonistic matter.

UP in *swsn-2.2(RNAi)* and DOWN in *ham-3(RNAi)*			
Gene name	**CDS**	**Chr.**	**DAF-16 related**
clec-41	B0365.6	V	YES
C06G8.1	C06G8.1	IV	YES
dod-21	C32H11.10	IV	YES
dod-24	C32H11.12	IV	YES
C32H11.9	C32H11.9	IV	YES
C49G7.7	C49G7.7	V	
C50F4.8	C50F4.8	V	
ugt-43	F01D4.1	IV	
F01D5.1	F01D5.1	II	YES
F01D5.2	F01D5.2	II	
F35E12.8	F35E12.8	V	YES
gst-38	F35E8.8	V	YES
F55G11.4	F55G11.4	IV	YES
dod-17	K10D11.1	IV	YES
Y37H2A.14	Y37H2A.14	V	
mtl-7	ZK430.8	II	
ZK6.11	ZK6.11	V	YES
UP in *ham-3(RNAi)* and DOWN in *swsn-2.2(RNAi)*			
cpt-5	F09F3.9	V	

Table.R.2: Genes differentially regulated by HAM-3 and SWSN-2.2. A total of 18 genes was found to be differentially regulated by HAM-3 and SWSN-2.2 in both replicates of the RNA-seq. The genes labeled in dark grey were chosen for further validation by qPCR. A list of genes regulated by DAF-16 was retrieved from Pinkston-Gosse & Kenyon, 2007.

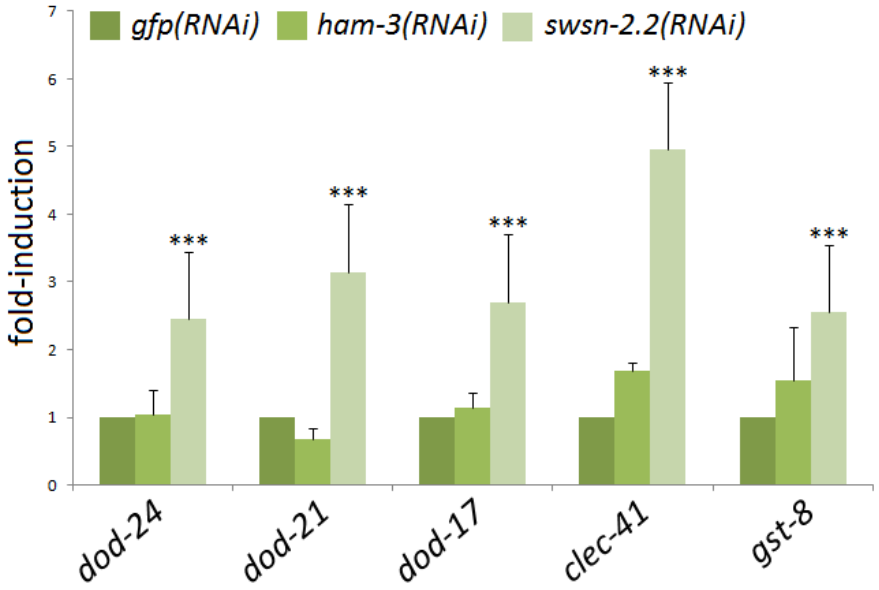

Fig.R.31: Expression levels of DAF-16 related genes in response to *ham-3(RNAi)* and *swsn-2.2(RNAi).* Expression levels of genes found to be differentially regulated in response to *ham-3(RNAi)* and *swsn-2.2(RNAi)* by RNA-seq were determined by qPCR. Expression data of all samples were normalized to the transcript levels of *act-1.* The transcript levels of the *ham-3(RNAi)* and *swsn-2.2(RNA)* worms related to the control animals [*gfp(RNAi)*]. Three asterisks indicate p<0.001.

R.6.3. *swsn-2.2* affects DAF-16 localization

As mentioned above, the differential regulation of some DAF-16 targets found in RNA-seq could be caused by an indirect effect.

To explore this possibility, we employed a reporter strain expressing DAF-16::GFP. RNAi of *ham-3* and *swsn-2.2* was performed and DAF-16 localization and thereby its activation state was studied by fluorescence microscopy.

Under favorable conditions, the transcription factor DAF-16 is inhibited by signals from the DAF-2 receptor and consequently localized in the cytoplasm. In response to stress stimuli, e.g. starvation or high temperatures, this inhibitory signaling stops and DAF-16 translocates to the nucleus where it induces the expression of its target genes (Barbieri et al., 2003; Baugh & Sternberg, 2006).

As expected, in control animals DAF-16 was predominantly found in the cytoplasm (Fig.R.32). *ham-3(RNAi)* did not have an obvious effect on the localization of the transcription factor (Fig.R.32). Interestingly, knock-down of *swsn-2.2* resulted in nuclear localization of DAF-16 in approximately 30% of the animals (Fig.R.32).

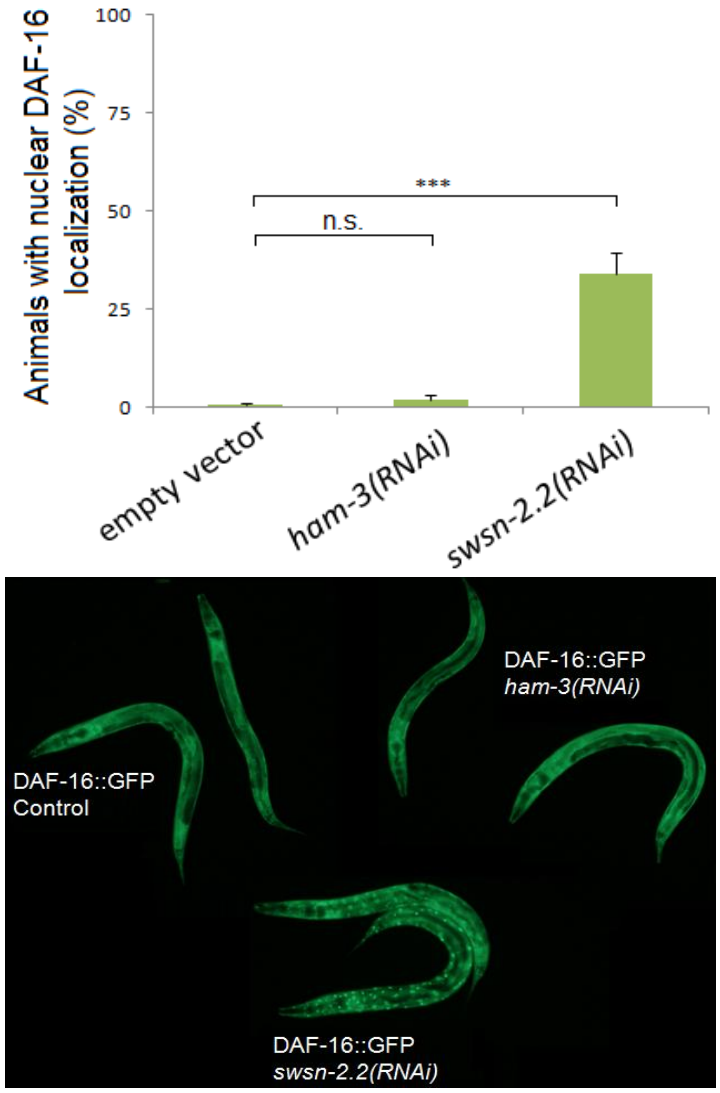

Fig.R.32: *swsn-2.2(RNAi)* affects the localization of the transcription factor DAF-16. Synchronized populations of animals expressing DAF-16::GFP were seeded on the respective RNAi plates or a control and incubated at 25°C for 36h. The localization of DAF-16 was scored under the dissection microscope (n≤300). While DAF-16 is predominantly found in the cytoplasm of control and *ham-3(RNAi)* animals, knock-down of *swsn-2.2* causes nuclear localization in some animals. Error bars represent the standard deviation between experimental triplicates. P values were calculated using a student's T-test. Three asterisks indicate $p<0.001$.

R.7. Identification of SWSN-2.2 interactors

R.7.1. Co-Immunoprecipitation of SWSN-2.2 and mass spectrometry

We employed our specific α-SWSN-2.2 antibody to immunopurify SWSN-2.2-containing complexes from wild type (N2) mixed-stage populations in two biological replicates. The success and specificity of the immunoprecipitation was confirmed by Western blotting (Fig.R.33). Samples were analyzed by mass spectrometry.
In both experiments we identified various SWI/SNF components, amongst them the enzymatic subunit SWSN-1 and the core proteins SWSN-4 and SWSN-5 (Table R.3). In none of the two experiments HAM-3 was co-immunoprecipitated, what lets suggests that, as their human homologs, HAM-3 and SWSN-2.2 are mutually exclusive in a given complex.

In both biological replicates we identified proteins that have previously been shown to have functions in embryonic development (Table R.3).
Amongst these proteins was SAO-1 that negatively regulates *aph-1* activity in the early embryo (Table R.3). APH-1 is a component of the γ-Secretase complex that cleaves the intracellular domain of the Notch receptor and SAO-1 has been shown to influence Notch signaling events (Hale et al., 2012). Another protein identified was ATX-2, a homolog of human ataxin-2 that is required for early embryonic patterning (Table R.3) (Kiel, Shibata & Pulst, 2000). Beyond its function in embryonic development, *atx-2* promotes germline proliferation (Ciosk, DePalma & Priess, 2004; Maine et al., 2004).

We also identified components of the nuclear envelope to interact with SWSN-2.2. MEL-28 for instance, is required for the assembly of the zygotic nuclear envelope (Table R.3) (Galy et al., 2006). Interestingly, it was previously shown that MEL-28 interacts with NPP-9 in early embryos (Fernandez & Piano, 2006). NPP-9 is a nuclear pore protein and was also identified to be an interactor of SWSN-2.2 by Co-immunoprecitation (Table R.3).
The interactions of SWSN-2.2 with these proteins might explain the failures in embryogenesis in response to *swsn-2.2* loss-of-function.

Another class of SWSN-2.2 interactors identified by Co-IP and Mass spectrometry were myosin related proteins (Table R.3). Traditionally, myosins were thought to act exclusively in the cytoplasm. However, more recent studies showed that members of this protein family have also functions in the nucleus and are probably involved in transcription and cell cycle regulation (Lanerolle & Serebryannyy, 2011). The observation that myosin-related proteins and SWSN-2.2 interact might implicate that they require SWI/SNF complexes for these functions.

We also identified a transcription factor, TAF-9 to interact with SWSN-2.2, what is concurrent with the role of SWI/SNF complexes in transcriptional regulation (Table R.3).

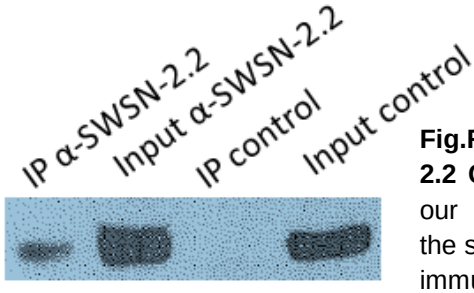

Fig.R.33: Western blot of SWSN-2.2 Co-immunoprecipitation. Using our specific α-SWSN-2.2 antibody the success and specificity of the Co-immunoprecipation was confirmed.

Protein	Function	IP1	IP2
		# Peptides	# Peptides
SWSN-1	SWI/SNF subunit	11	16
SWSN-2.2	SWI/SNF subunit	6	10
SWSN-3	SWI/SNF subunit	1	5
SWSN-4	SWI/SNF subunit	0	4
SWSN-5 (SNFC-5)	SWI/SNF subunit	0	2
SWSN-6	SWI/SNF subunit	0	2
SWSN-7	SWI/SNF subunit	0	1
SAO-1	Early embryo	1	4
ATX-2	Early embryo	0	3
NPP-2	Nuclear envelope	0	1
NPP-9, isoform a	Nuclear envelope	2	1
MEL-28	Nuclear envelope interacts with NNP-9*	1	0
HUM-5	Myosin-related	10	0
HUM-2	Myosin-related	2	0
MLC-6	Myosin-related	3	1
MLC-7	Myosin-related	4	0
TNT-4	Myosin-related	4	0
C30H6.7	Acetyltransferase	7	4
LEC-6	Lectin	0	3
H03A11.2	n/a	0	3
B0303.3	n/a	2	0
LYS-1	lysozyme	2	0
TFG-1	Protein secretion and oncogénesis	0	2
ZK973.9	Arp2/3 complex	0	2
TAF-9	Transcription	1	1

Table R.3: Proteins identified as interactors of SWSN-2.2 by Co-Immunoprecipitation. * Fernandez & Piano, 2006

R.7.2. SWSN-2.2 and MEL-28::GFP co-localize in developing oocytes and early embryos

In order to verify the interactions between SWSN-2.2 and MEL-28, we performed immunostaining in germlines and embryos of the strain BN311 expressing MEL-28::GFP. We found that both proteins, SWSN-2.2 and MEL-28::GFP were localized in the nuclei of early embryos and developing oocytes (Fig.R.34, Fig.R.35). This co-localization of the two proteins further supports the suggestion that SWSN-2.2 and MEL-28 might interact.

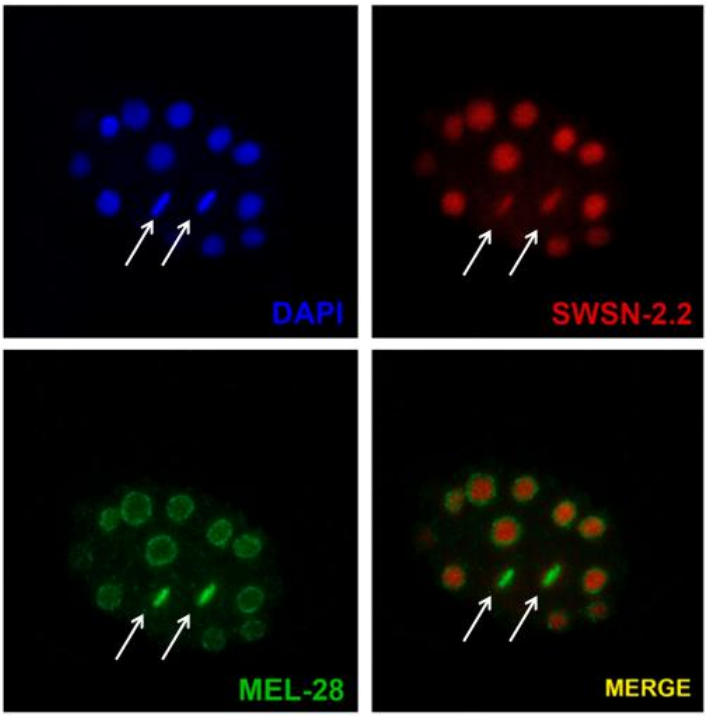

Fig.R.34: Immunostaining of SWSN-2.2 and MEL-28::GFP in early embryos. Immunostaining of SWSN-2.2 and MEL-28::GFP was performed in the embryos of the strain BN311 expressing MEL-28::GFP. Co-localization of the two proteins in early embryonic nuclei and at condensed chromosomes of mitotic cells (arrows) was observed.

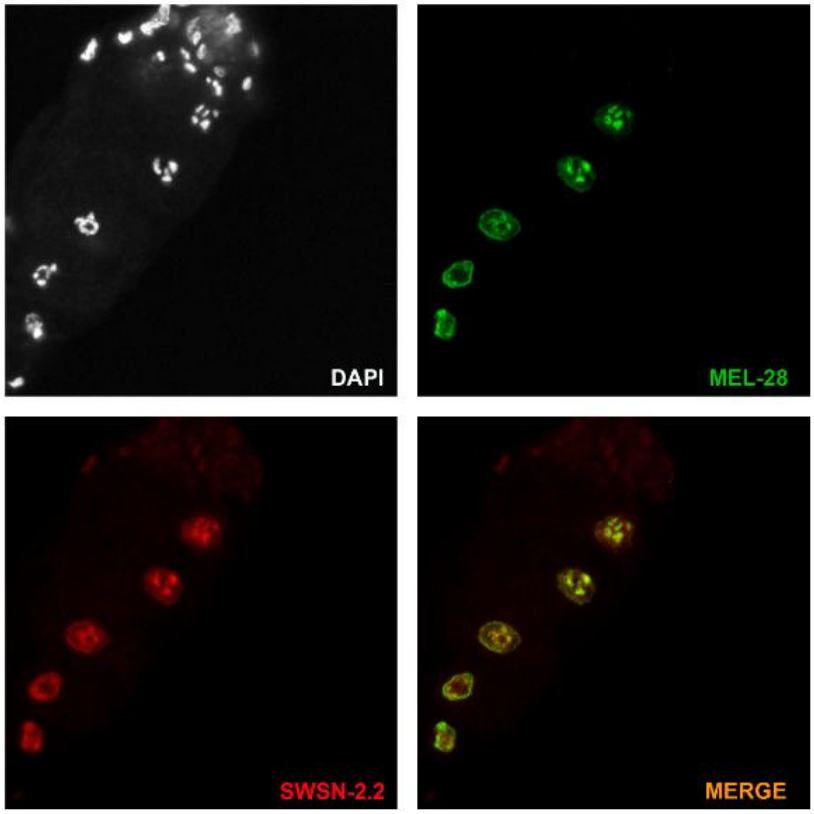

Fig.R.35: Immunostaining of SWSN-2.2 and MEL-28::GFP in developing oocytes in the germline. Immunostaining of SWSN-2.2 and MEL-28::GFP was performed in germlines of the strain BN311 expressing MEL-28::GFP. Co-localization of the two proteins in the developing oocytes was observed.

Discussion

Discussion

D.1. *ham-3* and *swsn-2.2* act redundantly in mechanisms required for fertility

We observed that *ham-3* or *swsn-2.2* loss-of-function causes reduced brood sizes and alterations of the gonads (Fig.R.8; Fig.R.9), what is concurrent to results published by others (Large & Mathies, 2014). However, despite of the negative effect of the absence of functional HAM-3 or SWSN-2.2 on the germline, *ham-3* and *swsn-2.2* mutants maintain the ability to produce eggs (Fig.R.11).

Interestingly, when RNAi by feeding is started in L1 stage, simultaneous knock-down of *ham-3* and *swsn-2.2* causes sterility due to a failure in the production of oocytes (Fig.R.11). The complete penetrance of this phenotype strongly implicates redundant functions of the two genes in this context.

We found that, although all types of germ cells are present, animals develop smaller gonads in response to double RNAi of *ham-3* and *swsn-2.2* (Fig.R.13). The oocytes seem to undergo normal development, but instead of entering the spermatheca and get fertilized, mature oocytes are trapped in the gonad arms and perform endoreplication (Fig.D.1).

Endomitotic oocytes in the gonad arm (Emo) are caused by ovulation defects (Iwasaki et al., 1996). In wild types, ovulation is induced by the major sperm protein (MSP) as well as by signals shed by the mature oocyte. In response to these signals the somatic sheath contracts and pushes the mature oocytes into the spermatheca (Miller et al., 2001; Iwasaki et al., 1996). Failures of ovulation can be caused by defects in the coordination between the

somatic gonad and the germline. For instance, the inductive signaling between the mature oocyte and the somatic sheath cells can be impaired (Miller et al., 2001; Iwasaki et al., 1996). Also abnormalities of the spermatheca were shown to cause endomitotic oocytes (McCarter et al, 1997).

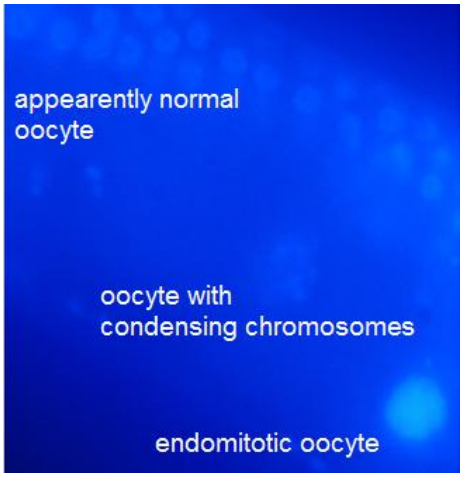

Fig.D.1: Emo phenotype caused by double RNAi of *ham-3* and *swsn-2.2*. In response to simultaneous inactivation of *ham-3* and *swsn-2.2* oocytes undergo endomitotic replication in the gonad arm.

SWI/SNF complexes are involved in the development of the distal tip cells (DTCs), which form part of the somatic gonad. Loss of the enzymatic subunit SWSN-4, the core subunit SWSN-1, as well as the signature subunits of the BAF and the PBAF complex (LET-526 and PBRM-1 respectively) cause loss of one or both DTCs (Cui, Fay & Han, 2004; Shibata et al., 2012; Large & Mathies, 2014).

We observed that, in contrast to individual RNAi, also double RNAi of *ham-3* and *swsn-2.2* often causes loss of one DTC, implicating redundant functions (Fig.R.15). It was previously shown that both genes interact with *ehn-3*, a gene that is specifically expressed in Somatic Gonad Precursors (SGPs) and required for their development into differentiated tissues (Large & Mathies, 2014). Thus, it is probable that the loss of DTCs in response to

inactivation of *ham-3* and *swsn-2.2* is caused due to failures in the differentiation of the SGPs. However, it cannot be excluded that the genes have also other functions, e.g. in the generation of the SGPs (Fig.D.2).

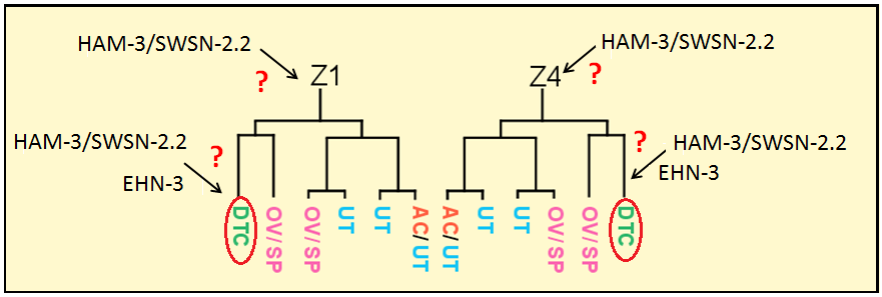

Fig.D.2: Model for the implications of HAM-3 and SWSN-2.2 in the development of the somatic gonad. Either HAM-3 or SWSN-2.2 is required for correct development of the distal tip cells. The two proteins might be involved in the generation of the SGPs (Z1 and Z4) or in the development of the DTCs.

Taking all these observations in consideration, we suggest that the ovulation defects in response to double RNAi of *ham-3* and *swsn-2.2* are at least partially caused by failures in the development of the somatic gonad.

Besides the somatic gonad defects, animals develop smaller germlines in response to double RNAi of *ham-3* and *swsn-2.2* (Fig.R.13). We therefore wondered, whether *ham-3* and *swsn-2.2* could be also involved in the maintenance of germline proliferation. The distal tip cells secrete the ligand LAG-2 and thereby induce proliferation of the germ cells through one of the LIN-12/Notch family receptors, GLP-1. Strong *glp-1* gain-of-function mutations result in the failure of the germ cells to exit mitosis and consequently in a tumorous germline consisting exclusively of a

proliferative zone (Hansen, Hubbard & Schedl, 2004). Single and double RNAi of *ham-3* and *swsn-2.2* caused smaller gonads in *glp-1*(gf) mutants (Fig.R.14). Since only mitotic, but no meiotic cells were found in the germlines of these animals, the effect of inactivation of *ham-3*, *swsn-2.2* and both genes must be regarded as a partial rescue of the *glp-1*(gf) phenotype. The used strain bears also the *rrf-1(pk1416)* loss-of-function allele, and the effect of the RNAi must therefore be soma-independent. Thus, we believe that *ham-3* and *swsn-2.2* play a role in the mitotic proliferation of germ cells.

While in adult stage germline proliferation is exclusively regulated by GLP-1 activity, cells of the somatic gonad influence the division of the germ cells during larval development (Kimble & Crittenden, 2005; Korta & Hubbard, 2010). Besides the two AC/VU (anchor cell/ventral uterine cell) progenitors that produce LAG-2, also the SS (sheath/spermathecal) precursors or their descendents have been shown to stimulate germline proliferation (Kimble & Crittenden, 2005; Korta & Hubbard, 2010). Thus, it is possible that abnormalities of the somatic gonad play an additional role in the reduced gonad size upon inactivation of *ham-3* and *swsn-2.2* in the wild type background.

In summary, our results implicate that *ham-3* or *swsn-2.2* act redundantly in germline proliferation as well as in the development of the somatic gonad. At least one of the two genes has to be functional to provide fertilized embryos, since simultaneous loss-of-function results in ovulation defects.

D2. *ham-3* and *swsn-2.2* are implicated in vulval development

D.2.1 Vulva muscle cells and egg-laying-defects

All studied loss-of-function alleles of *ham-3* and *ham-3(RNAi)* cause severe Egg-laying-defects frequently resulting in the death of adult hermaphrodites (Table R.1; Fig.R.12). It was previously shown that inactivation of *ham-3* affects the development of the hermaphrodite-specific neurons (HSN) (Desai et al., 1988). The HSNs use the neurotransmitter serotonin to stimulate the muscle cells of the vulva and thereby cause the disposal of the eggs. *ham-3* loss-of-function impairs this signaling and therefore results in the Egl phenotype. More recently it was demonstrated that this specific neuronal phenotype is caused by changes in the expression of the two Zinc-finger transcription factors *ham-2* and *sem-4* (Weinberg et al., 2013).

Given the complete penetrance of the Egl phenotype in all studied *ham-3* mutants (Table R.1), it is not probable that HAM-3 and SWSN-2.2 are redundant in this context.

However, also inactivation of *swsn-2.2* by mutation or RNAi results in Egg-laying-defects, but at lower penetrances (Table R.1; Fig.R.12). Thus, we conclude that *swsn-2.2* plays a role in the development of the egg-lay apparatus with less influence than its paralog.

D.2.2. The Pvl phenotype

Hermaphrodites with the protruding vulva (Pvl) phenotype produce vulva tissue, but fail to develop the wild type vulva structure. Since the tissue is nevertheless everted, they show a single protrusion at

the site of the vulva (Eisenmann & Kim, 2000). The Pvl phenotype can be caused by defects in all stages of vulval development. Mutations causing Pvl have been shown to affect genes that act in Vulval Precursor Cell (VPC) fate specification, VPCs survival, VPCs fate execution or in morphogenesis (Eisenmann & Kim, 2000). Simultaneous loss of *ham-3* and *swsn-2.2* causes Pvl at almost complete penetrance (Fig.R.16). Thus, these two proteins must have redundant functions in at least one of the steps in vulval development.

The induction of the vulval precursor cells is driven by the *let-60*/Ras pathway and is negatively regulated by synMuv genes. Different classes of synMuv genes exist and simultaneous loss-of-function in genes of different synMuv classes results in the Muv phenotype (Ceol et al., 2006). RNAi of *ham-3* and *swsn-2.2* in a strain bearing loss-of-function mutations in two synMuv genes (class A and B) enhanced the Multivulva phenotype (Fig.R.17). Beyond that, it has previously been shown that *ham-3* and *swsn-2.2* genetically interact with *lin-35*/Rb that represents a synMuv class B gene (Ceron et al., 2007; Cui, Fay & Han, 2004). Thus, it must be concluded that the two genes negatively regulate the induction of the VPCs (Fig.D.3).

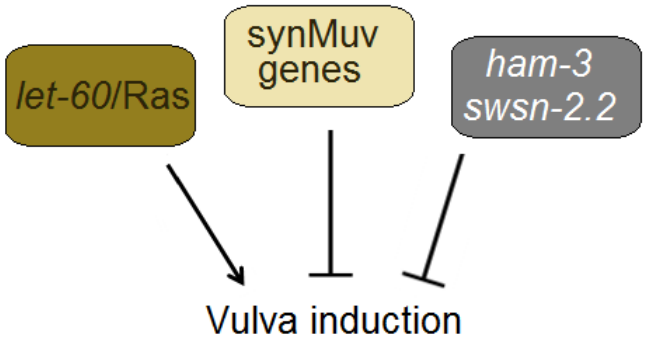

Fig.D.3: Regulation of vulva induction. Vulva induction is positively regulated by the *let-60*/Ras pathway and inhibited by different classes of synMuv genes. *ham-3* and *swsn-2.2* act in the negative regulation of vulva induction.

RNAi of *ham-3* and *swsn-2.2,* and especially simultaneous inactivation of both genes resulted in an enhancement of the Muv phenotype in a *let-60* gain-of-function background. (Fig.R.18). This observation suggests that *ham-3* and *swsn-2.2* act redundantly in the negative regulation of the *let-60*/Ras pathway.

Speculating about the precise mode of action of *ham-3* and *swsn-2.2* in vulva induction, there are two alternatives. I) The genes could act together with the synMuv B gene *lin-35*/Rb (Fig.D.4).

II) Another possibility is that HAM-3 and SWSN-2.2 cooperate with the Zinc-finger protein SOMI-1. HAM-3 cooperates with SOMI-1 in the differentiation of the hypodermis (Hayes, Riedel & Ruvkun, 2011). Beyond that, SOMI-1 was also shown to inhibit the induction of the vulval precursor cells and to bind the promoter of *let-60*/Ras (Hayes, Riedel & Ruvkun, 2011).Given the facts that *ham-3* and *somi-1* cooperate in hypodermal differentiation and that HAM-3 and SWSN-2.2 have redundant functions in *let-60*/Ras signaling, it is possible that the two proteins cooperate with SOMI-1 to inhibit *let-60* activity in the VPCs (Fig.D.4). Inactivation of *ham-3* and *swsn-2.2* might cause changes in the signaling cascade responsible for

the specification of the VPCs that explain the abnormal morphology of the vulva in response to individual and simultaneous silencing of both genes.

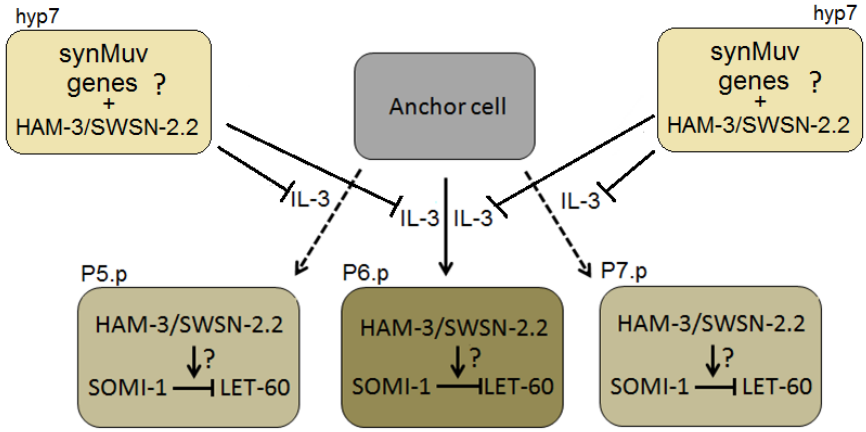

Fig.D.4: Model of action for *ham-3* and *swsn-2.2* functions in vulval development. HAM-3 and SWSN-2.2 may cooperate with the Zinc-finger protein SOMI-1 or the synMuv gene *lin-35* to inhibit *let-60*/Ras activity in the vulval precursor cells.

D.3. *swsn-2.2* has a specific function in embryogenesis

Concurrently with previous publications, we observed that inactivation of *swsn-2.2* by mutation results in embryonic lethality at high penetrances (Fig.R.19) (Sawa, Kouike & Okano, 2000; Large & Mathies, 2014).

Immunostaining showed the presence of SWSN-2.2 in developing oocytes and early embryos (Fig.R.22), implicating functions in the initial steps of embryogenesis. Indeed, microscopy and lineage analysis showed that the embryonic development of *swsn-2.2(ok3161)* mutants fails in early stages due to defects in cell division (Fig.R.21).

Co-immunoprecipition and Mass spectrometry allowed the identification of proteins that are involved in embryogenesis, such as SAO-1, ATX-2 and the transcription factor TAF-9 as interactors of SWSN-2.2 (Table R.3). SAO-1 presents a negative regulator of Notch signaling in the early embryo, while ATX-2 is required for early embryonic patterning (Hale et al., 2012; Kiel, Shibata & Pulst, 2000).

Interestingly, we also identified proteins of the nuclear membrane to be interactors of SWSN-2.2, amongst them MEL-28 (Table R.3). The nuclear envelope breaks down and re-establishes during every round of cell cycle. MEL-28 has been shown to be required for this process in the *C. elegans* embryo (Galy et al., 2006). Inactivation of *mel-28* by mutation or RNAi causes changes of the nuclear morphology and abnormal distribution of the nuclear pore complexes, as well as other proteins integrated in the nuclear envelope (Galy et al., 2006). The localization of MEL-28 is dynamic and depends on the stage of the cell cycle. During interphase the protein was observed to be associated with nuclear pore

complexes, while it was found at the kinetochores at the onset of mitosis and on chromatin in late mitosis (Galy et al., 2006).

To confirm the interaction between SWSN-2.2 and MEL-28, we performed immunostaining and indeed observed co-localization of the two proteins in the nuclei of developing oocytes and early embryos (Fig.R.34; Fig.R.35). MEL-28 is, besides its function in the assembly of the nuclear envelope, also involved in chromatin maintenance. Beyond that, it is apparently required for the correct segregation of the chromosomes during mitosis (Galy et al., 2006, Fernandez & Piano, 2006). We found SWSN-2.2 and MEL-28 to be co-localized to condensed chromosomes of mitotic cells in the early embryo (Fig.R.34), what could mean that the two proteins cooperate in this process.

MEL-28 has, amongst others, previously been shown to interact with the nuclear pore protein NPP-9, which is apparently required for its correct localization to chromatin and nuclear membranes in the early embryo (Fernandez & Piano, 2006). Interestingly, in the course of Co-Immunopreciptation and Mass spectrometry we identified also NPP-9 to interact with SWSN-2.2 (Table R.3). The observation that SWSN-2.2 interacts with both, MEL-28 and NPP-9 might implicate that SWSN-2.2 is also involved in the localization of MEL-28.

A third component of the nuclear envelope found to interact with SWSN-2.2 is NPP-2. *npp-2* has previously been shown to genetically interact with *mel-28* (Fernandez et al., 2014). However, it is unknown in which processes the two genes cooperate.

The nuclear lamins are, apart from their structural functions, also thought to be involved in processes such as replication, transcription and chromatin organization (Dechat et al., 2008). It was previously shown in human cells that SWI/SNF complexes are

associated with the nuclear lamina (Euskirchen et al., 2011). Our results might suggest that also in *C. elegans* SWI/SNF complexes and components of the nuclear envelope cooperate to provide correct organization of the chromatin.

In contrast to *swsn-2.2* alleles, mutations of *ham-3* cause embryonic lethality at low penetrance (Fig.R.19), what lets suggest that HAM-3 has different functions in embryonic development.
Differently from *swsn-2.2* mutant embryos, loss of functional *ham-3* does not cause defects in early embryonic cell divisions. Lineage analysis showed that a small fraction of *ham-3(he159)* embryos have defects in the orientation of the mitotic spindle at the 8 cell-stage (Fig.R.23). While in wild types three of the four spindles present in this stage are aligned in parallel, one is orientated perpendicular to the others (Rocheleau et al., 1997). In 1 out of 12 analyzed *ham-3* mutant embryos this perpendicular orientation was not given, but all four spindles were aligned in parallel, implicating a function of *ham-3* in Wnt signaling (Walston et al., 2004; Gómez-Orte et al., 2013).
Still, the predominant embryonic phenotype of *ham-3* mutants is a defective E lineage in later stages of embryogenesis (Fig.R.24).

Nevertheless, we observed that simultaneous knock-down of *ham-3* and *swsn-2.2* results in embryonic lethality at complete penetrance (Fig.R.20). Thus, the two genes must, apart from their independent functions in embryogenesis, also act redundantly at a certain level.

In conclusion, null activity of *ham-3* and *swsn-2.2* produces different embryonic phenotypes indicating specific functions in this

context. While *swsn-2.2* is indispensible for proper cell division during the initial stages of embryonic development, *ham-3* is not required in this process.

Nevertheless, since partial depletion of both genes by RNAi causes a highly penetrant synthetic phenotype, there must exist embryonic functions where the two genes cooperate.

D.4. *ham-3* and *swsn-2.2* have common functions in intestinal cell cycle regulation

Lineage analysis of two different mutant strains showed that *ham-3* loss-of-function results in an increase of the intestinal cell number due to extra cell divisions during embryogenesis (Fig.R.24). This observation suggests that HAM-3 is involved in the negative regulation of the cell cycle specifically in the E lineage.

Several independent pathways have been shown to regulate the intestinal cell number during embryonic development. The *cki-1* and *lin-35* pathways act redundantly and cooperate in the regulation of the entry into the S phase. Both signaling cascades are inhibited by signals from CYD-1/CDK-4 complexes (Boxem & van den Heuvel, 2001). A third pathway regulating proliferation in the E lineage involves the CDC25.1 phosphatase and CYE-1 (Kostić & Roy, 2002).

In wild type animals, only four of the cells present at the 16E stage continue proliferation, while the rest stops to divide, resulting in a total of 20 intestinal cells at hatching (Fig.D.5). In *cki-1* mutants these 16 cells fail to cease proliferation and undergo additional cell divisions (Fig.D.5). The extra intestinal cells of *cdc25.1* gain-of-function mutants in contrast, derive from additional cell divisions after the 8E stage (Fig.D.5) (Kostić & Roy, 2002). In other words, these cells divide faster.

The E lineages of the *ham-3* mutants show similarities to those of *cki-1* mutants. As *cki-1* loss-of-function alleles, absence of functional *ham-3* results in extra divisions of cells that should have stopped to proliferate (Fig.D.5). This lets suggest that *ham-3* is not part of the *cdc25.1* pathway, but rather acts in the *cki-1* signaling cascade (Fig.D.6).

A functional relation between *ham-3* and *cki-1* could also explain the somatic gonad phenotypes, since the levels of CKI-1 are critical for the specification of all cell types of the somatic gonad (Fujita, Takeshita & Sawa, 2007).

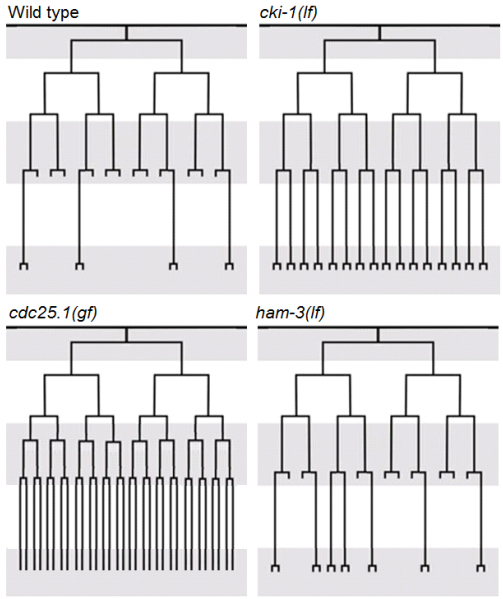

Fig.D.5: E lineages of *cki-1*(lf), *cdc25.1*(gf) and *ham-3*(lf) mutants compared to wild type. *cki-1* loss-of-function results in extra divisions of cells that should have stopped to proliferate. *cdc25.1* gain-of-function in contrast, causes extra cell divisions after the 8-cell stage. Similarly to *cki-1*(lf), *ham-3* loss-of-function results in extra intestinal cells due to cells that fail to cease proliferation.

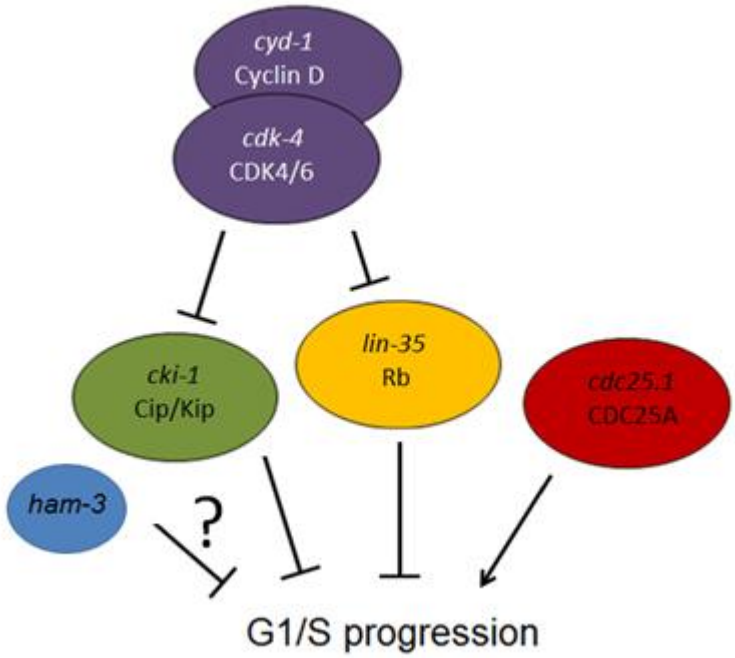

Fig.D.6: *ham-3* functions in cell cycle regulation in the E lineage. HAM-3 has a function in the control of G1/S phase transition in the E lineage. While it has rather no function in the *cdc.25-1* pathway, it might be involved in the *cki-1* signaling cascade. [Rb: Retinoblastoma protein; Cip/Kip: CDK interacting protein/Kinase inhibitory protein]

Also *swsn-2.2* mutant larvae have an increased number of intestinal nuclei at hatching (Fig.R.25), so it must be supposed that the gene also plays a role in the regulation of the cell cycle in the E lineage.

Since double RNAi of *ham-3* and *swsn-2.2* results in sterility or embryonic lethality at complete penetrance, it was not determinable, whether the two paralogs act redundantly in the cell cycle regulation of embryos, but we addressed this question at postembryonic stages.

The intestine of wild type larvae at hatching consists of 20 cells with one nucleus each. During L1 stage the nuclei of a variable

number of the intestinal cells divide, giving rise to the 30-34 nuclei found in a normal adult intestine.
RNAi of *ham-3* and *swsn-2.2* started in L1 stage caused an increase of the number of intestinal cells in the adult worm (Fig.R.26). Thus, the two proteins must also play a role in the postembryonic development of the intestine. In two different approaches the question whether *ham-3* and *swsn-2.2* cooperate in this context was addressed (Fig.R.26). In both cases an enhancement of the intestinal phenotype was observed in response to simultaneous loss of both genes, implicating common functions at this level of intestinal development.

In summary, we show that *ham-3* and *swsn-2.2* are involved in the regulation of the E lineage during embryogenesis. *ham-3* acts downstream CYD-1 (Fig.R.27) and the E lineage of *ham-3* mutants resembles those of animals with defects in the *cki-1* pathway (Fig.D.5). Beyond that, *ham-3* and *swsn-2.2* have common functions in the post-embryonic development of the intestine.

20% of human cancers show inactivating mutations of SWI/SNF components (Hohmann & Vakoc, 2014). Our observations suggest that SWI/SNF has also tumor suppressor-like functions in *C. elegans.*

D.5. *swsn-2.2* and *ham-3* have a function in IIS signaling

It was recently shown that SWI/SNF complexes are involved in the IIS pathway (Riedel et al., 2013). The FOXO transcription factor DAF-16 and SWI/SNF form complexes that bind the promoters of genes, thereby inducing their expression (Riedel et al., 2013). Thus, SWI/SNF complexes are required for the DAF-16 mediated induction of dauer formation, longevity and stress resistance (Riedel et al., 2013).

ham-3 and *swsn-2.2* were not studied extensively and they might interact with *daf-16* in contexts that were not addressed.

Performing RNA-seq, we identified genes whose expression is repressed or activated by HAM-3 and SWSN-2.2 (Fig.R.30). Interestingly, many of these targets overlapped with targets of DAF-16 (Fig.D.7). Amongst these DAF-16 regulated targets, genes were found to be activated, co-activated, repressed and co-repressed by HAM-3 and SWSN-2.2 (Fig.D.7). This observation implicates independent and common functions of the two genes in the IIS pathway. The numbers of genes activated or repressed in response to *ham-3(RNAi)* and *swsn-2.2(RNAi)* suggest that HAM-3 is rather involved in the activation of expression, while SWSN-2.2 plays a major role in gene repression (Fig.D.7). We also identified DAF-16 targets to be antagonistically regulated by HAM-3 and SWSN-2.2 (Fig.D.7). This differential regulation could be caused by a direct effect, what means that a SWI/SNF complex might induce the expression of a gene when one of the two paralogs is incorporated, while repressing it upon presence of the other paralog. Another possibility is that HAM-3 and SWSN-2.2 have an indirect effect on the IIS pathway playing distinct roles in this context.

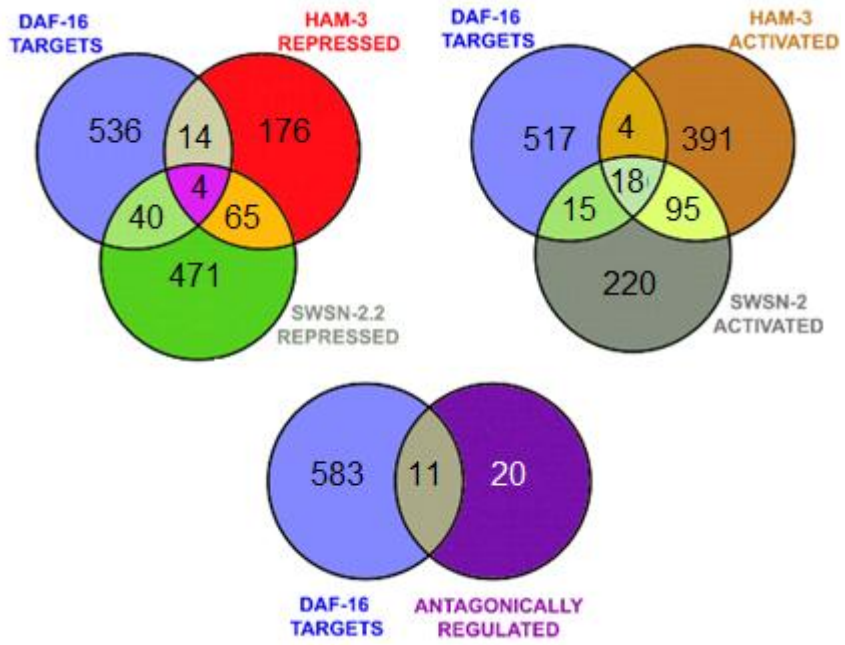

Fig.D.7: The transcriptional targets of HAM-3, SWSN-2.2 and DAF-16 are partly overlapping. RNA-seq revealed that DAF-16 targets are amongst the genes regulated by HAM-3 and/or SWSN-2.2. The list of genes regulated by DAF-16 was retrieved from Pinkston-Gosse & Kenyon, 2007.

The hypothesis that HAM-3 and SWSN-2.2 have an indirect effect on the IIS pathway was investigated by RNAi experiments in a strain expressing DAF-16::GFP (Fig.R.32). RNAi of *ham-3* and *swsn-2.2* was performed under the same conditions as for the RNA-seq, and the localization of DAF-16 observed. We found that inactivation of *swsn-2.2* caused alterations in the localization of DAF-16, while *ham-3(RNAi)* did apparently not have any effect (Fig.R.32). Under favorable conditions, the transcription factor DAF-16 is supposed to be inactive and in the cytoplasm. However, due to silencing of *swsn-2.2*, DAF-16 was partly found in the nucleus. This could indicate that SWSN-2.2 is involved in the

inactivation of DAF-16 and has an indirect effect on the IIS pathway. The observation that DAF-16 might present higher activity in response to *swsn-2.2(RNAi)* is congruent with the higher expression levels of genes under the control of DAF-16 in response to inactivation of *swsn-2.2* (Table R.2).

However, the differential regulation could also be caused by a combination of a direct and an indirect effect. ChIP-seq experiments could help to clear the question whether HAM-3 and SWSN-2.2 show a distinct binding to promoter regions of DAF-16 target genes.

We observed that both, *ham-3* and *swsn-2.2* are significantly down-regulated in arrested L1 and dauer larvae, hence in response to low IIS. However, the amount of protein that is produced before the entry into developmental arrest might be sufficient to provide the function of the proteins in this pathway.

To summarize, our results indicate that *ham-3* and *swsn-2.2* have independent and common functions in the IIS pathway. In contrast to *ham-3(RNAi)*, *swsn-2.2(RNAi)* has an influence on DAF-16 localization.

D.6. *ham-3* and *swsn-2.2* are genetic hubs with unique, redundant and shared functions

The human BAF60 proteins are mutually exclusive in a given complex. Since we did not co-purify HAM-3 upon immunopreciptation of SWSN-2.2 (Table R.3), we believe that the same is true for their *C. elegans* homologs.

It was previously described that two subunits of SWI/SNF complexes in *Arabidopsis thaliana* can have redundant, unique and shared functions (Kwon & Wagner, 2007). This means that a given SWI/SNF complex can incorporate either of the two proteins in order to regulate a certain target (redundant), while it requires the presence of a specific subunit to act on others (unique). In some cases several SWI/SNF complexes regulate a target, whereby they contain different subunits (shared). Our results implicate that this model of action might also true for the *C. elegans* accessory subunits HAM-3 and SWSN-2.2.

For instance, silencing of one of the two genes by RNAi does not have a strong effect on the induction of the VPCs and germline development, while simultaneous inactivation of both paralogs causes phenotypes at (almost) complete penetrance (Pvl and Ste, respectively) (Fig.R.11; Fig.R.16). This implicates that loss-of-function of one gene can be compensated by its paralog and the gene pair has redundant functions in these contexts.

In others cases, such as early embryonic cell division, HAM-3 and SWSN-2.2 seem to have unique functions, since loss of one paralog only, in this case SWSN-2.2, gives a highly penetrant phenotype (Fig.R.19).

We suppose shared functions of HAM-3 and SWSN-2.2 in intestinal cell cycle regulation in postembryonic stages. Inactivation of both

genes causes an increase of the intestinal nuclei number, but this effect is not intensively enhanced upon knock-down of both paralogs (Fig.R.26).

Studies in *C. elegans* allowed the identification of a group of genes whose inactivation causes the enhancement of the effects of mutations in many different genes, so-called hub genes (Lehner et al., 2006). It was shown that hub genes are also present in other organisms, including the human, and act as genetic buffers that can (partly) compensate mutations in other genes. As a consequence, the inactivation of hub genes can cause various different diseases and conditions (Lehner et al., 2006). In *C. elegans,* all the identified hub genes encode chromatin remodelers (Lehner et al., 2006).
Our study showed that *ham-3* and *swsn-2.2* function in various independent pathways and processes. We related both genes with the development of the somatic gonad and the germline, the regulation of the intestinal cell cycle and embryogenesis.
We showed that *ham-3* and *swsn-2.2* might be involved in the *let-60*/Ras, the Notch and the IIS pathway. Further, we suppose that *ham-3* plays a role in Wnt signaling.
Thus, we believe that the two genes must, as other genes encoding chromatin remodelers, be regarded as genetic hubs.

Mutations in components of the SWI/SNF complex were shown to be involved in the pathogenesis of human diseases, such as cancer (Biegel, Busse & Weissmann, 2014). Several studies suggest that also the accessory subunits BAF60a, BAF60b and BAF60c play a role in tumorigenesis when mutated (Reisman, Glaros & Thompson, 2009; Stephens et al., 2012, Sgroi et al.,

1999; Weissman & Knudsen, 2009). Our study supports this hypothesis, since *ham-3* and *swsn-2.2* are highly similar to their human counterparts and we showed that they act in cell cycle regulation, in chromosomal and nuclear stability and in pathways related with tumorigenesis such as Wnt and Ras.

Material and Methods

MM.1. General methods

NGM plates and OP50 cultures were prepared according to the standard protocols (Brenner, 1974). Worms were grown in incubators at 15°C, 20°C or 25°C according to their intended use.
For harvesting and washing of populations, M9 buffer was used. Single individuals were transferred with a worm picker. To make this tool, platinum wire (ø 0.2mm, approximately 1.5cm length) was placed in a glass Pasteur pipette and fixed by melting the tip in the flame of a Bunsen burner.
To create new strains, males were generated and employed for crossing. Efficient mating was achieved by placing several males with single hermaphrodites on plates seeded with a small drop of OP50.

NGM plates:

Bacto-Agar™ (g)	17	
NaCl (g)	3	
Bacto-Peptone™ (g)	2.5	
ddH_2O (ml)	975	Autoclave
Kalium phosphate buffer 1M pH 6.0 (ml)		25
$CaCl_2$ 1M (ml)		1
$MgCl_2$ 1M (ml)		1
Cholesterol (5mg/ml in 96% EtOH) (ml)		1

Kalium phosphate buffer 1M

KH_2PO_4 (g)	108.3	
K_2HPO_4 (g)	35.6	
ddH_2O	up to 1l	Autoclave

1xM9 buffer:

KH_2PO_4 (g)	3	
Na_2HPO_4 (g)	6	
NaCl (g)	5	
ddH_2O	up to 1l	Autoclave
$MgSO_4$ 1M (ml)	1	

Generation of males:

- Transfer of L4 hermaphrodites to NGM plates seeded with OP50 (six plates with 10 worms each)
- Heat shock at 30°C for 3 hours
- Down-shift to 25°C
- Some males should be found in F1

MM.2. Molecular analysis of mutant alleles

MM.2.1. Genotyping of mutant alleles

Preparation of worm lysates:

Single individuals or pools of worms were transferred into 10µl Lysis buffer with a worm picker. To crack the tissue, 5 freeze/thaw cycles were performed using dry ice combined with 96% EtOH, and a water bath at 37°C. The samples were subsequently incubated in a thermocycler for 1h at 60°C and 15min. at 95°C to inactivate the Proteinase K.

1xLysis buffer

H_2O	135
10x NH4 Reaction Buffer* (µl)	15
Proteinase K (10mg/ml) (µl)	1

* BIOTAQ™ PCR Kit

PCR for amplification of WT and mutant sequences:

For each sample a master mix was prepared. All required components came from the BIOTAQ™ PCR Kit (Cat. No. 21060), and were handled according to the manufacturer's instructions. PCR reactions were performed according to the annealing temperature of the respective primers and the length of the amplicon.

ham-3(he159)	**primer fw**	GAGAAGGAAGGCGACGATGC
	primer rev	GAGACTTTGCTCCAGCTCGG
ham-3(tm3309)	**primer fw**	CAAGATTCAACCATCCGGTA
	primer rev	GGATCAGGCTGTTGCAAGAGTTGATGAAG
swsn-2.2(ok3161)	**primer fw**	GACACCAGGAAGTGCTC
	primer rev	TACCTCGAGCAGGTCCGAATTCTGGC
swsn-2.2(tm3395)	**primer fw**	GACACCAGGAAGTGCTC
	primer rev	AACTCGTGTCGCTTCTGGTT

Master Mix:

10x Reaction buffer* (µl)	2.5
10mM dNTPs* (µl)	1
Primer fwd (µl)	1.25
Primer rev (µl)	1.25
$MgCl_2$* 50mM **(**µl)	1
BIOTAG DNA Polymerase* (µl)	0.2
template (µl)	1
H_20* (µl)	16.8
total Volume (µl)	25

* BIOTAQ™ PCR Kit

Program:

Initial Denaturation	2 min.	96°C
Denaturation	30sec.	96°C
Annealing	30sec.	X*
Elongation	X**	72°C
Final Elongation	10min.	72°C

* depends on Tm of primers

** depends on length of amplicon
(BIOTAQ™ DNA Polymerase transcribes 0.5kb/min)

MM.2.2. Sequencing of the novel allele *ham-3(he159)* and the point mutation *ham-3(n1654)*

Primers flanking the mutation were designed and PCR performed with lysates of the worms to be sequenced. The PCR product was applied on a 1% agarose gel and the band of the expected size excised with a scalpel.

The DNA was extracted from the gel using the QIAquick Gel Extraction Kit (Qiagen, Cat. No. 28704) according to the manufacturer's instructions. The concentration of the DNA solution was determined using a Nanodrop ND-1000 spectrophotometer and the reaction mix prepared for forward and reverse primer of each sample. The sequencing reaction was performed in a thermocycler and the product sent to the IDIBELL sequencing facility.

Master Mix:

Big dye (µl)	1
Buffer (µl)	1
fw/rev primer (µl)	0.5
DNA (ng)	500
H_20 up to 10µl	

Sequencing reaction:

96°C	1min.
96°C	30sec.
50°C	5sec.
60°C	4min.
25 cycles	

he159	**primer fw 1**	CAACAAAAGCTGCATGCGCC
	primer rev 1	CCAGTTTACAGGTCGGCAGAGGG
	primer fw 2	GAGAAGGAAGGCGACGATGC
	primer rev 2	GAGACTTTGCTCCAGCTCGG
n1654	**primer fw 1**	CAAACTCAAGCGCGGCCAC
	primer rev 1	TTTGCTCCAGCTCGGCTCGTT
	primer fw 2	GCAGGGGCCAAGATTCAACCATC
	primer rev 2	GGCATATCGCTTTTTCTTTTTCGGAGG

MM.2.3. Reverse-Transcription PCR of gene products encoded by *ham-3* and *swsn-2.2* mutant alleles

RNA isolation:

Worms were harvested with M9 and washed several times (1.500rpm; 1min.). To remove bacteria from the gut, the animals were incubated for 30min. at RT with agitation and washed again. The worm pellet was resuspended in the 7x volume of TRI Reagent® (Cat. No. TR-118) and vigorously vortexed. Afterwards 5 freeze/thaw cycles were performed using dry ice combined with 96% EtOH and a water bath at 37°C. The suspension was vigorously vortexed for 30sec., and let stand at RT for 30sec. This step was repeated 5 times.

After 5min. incubation at RT, the sample was mixed with chloroform and vortexted. The quantity of chloroform depended on the amount of TRI Reagent® initially used (0.2ml chloroform/1ml TRI Reagent®).

Phase separation was achieved by incubation of 15min. at RT, followed by centrifugation (13.200rpm; 15min; 4°C). The aqueous phase was transferred to a new Eppendorf, united with isopropanol (0.5ml/ml TRI Reagent®) and incubated at RT for 10min. Afterwards the RNA was pelleted (13.200rpm; 30min.; 4°C) and washed in 75% ethanol (diluted with DEPC-water) (9.000rpm; 5min.; 4°C). The pellet was air-dried and subsequently resuspended in 30µl DEPC-water. The concentration and purity of the RNA was determined using a Nanodrop ND-1000 spectrophotometer.

DNase treatment:

To eliminate DNA contaminations, the DNAse I, Amplification Grade system (Invitrogen™, Cat. No. 18068-015) was used. 1µg RNA was united with 1µl DNAse I in 1xDNAse I Reaction buffer (total reaction volume 10µl) and incubated for 30min. at 37°C. Afterwards 1µl 25mM EDTA was added and the sample incubated for 10min. at 65°C to stop the reaction.

cDNA synthesis:

For each sample a master mix was prepared using the RevertAid H Minus First Strand cDNA Synthesis Kit (Thermo Scientific, # K1612) and incubated for 1h at 42°C and 5min. at 25°C.

Master Mix:

RNA template (from previous reaction) (µl)	11
5x RT reaction buffer (ul)	1
dNTP mix 10mM (µl)	2
oligo(dT) Primer 100uM (µl)	1
RiboLock RNase Inhibitor (20u/ul) (ul)	1
RevertAid H Minus M-MuLV Reverse Transcriptase (ul)	1

Amplification of cDNA:

To avoid the amplification of genomic DNA at least one primer was designed to span an exon/exon junction. cDNA of heterozygote or wild type animals was used as control.

ham-3(he159)	**primer fw**	TCAACCATCCGGCAACACCACAG
	primer rev	TTTGCTCCAGCTCGGCTCGTT
ham-3(tm3309)	**primer fw**	TCAACCATCCGGCAACACCACAG
	primer rev	TTTGCTCCAGCTCGGCTCGTT
ham-3(1654)	**primer fw**	TCAACCATCCGGCAACACCACAG
	primer rev	GGATCAGGCTGTTGCAAGAGTTGATGAAG
swsn-2.2(ok3161)	**primer fw**	CATTCTAGAGACACCAGGAAGTGCTC
	primer rev	TACCTCGAGCAGGTCCGAATTCTGGC
swsn-2.2(tm3395)	**primer fw**	CATTCTAGAGACACCAGGAAGTGCTC
	primer rev	AACTCGTGTCGCTTCTGGTT
act-1	**primer fw**	TTGAGCACGGTATCGTCACCAACT
	primer rev	TCAGCGGTGGTGGTGAAAGAGTAA

MM.2.4. *In silico* analyses of mutant alleles

Genomic sequences of *ham-3*, *swsn-2.2* and their mutant alleles were downloaded from “worm base” (www.wormbase.org) or, in the case of the novel *ham-3* allele *he159*, determined by sequencing. Alignments were done with “Blast” (www.ncbi.nlm.nih.gov/blast/) and virtual translation into protein sequences with “Expasy” (www.expasy.org/translate).

MM.2.5. Western blots

Sample preparation:

Worms were harvested with M9 and washed at least twice (1500rpm; 1min.). After the last washing step as much supernatant as possible was removed and the equal volume of 2x Lysis buffer added to the worm pellets. The samples were cooked at 95°C for 10min. After spinning down remaining solid particles (13.000rpm; 2min.), the protein solutions were transferred to fresh Eppendorf tubes. In order to perform western blots with the same protein amount of all samples, protein concentrations were measured with the BioRad DC protein assay (Cat. No. 500-0113-15) following the manufacturer's instructions. The required quantities were brought to a volume of 16µl with 1x Lysis buffer and united with 4µl 5x Laemmli buffer before applying them onto the SDS gel.

1x Laemmli:

Tris-HCl 60mM; pH 6.8
2% SDS
5% β-Mercaptoethanol
0.005% Bromophenol blue
5% Glycerol

2x Lysis buffer:

4%SDS
Tris-HCl 100mM; pH 6.8
2% Glycerol
Protease and phosphates inhibitors
(Roche, Cat. No. 1187350001)

SDS-Page:

The concentration of the acrylamide gel was chosen according to the size of the protein(s) to be detected. After pouring the resolving gel, it was covered with isopropanol to flatten the surface and prevent its drying out. Rests of isopropanol were removed by flushing with sterile water before pouring the stacking gel. The gel was transferred to a cuvette with 1x TGS buffer. All slots were filled with equal volumes of either protein samples in 5x Laemmli buffer or 1x Lysis buffer with 5x Laemmli buffer to provide an even run. Gels were run on 120V for approximately 1h.

	Resolving gel			**Stacking gel**
% Polyacrylamide	7.5	10	15	4
H_2O (ml)	5.5	4.9	3.6	6
Tris-HCl 1.5M pH 8.8 (ml)	2.5			-
Tris-HCl 1.5M pH 6.8 (ml)	-			2.5
10% SDS (µl)	100			
Acrylamide/Bis-acrylamide* (37.5:1) (ml) (AppliChem; Cat. No. A3658)	1.9	2.5	3.8	1.4
10% APS (µl)	20			
TEMED (µl)	40			

1x TGS:

Tris OH 25mM; pH 8.3
Glycine192mM
0.1% SDS

Transfer:

The extracted proteins were transferred to the membrane in 1xTransfer buffer (300mA; 1h). To confirm the success of the process, the membrane was subsequently stained with Ponceau S

(5min.; RT; with agitation). De-staining was achieved by flushing the membrane several times with sterile water.

Ponceau:

0.5% Ponceau (w/v)
1% Glacial acetic acid

1xTransfer buffer

Tris OH 50mM; pH 8.3
Glycine 386mM
20% MeOH

Blocking and incubation with primary antibody:

The membrane was blocked in 5% non-fat milk in TBS-t for 1h at RT. Subsequently the primary antibody (see table below) was diluted in the same solution and incubated with the membrane o/n at 4°C with agitation. The membrane was washed three times with TBS-t for 5min. and incubated with the respective secondary antibody in the same buffer for 45min. at RT. Afterwards two washing steps with TBS-t and one with TBS were performed.

1xTBS:

Tris-HCl 100mM; pH 6.8
NaCl 137mM

TBS-t

TBS
0.1% Tween-20
Thermo Scientific (# 3604596)

Reference	Commercial	Feature	Target	Species	Dilution
Q5536	SDIX	1ary	SWSN-2.2*	rabbit	1:500
69100	MP Biomedicals	1ary	ACT-1	mouse	1:500
P 0448	Dako	2ary	α-rabbit	goat	1:2000
P 0260	Dako	2ary	α-mouse	rabbit	1:2000

* The α-SWSN-2.2 antibody was generated on our request

Developing of the films:

1% Enhancer solution was added to the required volume of Luminol (2ml per membrane to be developed) and applied on the membrane. After one minute of incubation, the membrane was exposed to autoradiographic films (CL-XPosure™ Films, Cultek S.A.)

Luminol:

Luminol sodic (Sigma A-4685) (mg)	125
Tris-HCl 1.5 M pH 8.8 (ml)	33.25
Hydrogen peroxide (µl)	155
H_2O (ml)	466.8

Enhancer p-CU

p-coumaric acid (Sigma-9008) (mg)	27.5
DMSO 99.5% (Sigma 41639) (ml)	25

MM.3. Expression during development

MM.3.1. Reverse-Transcription PCR

Sodium hypochlorite treatment (Bleaching):

The eggs of *C. elegans* are surrounded by a cuticle protecting them from harmful environmental factors such as chemicals. This feature is used to obtain synchronized populations. Treatment of pregnant worms with bleaching solution causes the degradation of adult tissues, but does not harm the embryos if stopped in time. Since L1 larvae that hatch in the absence of food do not start post-embryonic development, all larvae are in the same developmental stage when seeded (Porta-de-la-Riva et al., 2012).

Mixed populations with gravid hermaphrodites were harvested in M9, washed several times (1500rpm; 1min.) and resuspended in 3ml buffer. Digestion of the mothers was achieved by adding the same volume of bleaching solution and incubation for approximately 5min. under vigorous shaking. To avoid an excess of the reaction and thereby damage of the embryos, the destruction of the adult tissue was monitored under the dissection microscope. The reaction was quenched by addition of M9. At least three washing steps (1.500rpm; 1min.) were performed to get rid of rest of the bleaching solution. To remove remaining carcasses, the solution was filtered (BD Falcon™ Cell Strainers, 40µm). The embryos were incubated on 15°C for 24h under rotation.

Bleaching solution:

NaOH 1N (ml)	2.5
Hypochlorite solution (ml)	1
ddH_2O (ml)	0.5

Preparation of samples:

Synchronized L1 larvae were seeded on NGM plates and incubated on 20°C. Fractions of the animals were harvested in different developmental stages. RNA isolation and cDNA synthesis was performed as described in MM.2.3.

Reverse-Transcription PCR:

To avoid the amplification of genomic DNA at least one primer was designed to span an exon/exon junction. Primers targeting the housekeeping gene *act-1* were used to provide a loading control. PCR products were analyzed on a 1% agarose gel.

ham-3	**primer fw**	TCAACCATCCGGCAACACCACAG
	primer rev	TTTGCTCCAGCTCGGCTCGTT
swsn-2.2	**primer fw**	CATTCTAGAGACACCAGGAAGTGCTC
	primer rev	TACCTCGAGCAGGTCCGAATTCTGGC
act-1	**primer fw**	TTGAGCACGGTATCGTCACCAACT
	primer rev	TCAGCGGTGGTGGTGAAAGAGTAA

MM.3.2. qPCR

Preparation of samples:

Worms were cultivated as described in MM.3.1. cDNA samples produced (described in MM.2.3) and diluted 1:10. For reactions targeting housekeeping genes, cDNA templates were diluted 1:100.

Primer design:

Primers were designed that span exon/exon junctions to avoid the amplification of genomic DNA. All primers had approximately the same annealing temperatures (ideally 60°C), a GC-content of 40-60% and produced amplicons of roughly the same length (100-120bp).

qPCR:

For the quantification of gene expression levels, the Roche LightCycler 480 Instrument I and the LightCycler 480 SYBR green I Master Kit (Cat. No. 04 707 516 001) were used according to the manufacturer's instructions. Gene expression was normalized to transcript levels of the housekeeping gene *act-1*.
To exclude contaminations, for each primer pair a water sample was run in parallel. All experiments were performed in triplicates.

Master Mix:

cDNA (1:10 or 1:100) (µl)	2
SYBR green (µl)	5
Primer fw (µl)	1
Primer rev (µl)	1
H_2O (µl)	1

ham-3	**primer fw**	TCAACCATCCGGCAACACCACAG
	primer rev	CGGCATATCGCTTTTTCTTTTTCGGAG
swsn-2.2	**primer fw**	CCTATGGGACACCAGGAAGTGCTC
	primer rev	CCGCATACTTCTTCTTTTTCGGCAATGG
act-1	**primer fw**	GAGGCCCAATCCAAGAGAGGTATC
	primer rev	GGGGCAACACGAAGCTCATTGTAG

MM.4. Staining methods

MM.4.1. Fixation with Carnoy's solution

The animals were flushed from the plate with PBS-t, washed until all bacteria was removed and pelleted (1500rpm; 1min.). The supernatant was discarded and the 50x volume of Carnoy's solution added to the pellet. Fixation was performed at least for 1h, then the worms were spinned down and as much supernatant as possible was removed. Re-hydration was achieved by addition of increasing amounts of PBS-t over at least 1h. Subsequently, two more washing steps with PBS-t were performed, the worm resuspended in a small quantity of PBS-t and dropped onto a microscope slide.

Carnoy's solution		**PBS-t**
EtOH (ml)	3	**PBS**
Acetic acid (ml)	1.5	**0.05% Tween-20**
Chloroform (ml)	0.5	

MM.4.2. Fixation with EtOH:

10µl M9 were applied onto a microscope slide and worms were transferred to the drop using a worm picker. Using a filter paper, as much liquid as possible was soaked off, whereby drying-out of the worms was avoided. 10µl 90% EtOH was added. After several minutes, the procedure was repeated and the EtOH allowed to evaporate completely before DAPI staining.

MM.4.3. DAPI staining:

A drop of DAPI Fluoromount-G (Southern Biotech; Cat. No. 0100-20) was applied onto the fixed animals and the sample sealed with nail polish and a coverslip. After at least 15min. of incubation, the stained worms were studied under the fluorescence microscope.

MM.4.4. Staining of germ cells

Animals were harvested with M9 and washed several times with PBS-t in a glass multi-well (Pyrex® Plate, Cat. No. 71563-01). As much supernatant as possible was removed and Levamisole solution added to paralyze the worms. When the animals were immobilized, two syringes were used to cut their necks causing the expulsion of the intact gonad arms. For fixation, the dissected gonads were incubated for 20min. in 4% Formaldehyde solution. After three washing steps with PBS-t, DAPI staining was performed as described in MM.4.3.

Formaldehyde solution

4% Formaldehyde (in PBS-t)

Levamisole 0.3mM (in PBS-t)

MM.5. RNA-mediated interference (RNAi)

MM.5.1. RNAi by feeding

RNAi feeding libraries:

Two different RNAi libraries exist that together cover 94% of the *C. elegans* genome (Ahringer, 2006).
The group of Julie Ahringer developed a library under the usage of genomic DNA fragments that were amplified by PCR (Kamath & Ahringer, 2003). Fragments encoding genes were cloned into the vector L4440 and transformed into the bacterial strain HT115. This *E. coli* strain lacks functional RNAse III and thereby allows accumulation of large quantities of dsRNA in the cell.
The second RNAi library was generated by the group of Marc Vidal and used cDNA as template for amplification (Rual et al., 2004). Thus, it contains only clones targeting expressed genes. As for the Ahringer library, also the "ORFeome" library employs HT115 as bacterial host strain for the L4440 vector. Thus, in both cases the expression of the respective insert is controlled by a promoter inducible by IPTG that must be added to the RNAi plates.

RNAi clones:

The position of a desired clone in the RNAi feeding libraries was searched on "wormbase" (www.wormbase.org). A streak of the respective clone was made on a LB-Ampicillin plate (50µg/ml) and incubated o/n at 37°C. To confirm that the insert had the expected length, single-colony PCR was performed using primers flanking

the multiple cloning site of the inserts. For final validation the respective band were sequenced.

In the case of *swsn-2.2* no RNAi clone was available in any of the two RNAi libraries. Thus, cDNA of wild type (N2) animals was used as template and PCR using specific primers for *swsn-2.2* was performed. Using the MultiSite Gateway Vector Construction Kit the insert was cloned into the L4440 vector and transformed into the bacterial strain DH5α. PCR was performed to test that the insert had the expected length and, for final validation, its identity was confirmed by sequencing. Afterwards the plasmid was transformed into the bacterial host strain HT115.

For detailed information about the *ham-3* and *swsn-2.2* RNAi clones used for this study, see Annex 5.

L4440 sequencing	**primer fw**	TCAACCATCCGGCAACACCACAG
	primer rev	CGGCATATCGCTTTTTCTTTTTCGGAG

Preparation of RNAi plates:

Single colonies of the respective RNAi clones were inoculated in 5ml selective media and allowed to grow at 37°C o/n. The culture was concentrated 2x, seeded on RNAi plates and allowed to grow for 24h at RT or for 6h at 37°C. Plates were stored at 4°C.

Selective media:

LB media		
Tetracycline (12.5mg/ml) (ml)	1	
Amplicline (50mg/ml)	1	

RNAi plates:

Bacto-Agar™ (g)	17	
NaCl (g)	3	
Bacto- Peptone™ (g)	2.5	
ddH_2O (ml)	975	Autoclave
Kalium phosphate buffer 1M (ml)	25	
$CaCl_2$ 1M (ml)	1	Add after cooling down
$MgCl_2$ 1M (ml)	1	
Cholesterol (5mg/ml) (ml)	1	
Tetracycline (12.5mg/ml)	1	
Ampicilin (50mg/ml)	1	Add after cooling down
IPTG 3mM (ml)	1	

RNA-mediated interference:

Worm populations were synchronized as described in MM.3.1. In general the experiments were performed at 25°C. Experiments with temperature-sensitive mutants were done at 20°C.

MM.5.2. RNAi by microinjection

***In vitro* transcription of dsRNA for microinjection:**

For *in vitro* transcription the template must contain a RNA polymerase promoter site. The vector L4440 used for both *C. elegans* RNAi libraries contains two RNA polymerase T7 promoters flanking the multicloning site that allow the synthesis of the transcribed *sense* and *antisense* strands of the cloned fragment. Thus, RNA clones of the feeding libraries can be used as templates for the synthesis of dsRNA.

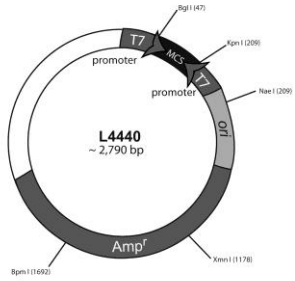

T7 promoter CCGGCAGATCTGATATCATCGATGAATTCGAGCTCCACCGCGGTGGCGGCCGCTC

TAGATCTAGAACTAGTGGATCCCACCGGTTCCATGGCTAGCCACGTGACGCGTGGATCCCCCGGGCTGCA

GGAATTCGATATCAAGCTTATCGATACCGTCGACCTCGAGGGGGGGCCCGGTACCCAATT T7 promoter

Synthesis of dsRNA:

The respective RNAi clones were obtained as described in MM.6.1. and PCR performed using primers flanking the RNA polymerase T7 promoters adjacent to the multiple cloning site of the L4440 vector. For *in vitro* transcription the MEGAscript® T7 Kit (Cat. No. AM1333) was employed. The reaction mix was prepared at RT to avoid precipitation of the spermidine. The samples were incubated for 3h on 37°C, supplied with 1µl TURBO DNase and incubated for 15min. on the same temperature.

L4440 RNAi	**primer fw**	CAGTCACGACGTTGTAAAACG
	primer rev	GCAACCTGGCTTATCGAAAT

Reaction Mix

ATP solution (µl)	2
CTP solution (µl)	2
GTP solution (µl)	2
UTP solution (µl)	2
10x Reaction Buffer (µl)	2
PCR-product template (µg)	0.1-0.2
Enzyme mix (µl)	2
DEPC- water	up to 20µl

Recovery of RNA:

The RNA was precipitated by addition of 30µl DEPC-water and 30µl LiCl Precipitation Solution, followed by incubation for 30min. at -20°C. The RNA was pelleted and (13.000 rpm; 4°C; 15min.), washed with 70% EtOH and resuspended in 30µl DEPC-water. Double strand hybridization was achieved by heating the sample at 72°C for 10min. After cooling down, the RNA quantity was determined using a Nanodrop ND-1000 spectrophotometer. To confirm the quality of the dsRNA, 2µl were run on an agarose gel.

Microinjection:

The dsRNA was brought to the desired concentration with M9 and loaded into the injection needle (Femtotips® microinjection capillaries, Eppendorf, Cat. No. 5242 952.008) using a special pipette tip (Microloader, Eppendorf, Cat. No. 5242 956.003). The needle was installed in the micromanipulator and the tip, if required, opened by pushing it slightly against a glass cover slight.
Animals in L4/young adult stage were selected and transferred into a drop of Halocarbon oil 700 (Sigma; Cat. No. H8898) on an agarose pad. The worms were allowed to gravity settle in the drop and slightly pressed to the surface of the agarose pad with a picker to achieve their attachment to the agarose surface.
The dsRNA was injected into the gonads or the intestine of the immobilized worms. After injecting all animals, M9 was applied onto this drop, so that the worms were released from the oil. The animals were carefully transferred into a drop M9 on a NGM plate and allowed to recover at 15 °C o/n. The following day they were singled out and, in order to synchronize the progeny, transferred to

new plates twice a day over two days. The phenotypes were studied in the F1 progeny.

MM.6. Generation of HAM-3 transgenics

For the generation of transgenic HAM-3 animals, the transgene [P*ham*3:GFP:*ham-3*ORF + 3'UTR + P*myo*3:mCherry + P*rab3:*mCherry] was injected into the germlines of wild type animals in young adult stage. Microinjection was performed as described in MM.6.2. Transgenic animals in the F1 generation could be identified due to the presence of the red fluorescent protein mCherry expressed in muscle and neuronal cells.

Injection mix:

P*ham*-3:GFP:*ham-3*ORF+3'UTR (ng/µl)	2
P*myo*-3:mCherry (ng/µl)	5
P*rab-3:*mCherry (ng/µl)	10
DNA ladder	up to 100ng/µl

MM.7. Immunostaining

MM.7.1. Immunostaining of gonads

Gonads were dissected and fixated in a spot plate as described in MM.4.4. To prevent drying out of the samples, all incubation steps were performed in a sealed tupper box with water-soaked paper towels providing humidity.

After three washing steps with PBS-t, blocking in PBS-t plus BSA was performed for 1h at RT. Afterwards, the two primary antibodies (specific and control antibody, see table below) diluted in the same solution (1:500) were added and incubated with the fixed gonads o/n at 4°C. Afterwards the samples were let acclimatize to RT for 1h and three washing steps were performed. The respective secondary antibodies diluted in PBS-t (1:500) were applied and the samples incubated for 2h at RT. After three additional washing steps, the gonads were counter-stained with DAPI as described in M.4.3.

MM.7.2. Immunostaining of embryos:

Preparation of sample:

Worms were harvested with PBS and washed several times. A drop of worm suspension was transferred to a polylysine coated slide and worms were allowed to settle for at least 1min. As much liquid as possible was removed with a pipette or filter paper. A coverslip was placed on the microscope slide at the right angle, so that the edge of the coverslip extended over the edge of the slide. By giving pressure on the coverslip with a pair of forceps, the

gravid animals were broken and the embryos released. To avoid damage of the embryos by excessive mechanic pressure, this process was performed under the microscope.

Preparation of polylysine coated slides:

- Covering of microscope slide with 50µl 1:10 polylysine solution (Sigma)
- Incubation of 5-10min. at RT
- Bake slides at 60°C for 15 min.

Fixation:

The slide was placed onto a pre-chilled aluminum block. In order to keep the block at the lowest temperature possible, it was located in a Styrofoam box and embedded in dry ice. When the sample was completely frozen (approx. 10min.), the coverslip was fitfully popped off and the slide immediately transferred into coplin jar with pre-chilled methanol. After 20min. incubation at -20°C, the slide was transferred to another coplin jar with pre-cooled acetone and incubated for 10min. at the same temperature.

For all following washing steps, as well as for the dilution of the antibodies, PBT was used. To avoid drying out of the samples, incubation steps were performed in a humidity chamber. The slides were three times washed for 10min. and pre-incubated in PBT for 30min. The respective primary antibodies were diluted and 30µl applied on the samples. The slides were covered with parafilm and incubated at 4°C o/n in a humidity chamber. Three washing steps of 10min. were performed, the secondary antibodies diluted and 30µl of the dilution applied on the samples. After 2h of incubation

on RT, three more washing steps of 10min. were performed and the sample was DAPI-stained as described in MM4.3.

Reference	Commercial	Feature	Target	Species	Dilution
Q5536	SDIX	1ary	SWSN-2.2	rabbit	1:500
JL-8	Clontech	1ary	GFP	mouse	1:500
OICD14	DSHB	1ary	Germline P-granules	mouse	1:500
KT23	DSHB	1ary	Nuclear membrane	mouse	1:500
A11001	Molecular Probes, Inc.	2ary	mouse-AB	goat	1:500
A11001	Molecular Probes, Inc.	2ary	rabbit-AB	goat	1:500

MM.8. Study of embryonic phenotypes

MM.8.1. 4-D microscopy

The 4D microscope system (multifocal, time-lapse video recording system) enables the recording of the complete development of a single embryo. Using the appropriate software, single cell division events, the exact position of cells and their migration paths can be analyzed. Thereby, the development of the embryonic lineages, the fate of single cells and other events during embryonic development can be monitored.

MM.8.2. Lineage analysis

For this study, the development of *ham-3(he159)*, *ham-3(n1654)* and *swsn-2.2(ok3161)* embryos was recorded, using a Leica DM 6000 microscope fitted with Nomarski. The experiments were performed with embryos derived from homozygote mothers by dissection. Recording was performed at 25°C.

MM.8.3. Study of engulfment of apoptotic bodies

The entire development of *ham-3(he159)* embryos that did not suffer embryonic lethality was recorded using a Leica DM 6000 microscope fitted with Nomarski. This system combined with the appropriate software enables the monitoring of the fate of single lineages, including the apoptosis of certain cells, followed by the engulfment of their corpses. The engulfment time was compared to wild type embryos.

MM.9. RNA-seq

N2 were fed for 36h at 25°C with *ham-3* and *swsn-2.2* RNAi clones or a control. Subsequently the RNA was isolated as described in MM.2.3. To remove eventual contaminations with DNA, the PureLink® DNase Set (Cat. No. 12185-010) was used according to the manufacturer's instructions.

The samples of the first biological replicate were multiplexed in libraries for RNA-Sequencing Illumina Hiseq 2000 platform in the CNAC (Centre National d' Anàlisis Genòmica) sequencing facility at Barcelona Parc scientific. For the generation of BAM files more than 50 millions of reads per sample were mapped against the *C. elegans* worm version WS236 following the GEMTools pipeline (http://gemtools.github.io/). The files were analyzed using the Seqsolve software.

For the second biological replicate the worms were cultivated as described above, the RNA equally isolated and purified using the mir Vana™ miRNA Isolation Kit (Ambion). The purified RNA was analyzed in the in the CIBIR (Centro de Investigación Biomédica de La Rioja) using a Biorad Experion Bioanalyzer. Samples were multiplexed in libraries for RNA-sequencing using the Illumina *TruSeq RNA Sample Preparation Kit*. Quality of the libraries was confirmed and sequenced in the Illumina Genome Analyzer IIx to generate 150bp reads resulting in BAM files with approximately 10 millions of reads per sample.

For both RNA-seq experiments the BAM files were analyzed with the Seqsolve software filtering out reads mapping in multiple places in the genome.

For the validation of the results obtained by RNA-seq, qPCR was performed as described in MM3.2.

dod-24	**primer fw**	GAATTGCTCCAGAACGATGACTAC
	primer rev	CGAATAAACGACTTTGAAGCC
dod-21	**primer fw**	GATGATGCTCAATGACAATGACC
	primer rev	GACCAAACAACTTTGAATCCG
dod-17	**primer fw**	CTGGAAATGGTTGCACACTTG
	primer rev	CTGCCCATTATCCAGCTGAG
clec-41	**primer fw**	GGATTTGCTCCGGGATACC
	primer rev	CAGATAAAGTTCAGGCTCATTGTG
gst-38	**primer fw**	GGAAAAACCCCATACAACCAG
	primer rev	GCTTCTTCCCATCTGCTCTTTC
act-1	**primer fw**	GAGGCCCAATCCAAGAGAGGTATC
	primer rev	GGGGCAACACGAAGCTCATTGTAG

MM.10.Co-Immunoprecipitation of SWSN-2.2 and interaction partners

Cultivation of worms:

OP50 cultures were grown o/n on 37°C under agitation. The cultures were 10x concentrated, seeded on 150mm NGM plates and allowed to grow for 24h on RT.
N2 mixed populations were grown on at least six of these plates on 25°C and harvested before they lacked food or the plates became too crowded.

Preparation of protein sample:

Worms were harvested with M9 and washed several times to get rid of bacteria (1500rpm; 1min.). The last two washing steps were performed in IP buffer with phosphatase and protease inhibitors. After the last wash, the worm pellet was resuspended in the 2x volume of IP buffer. Small quantities of the worm suspension were dropped into a metal mortar with liquid nitrogen using a Pasteur pipette. Using pre-cooled mortar and pistil, the pearls were stamped to fine powder in liquid nitrogen, transferred to Eppendorf tubes and allowed to thaw on ice. By centrifugation (13.000rpm; 2min.) solid particles were separated from the proteins extract. The protein concentration of the sample was determined with the BioRad DC protein assay following the manufacturer's instructions.

Preparation of antibody-conjugated beads:

For each reaction (specific antibody and unspecific control) 2mg of Dynabeads were weighed in and washed twice in 1ml buffer C1. Since the pearls are magnetic, they can be pelleted by placing the

Eppendorf containing the beads solution in a magnetic rack (DynaMag™-2 magnet, Life Technologies, Cat. No. 12322D). After about one minute the beads concentrate on the back of the eppendorf and the supernatant can be easily removed. After washing, the beads were resuspended in C1 buffer containing the respective antibody (5µg/mg beads) to reach a concentration of 2mg beads/100µl buffer. The same volume of C2 buffer was added, thereby brining the solution to a final concentration of 1mg beads/100µl buffer. The beads and the respective antibodies were incubated at 37°C for 24h under rotation. Afterwards the beads are washed with HB, LB and SB buffer by resuspending them carefully. A last washing step in SB buffer was performed on RT for 15 min. under agitation. Subsequently the beads were resuspended in SB buffer to achieve a concentration of 1mg beads/100µl. Afterwards the pearls were washed twice in 900µl Extraction buffer. All required buffers came with the Dynabeads®Co-immunopreciptation Kit (Life Technologies, Cat. No. 14321D)

Immunoprecipitation and sample preparation for mass spec:

For both samples an initial amount of 3mg total protein was brought to a volume of 1ml with IP buffer plus phospatase and protease inhibitors. 1.5mg antibody-conjugated beads were washed twice with IP buffer, the protein sample added to the beads and incubated for 20min. on 4°C under rotation. Afterwards the pearls were washed three times with Extraction buffer and once with LWB.

Bound protein complexes were eluted by resuspending the pearls for 30sec. in 50µl Glycin pH2.5. Neutralization was achieved by adding 5µl Tris-HCl. To precipitate protein, the solution was united

with the 6-fold volume of ice-cold acetone and incubated at -20°C o/n. The sample was centrifuged (13.000rpm; 15min.) and the protein pellet washed in 90% ice-cold aceton (13.000rpm; 5min.). The pellet was air dried and stored at -20°C.

Check on success of precipitation:

To test if the precipitation of SWSN-2.2 was successful and specific, in parallel control reactions were performed with smaller amounts of the components. 1mg total protein was brought to a volume of 0.5ml and united with 0.5mg of antibody-conjugated pearls. Afterwards the bound protein complexes were dissolved by cooking the pearls in 50µl 2x Laemmli buffer 10min. on 95°C. During cooking, pearls were occasionally resuspended by pipetting. The pearls were removed by magnetic separation and the samples analyzed by western blotting as described in MM 2.5.

IP buffer* = Extraction buffer*

modified with: **NaCl** 100mM
Protease and phosphates inhibitors
(Roche, Cat. No. 1187350001)

Last wash buffer (LWB)*

modified with: **NaCl** 100mM
0.02% Tween-20

Glycin 0.2M pH 2.5

Tris-HCl 1M pH 10.4

* Dynabeads®Co-immunopreciptation Kit.

Strain Name	Genotype
BN311	*mel-28*::*gfp*
Bristol N2	*C. elegans* wild isolate; reference strain
BS3801	*rrf-1(pk1417)* I; *glp-1(oz264)* III
CB1370	*daf-2(e1370)* III
CER12	*cerEx06* [P*ham-3*:GFP:*ham-3*ORF + 3'UTR+P*myo-3*:mCherry+P*rab-3*:mCherry]
CER123	*ham-3 (he159)* III / hT2[bli-4(e937) let-? (q782)qIs48] I;III
CER30	*ham-3(he159)* III / hT2 [bli-4(e937) let-?(q782) qIs48]; rtIs18 [*elt-2p*::GFP+*osm-10*p::HtnQ150] (I; III)
CER31	*swsn-2.2(ok3161)*I / hT2 [bli-4(e937) let-?(q782) qIs48]; rtIs18 [*elt-2p*::GFP+*osm-10*p::HtnQ150] (I; III)
HA661	rtIs18 [*elt-2*p::GFP+*osm-10*p::HtnQ150] I
JK2049	*qIs19* [*lag-2p*::GFP::*unc-54 3'UTR* + *rol-6(su1006)*] V
MT12839	*lin-61(n3809)* I; *lin-8(n2731)* II
MT2124	*let-60 (n1046)* IV
MT3971	*ham-3(n1654)* III
OH11704	*ham-3(tm3309)* III / hT2 [*bli-4(e937) let-?(q782) qIs48*] I;III
RA440	*swsn-2.2(tm3395)* I / hT2 [*bli-4(e937) let-?(q782) qIs48*] I;III
SV329	*rol-1(e91) cyd-1(he116)*/ mnC1 *dpy-10(e128) unc-52(e444)* II
TJ356	*zIs356* [*daf-16p*::*daf-16a/b*::GFP + *rol-6*] IV
VC2789	*swsn-2.2(ok3161)*I / hT2[*bli-4(e937) let-? (q782)qIs48*] I;III

Index of abbreviations and acronyms

AC:	anchor cell
APS:	Ammonium persulfate
ATP:	Adenosine triphosphate
BAF:	BRG1- or HRBM-associated factors
Bag:	Bag of worms (phenotype)
BSA:	Bovine serum albumin
C. elegans:	*Caenorhabditis elegans*
Cdk:	cyclin dependent kinase
cDNA:	complementary DNA
CDS:	Coding DNA Sequence
CGC:	*Caenorhabditis* Genetics Center
CNAC:	Centre National d' Anàlisis Genòmica
CoIP:	Coimmunoprecipitation
DAPI:	4',6-diamidino-2-phenylindole
DEPC:	Diethylpyrocarbonate
DIC:	differential interference contrast
DNA:	Deoxyribonucleic acid
dsRNA:	double stranded RNA
DTC:	distal tip cell
E. coli:	*Escherichia coli*
EGF-like:	Epidermal growth factor
Egl:	Egg-laying-defect (phenotype)
Emb:	embryonic lethality (phenotype)
Emo:	Endomitotic oocytes (phenotype)
Evl:	Eversion of the vulva (phenotype)
F1:	Filial generation 1
G1 phase:	Growth 1/Gap1 phase
GFP:	Green Fluorescent Protein
H1:	Histone 1
H2A:	Histone 2A
H2B:	Histone 2B
H3:	Histone 3
H4:	Histone 4
HIL:	*hunchback* and Ikaros-like
HSN:	hermaphrodite-specific neurons

IGF:	insulin-like growth factor
IIS pathway:	insulin and insulin-like growth factor 1 signaling
IPTG:	Isopropyl-β-D-1-thiogalactopyranoside
L1-L4:	Larval stages 1 to 4
LB:	Lysogeny broth
Lva:	Larval arrest (phenotype)
MSP:	major sperm protein
Muv:	Multivulva (phenotype)
NGM:	Nematode growth media
NMD:	Nonsense Mediated Decay
N-terminal:	Amino-terminal
ORF:	Open Reading Frame
PBAF:	polybromo-associated BAF
PBS:	Phosphate-buffered Saline
PL3-Kinase:	Phosphatidylinositol-4,5-bisphosphate 3-kinase
PSA:	phasmid sock absent (phenotype)
PTC:	Premature Termination Codon
Pvl:	Protruding vulva (phenotype)
qPCR:	quantitative Real Time-Polymerase Chain Reaction
RNAi:	RNA-mediated interference
RNase III:	Ribonuclease III
RNA-seq:	RNA sequencing
RSC:	Chromatin structure remodeling
RT:	room temperature
RT-PCR:	Reverse-Transcription Polymerase Chain Reaction
Rup:	Rupturing vulva (phenotype)
S phase:	Synthesis phase
SDS:	Sodium dodecyl sulfate
SGP:	somatic gonad precursors
SWI/SNF:	Switching defective/Sucrose non-fermenting
SWIB:	SWI/SNF complex B
synMuv:	Synthetic Multivulva
TBS:	Tris-buffered Saline
TEMED:	Tetramethylethylenediamine
VC:	Ventral cord neuron
VPC:	Vulval precursor cells
Vul:	Vulvaless (phenotype)

Annex

A) *tm3309*

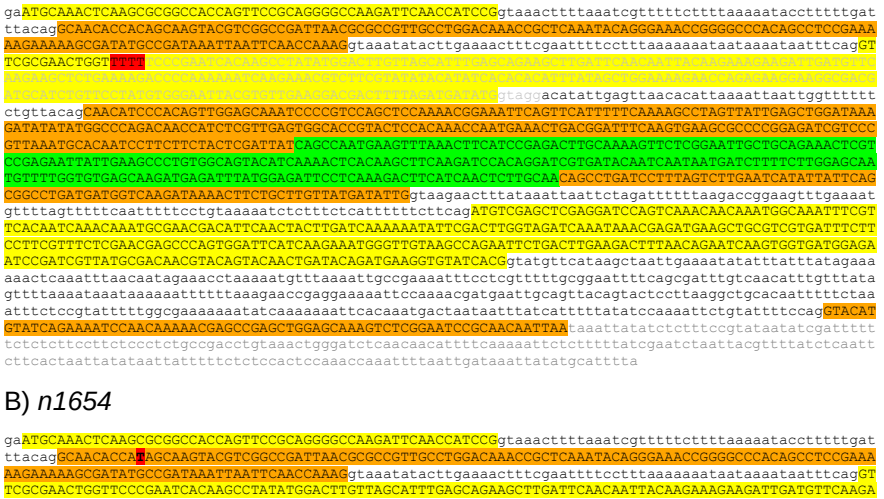

B) *n1654*

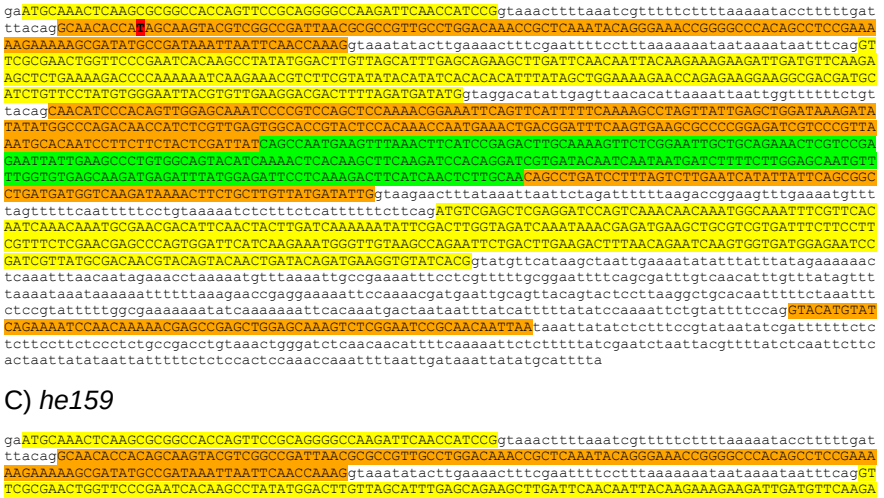

C) *he159*

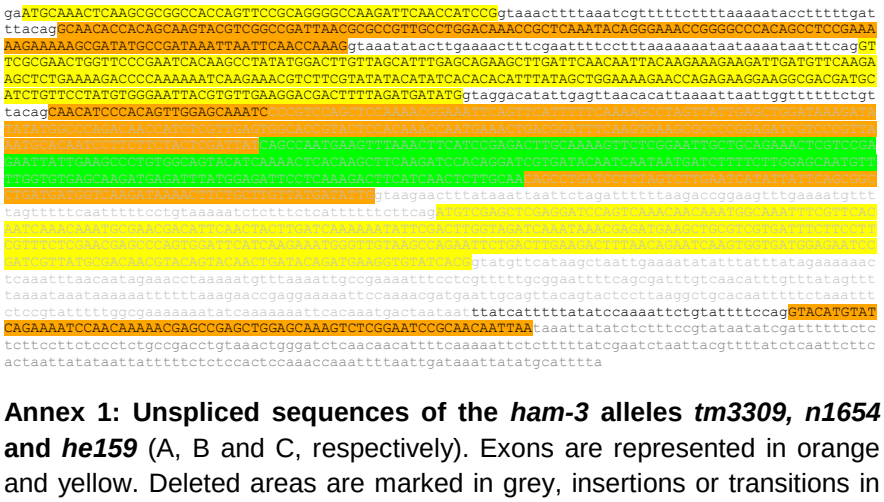

Annex 1: Unspliced sequences of the *ham-3* alleles *tm3309, n1654* and *he159* (A, B and C, respectively). Exons are represented in orange and yellow. Deleted areas are marked in grey, insertions or transitions in red letters. The SWIB/MDM2 domain is labeled in green.

A) Wild type

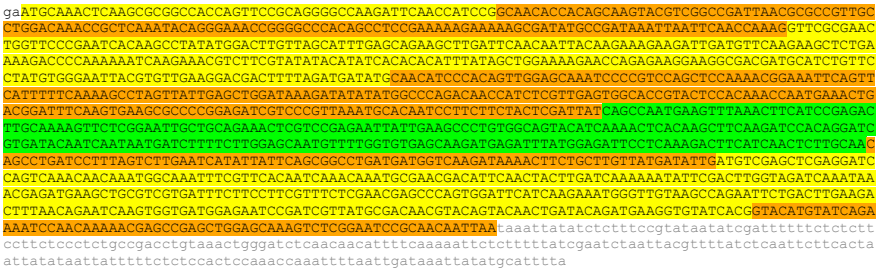

B) *tm3309*

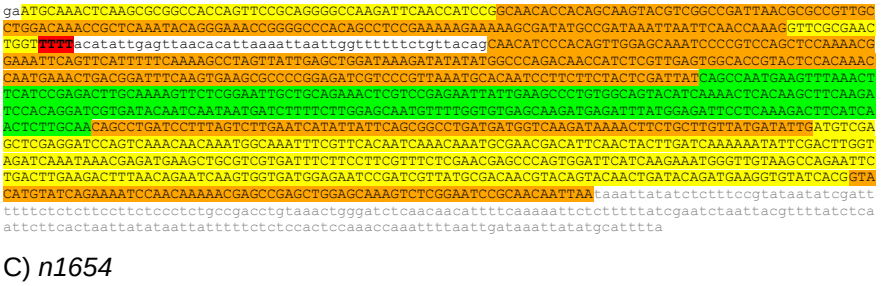

C) *n1654*

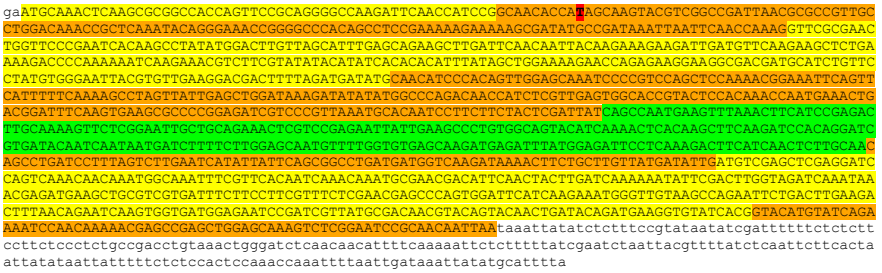

D) *he159*

Annex 2: **Spliced coding sequences of *ham-3* and the mutant alleles *tm3309*, *n1654* and *he159*.** Yellow and orange regions mark different exons. The green area labels the SWIB/MDM2 domain. Insertions or transitions are indicated in red. (A) Wild type *ham-3* sequence. (B) *tm3309* causes partial retention of the second intron and premature stop codons. (C) *n1654* presents a point mutation that produces a premature stop codon. (D) The deletion allele *he159* causes the loss of the sequence encoding the SWIB/MDM2 domain and partial retention of the last intron.

A) *ok3161*

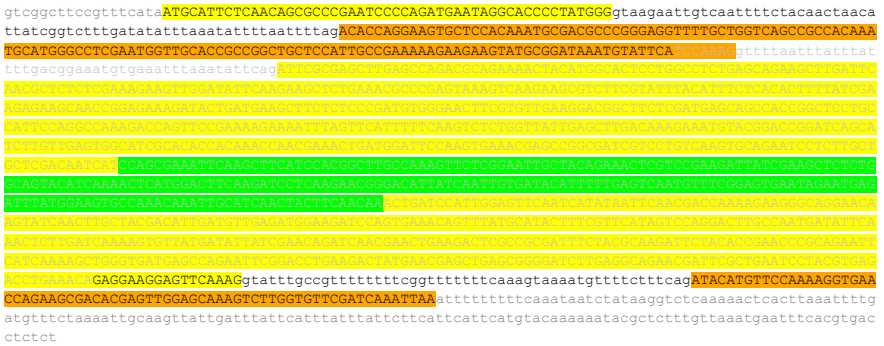

B) *tm3395*

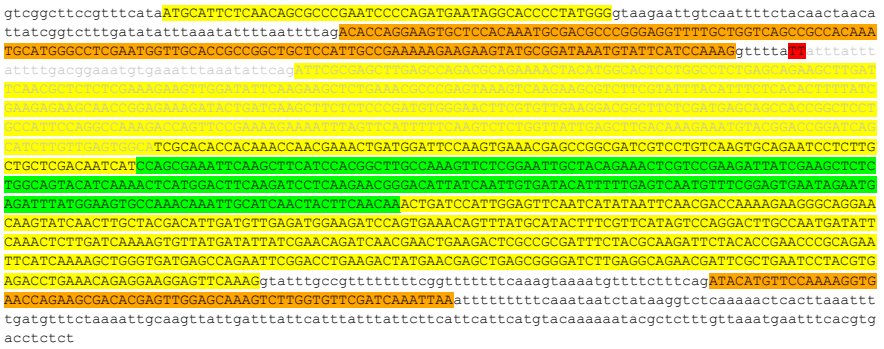

Annex 3: Unspliced sequence of the *swsn-2.2* alleles *ok3161 and tm3395* (A and B, respectively). Exons are represented in orange and yellow. Deleted areas are marked in grey and insertions in red letters. The SWIB/MDM2 domain is labeled in green.

A) Wild type

gtcggcttccgtttcataATGCATTCTCAACAGCGCCCGAATCCCCAGATGAATAGGCACCCCTATGGGACACCAGGAAGTGCTCCACAAATGCGACGC
CCGGGAGGTTTTGCTGGTCAGCCGCCACAAATGCATGGGCCTCGAATGGTTGCACCGCCGGCTGCTCCATTGCCGAAAAAGAAGAAGTATGCGGATAAA
TGTATTCATCCAAAGATTCGCGAGCTTGAGCCAGACGCAGAAAACTACATGGCACTCCTGGCCTCTGAGCAGAAGCTTGATTCAACGCTCTCTCGAAAG
AAGTTGGATATTCAAGAAGCTCTGAAACGCCCGAGTAAAGTCAAGAAGCGTCTTCGTATTTACATTTCTCACACTTTTATCGAAGAGAAGCAACCGGAG
AAAGATACTGATGAAGCTTCTCTCCCGATGTGGGAACTTCGTGTTGAAGGACGGCTTCTCGATGAGCAGCCACCGGCTCCTGCCATTCCAGGCCAAAGA
CCAGTTCCGAAAAGAAAATTTAGTTCATTTTTCAAGTCTCTGGTTATTGAGCTTGACAAAGAAATGTACGGACCGGATCAGCATCTTGTTGAGTGGCAT
CGCACACCACAAACCAACGAAACTGATGGATTCCAAGTGAAACGAGCCGGCGATCGTCCTGTCAAGTGCAGAATCCTCTTGCTGCTCGACAATCATCCA
GCGAAATTCAAGCTTCATCCACGGCTTGCCAAAGTTCTCGGAATTGCTACAGAAACTCGTCCGAAGATTATCGAAGCTCTCTGGCAGTACATCAAAACT
CATGGACTTCAAGATCCTCAAGAACGGGACATTATCAATTGTGATACATTTTTGAGTCAATGTTTCGGAGTGAATAGAATGAGATTTATGGAAGTGCCA
AACAAATTGCATCAACTACTTCAACAAACTGATCCATTGGAGTTCAATCATATAATTCAACGACCAAAAGAAGGGCAGGAACAAGTATCAACTTGCTAC
GACATTGATGTTGAGATGGAAGATCCAGTGAAACAGTTTATGCATACTTTCGTTCATAGTCCAGGACTTGCCAATGATATTCAAACTCTTGATCAAAAG
TGTTATGATATTATCGAACAGATCAACGAACTGAAGACTCGCCGCGATTTCTACGCAAGATTCTACACCGAACCCGCAGAATTCATCAAAAGCTGGGTG
ATGAGCCAGAATTCGGACCTGAAGACTATGAACGAGCTGAGCGGGGATCTTGAGGCAGAACGATTCGCTGAATCCTACGTGAGACCTGAAACAGAGGAA
GGAGTTCAAAGATACATGTTCCAAAAGGTGAACCAGAAGCGACACGAGTTGGAGCAAAGTCTTGGTGTTCGATCAAATTAAatttttttttcaaataat
ctataaggtctcaaaaactcacttaaattttgatgtttctaaaattgcaagttattgatttattcatttatttattcttcattcattcatgtacaaaaa
atacgctctttgttaaatgaatttcacgtgacctctct

B) *ok3161*

gtcggcttccgtttcataATGCATTCTCAACAGCGCCCGAATCCCCAGATGAATAGGCACCCCTATGGGACACCAGGAAGTGCTCCACAAATGCGACGC
CCGGGAGGTTTTGCTGGTCAGCCGCCACAAATGCATGGGCCTCGAATGGTTGCACCGCCGGCTGCTCCATTGCCGAAAAAGAAGAAGTATGCGGATAAA
TGTATTCAGAGGAAGGAGTTCAAAGATACATGTTCCAAAAGGTGAACCAGAAGCGACACGAGTTGGAGCAAAGTCTTGGTGTTCGATCAAATTAAattt
ttttttcaaataatctataaggtctcaaaaactcacttaaattttgatgtttctaaaattgcaagttattgatttattcatttatttattcttcattca
ttcatgtacaaaaaatacgctctttgttaaatgaatttcacgtgacctctct

C) *tm3395*

gtcggcttccgtttcataATGCATTCTCAACAGCGCCCGAATCCCCAGATGAATAGGCACCCCTATGGGACACCAGGAAGTGCTCCACAAATGCGACGC
CCGGGAGGTTTTGCTGGTCAGCCGCCACAAATGCATGGGCCTCGAATGGTTGCACCGCCGGCTGCTCCATTGCCGAAAAAGAAGAAGTATGCGGATAAA
TGTATTCATCCAAAGgttttaTTTCGCACACCACAAACCAACGAAACTGATGGATTCCAAGTGAAACGAGCCGGCGATCGTCCTGTCAAGTGCAGAATC
CTCTTGCTGCTCGACAATCATCCAGCGAAATTCAAGCTTCATCCACGGCTTGCCAAAGTTCTCGGAATTGCTACAGAAACTCGTCCGAAGATTATCGAA
GCTCTCTGGCAGTACATCAAAACTCATGGACTTCAAGATCCTCAAGAACGGGACATTATCAATTGTGATACATTTTTGAGTCAATGTTTCGGAGTGAAT
AGAATGAGATTTATGGAAGTGCCAAACAAATTGCATCAACTACTTCAACAAACTGATCCATTGGAGTTCAATCATATAATTCAACGACCAAAAGAAGGG
CAGGAACAAGTATCAACTTGCTACGACATTGATGTTGAGATGGAAGATCCAGTGAAACAGTTTATGCATACTTTCGTTCATAGTCCAGGACTTGCCAAT
GATATTCAAACTCTTGATCAAAAGTGTTATGATATTATCGAACAGATCAACGAACTGAAGACTCGCCGCGATTTCTACGCAAGATTCTACACCGAACCC
GCAGAATTCATCAAAAGCTGGGTGATGAGCCAGAATTCGGACCTGAAGACTATGAACGAGCTGAGCGGGGATCTTGAGGCAGAACGATTCGCTGAATCC
TACGTGAGACCTGAAACAGAGGAAGGAGTTCAAAGATACATGTTCCAAAAGGTGAACCAGAAGCGACACGAGTTGGAGCAAAGTCTTGGTGTTCGATCA
AATTAAatttttttttcaaataatctataaggtctcaaaaactcacttaaattttgatgtttctaaaattgcaagttattgatttattcatttatttat
tcttcattcattcatgtacaaaaaatacgctctttgttaaatgaatttcacgtgacctctct

Annex 4: Spliced sequences of *swsn-2.2* and the mutant alleles *ok3161* and *tm3395*. Yellow and orange regions mark different exons. The green area represents the SWIB/MDM2 domain. Insertions or transitions are indicated by red letters. (A) Wild type *swsn-2.2* sequence. (B) The allele *ok3161* causes the loss of the sequence encoding the SWIB/MDM2 domain. (C) *tm3395* causes partial retention of the second intron. The sequence encoding the SWIB/MDM2 domain is not affected by the mutation.

A)

B)

Annex 5: RNAi clones of *ham-3* and *swsn-2.2* (A and B, respectively). Exons are represented in orange and yellow. The parts of the sequences contained in the respective RNAi clone are underlined. The *ham-3* clone came from the Ahringer library. The clone for *swsn-2.2* was generated in our lab using cDNA of wild type worms.

References

References

A

Ahringer, J. (2006). Reverse genetics. *WormBook*, ed. The *C. elegans* Research Community, WormBook, doi/10.1895/wormbook.1.47.1

Altun, Z.F. & Hall, D.H. (2009). Introduction. In *WormAtlas*. doi:10.3908/wormatlas.1.1

Annunziato, A. (2008) DNA packaging: Nucleosomes and chromatin. Nature Education 1(1):26

B

Barbieri, M., Bonafè, M., Franceschi, C., & Paolisso, G. (2003). Insulin/IGF-I-signaling pathway: an evolutionarily conserved mechanism of longevity from yeast to humans. *American Journal of Physiology. Endocrinology and Metabolism*, *285*(5), E1064–71. doi:10.1152/ajpendo.00296.2003

Baugh, L.R. (2013). To grow or not to grow: nutritional control of development during *Caenorhabditis elegans* L1 arrest. *Genetics*, *194*(3), 539–55. doi:10.1534/genetics.113.150847

Baugh, L.R., & Sternberg, P.W. (2006). DAF-16/FOXO regulates transcription of *cki-1*/Cip/Kip and repression of *lin-4* during *C. elegans* L1 arrest. *Current Biology : CB*, *16*(8), 780–5. doi:10.1016/j.cub.2006.03.021

Bennett-Lovsey, R., Hart, S.E., Shirai, H., & Mizuguchi, K. (2002). The SWIB and the MDM2 domains are homologous and share a common fold. *Bioinformatics (Oxford, England)*, 18(4), 626–30.

Biegel, J.A., Busse, T.M: & Weissman, B.E. (2014) SWI/SNF chromatin remodeling complexes and cancer. Am J Med Genet C Semin Med Genet.; 166C(3):350-66. doi: 10.1002/ajmg.c.31410. Epub 2014 Aug 28.

Boxem, M., & van den Heuvel, S. (2001). *lin-35*/Rb and *cki-1*/Cip/Kip cooperate in developmental regulation of G1 progression in *C. elegans*. *Development (Cambridge, England)*, 128(21), 4349–59.

Brenner, S. (1974). The genetics of *Caenorhabditis elegans*. Genetics, 77(1), 71–94.

Bustin, M., Catez, F., & Lim, J-H. (2005). The dynamics of histone H1 function in chromatin. *Molecular Cell*, *17*(5), 617–20. doi:10.1016/j.molcel.2005.02.019

C

Cabello, J., Neukomm, L.J., Günesdogan, U., Burkart, K., Charette, S. J., Lochnit, G., Hengartner M.O., & Schnabel, R. (2010). The Wnt pathway controls cell death engulfment, spindle orientation, and migration through CED-10/Rac. *PLoS Biology*, *8*(2), e1000297. doi:10.1371/journal.pbio.1000297

Cairns, B.R., Lorch, Y., Li, Y., Zhang, M., Lacomis, L., Erdjument-Bromage, H., Tempst, P., Du, J., Laurent, B., & Kornberg, R.D. (1996). RSC, an essential, abundant chromatin-remodeling complex. *Cell*, *87*(7), 1249–60.

Ceol, C.J., Stegmeier, F., Harrison, M.M., & Horvitz, H.R. (2006). Identification and classification of genes that act antagonistically to *let-60*/Ras signaling in *Caenorhabditis elegans* vulval development. *Genetics*, *173*(2), 709–26. doi:10.1534/genetics.106.056465

Cerón, J., (2006). *Caenorhabditis elegans*: a gateway to metazoan systems biology (Book chapter). Book: Understanding and Exploiting System Biology in Biomedicine and Bioprocesses. Fundación Cajamurcia ISBN 84-611-1135-4.

Ceron, J., Rual, J-F., Chandra, A., Dupuy, D., Vidal, M., & van den Heuvel, S. (2007). Large-scale RNAi screens identify novel genes that interact with the *C. elegans* retinoblastoma pathway as well as splicing-related components with synMuv B activity. *BMC Developmental Biology*, *7*, 30. doi:10.1186/1471-213X-7-30

Church, D.L., Guan, K.L., & Lambie, E.J. (1995). Three genes of the MAP kinase cascade, *mek-2*, *mpk-1*/*sur-1* and l*et-60*/Ras, are required for meiotic cell cycle progression in *Caenorhabditis elegans*. *Development (Cambridge, England)*, *121*(8), 2525–35.

Ciosk, R., DePalma, M., & Priess J.R. (2004) ATX-2, the *C. elegans* ortholog of ataxin-2, functions in translational regulation in the germline. Development. 131(19):4831-41.

Collins, R.T., Furukawa, T., Tanese, N., & Treisman, J.E. (1999). Osa associates with the Brahma chromatin remodeling complex and promotes the activation of some target genes. *The EMBO Journal*, 18(24), 7029–40. doi:10.1093/emboj/18.24.7029

Cooper, G.M. (2000). The Cell. A molecular approach. 2nd edition. Sinauer Associates.

Cui, M., Fay, D.S., & Han, M. (2004). *lin-35*/Rb cooperates with the SWI/SNF complex to control *Caenorhabditis* elegans larval development. *Genetics*, 167(3), 1177–85. doi:10.1534/genetics. 103.024554

Cui., M., Chen., J., Myers, T.R., Hwang, B.J., Sternerg, P.W., Greenwald, I., & Han, M (2006) SynMuv genes redundantly inhibit lin-3/EGF expression to prevent inappropriate vulval induction in *C.elegans.* Dev Cell.;10(5):667-72.

D

Das, C., & Tyler, J.K. (2012). Histone exchange and histone modifications during transcription and aging. *Biochimica et Biophysica Acta (BBA) - Gene Regulatory Mechanisms*, *1819*(3-4), 332–342. doi:10.1016/j.bbagrm.2011.08.001

Das, C., Tyler, J.K., & Churchill, M.E.A. (2010). The histone shuffle: histone chaperones in an energetic dance. *Trends in Biochemical Sciences*, *35*(9), 476–89. doi:10.1016/j.tibs.2010.04.001

Dechat, T., Pfleghaar, K., Sengupta, K., Shimi, T., Shumaker, D.K., Solimando, L., & Goldman R.D. (2008) Nuclear lamins: major factors in the structural organization and function of the nucleus and chromatin.Gene Dev.22(7):832-53. doi: 10.1101/gad.1652708.

Desai, C., & Horvitz, H.R. (1989). *Caenorhabditis elegans* mutants defective in the functioning of the motor neurons responsible for egg laying. *Genetics*, *121*(4), 703–21

Draper, B.W., Mello, C.C., Bowerman, B., Hardin, J., & Priess, J.R. (1996). MEX-3 is a KH domain protein that regulates blastomere identity in early C. elegans embryos. *Cell*, *87*(2), 205–16.

E

Eisenmann, D,M., & Kim, S.K. (2000). Protruding vulva mutants identify novel loci and Wnt signaling factors that function during *Caenorhabditis elegans* vulva development. *Genetics*, *156*(3), 1097–116.

Euskirchen, G.M., Auerbach, R.K., Davidov, E., Gianoulis, T.A., Zhong, G., Rozowsky, J., Bhardwaj, N., Gerstein, M.B., & Snyder, M. (2011) Diverse roles and interactions of the SWI/SNF chromatin remodeling complex revealed using global approaches PLoS Genet 7(3):e1002008. doi: 10.1371/journal.pgen.1002008. Epub 2011 Mar 3

Euskirchen, G., Auerbach, R.K., & Snyder, M. (2012). SWI/SNF chromatin-remodeling factors: multiscale analyses and diverse functions. *The Journal of Biological Chemistry*, *287*(37), 30897–905. doi:10.1074/jbc.R111.309302

F

Fay, D.S., & Yochem, J. (2007). The SynMuv genes of Caenorhabditis elegans in vulval development and beyond. *Developmental Biology*, *306*(1), 1–9. doi:10.1016/j.ydbio.2007.03.016

Ferguson, E.L., & Horvitz, H.R. (1985). Identification and characterization of 22 genes that affect the vulval cell lineages of the nematode *Caenorhabditis elegans. Genetics*, *110*(1), 17–72.

Fernandez, A.G., Mis, E.K., Lai, A., Mauro, M., Quental A., Bock, C., & Piano, F. (2014) Uncovering buffered pleiotropy: a genome-scale screen for *mel-28* genetic interactors in *Caenorhabditis elegans.* G3 (Bethesa);4(1):185-96. doi: 10.1534/g3.113.008532.

Fernandez, A.G., & Piano, F. (2006). MEL-28 is downstream of the Ran cycle and is required for nuclear-envelope function and chromatin maintenance. *Curr Biol, 16*, 1757-63. doi:10.1016/j.cub.2006.07.071

Fujita, M., Takeshita, H., & Sawa, H. (2007) Cyclin E and CDK2 repress the terminal differentiation of quiescent cells after asymmetric division in *C. elegans. PLoS One;2(5):e407.*

G

Galy, V., Askjaer, P., Franz, C., Lopez-Iglesias, C. & Mattaj, I.W. (2006) MEL-28, a novel nuclear-envelope and kinetochore protein essential for zygotic nuclear-envelope assembly in *C. elegans*. Curr Biol.16(17):1748-56.

Gómez-Orte, E., Sáenz-Narciso, B., Moreno, S., & Cabello, J. (2013). Multiple functions of the noncanonical Wnt pathway. *Trends in Genetics : TIG*, *29*(9), 545–53. doi:10.1016/j.tig.2013.06.003

Gupta, B.P., Hanna-Rose, W., & Sternberg, P.W. (2005). Morphogenesis of the vulva and the vulval-uterine connection. *WormBook*, ed. The *C. elegans* Research Community, WormBook, doi/10.1895/wormbook.1.152.1

H

Hale, V.A., Guiney, E.L., Goldberg, L. Y., Haduong, J.H., Kwartler, C. S., Scangos, K. W., & Goutte, C. (2012) Notch signaling is antagonized by SAO-1, a novel GYF-domain protein that interacts with the E3 ubiquitin ligase SEL-10 in *Caenorhabditis elegans*. *Genetics*190(3):1043-57. doi: 10.1534/genetics.111.136804.

Hansen, D., Hubbard, E.J.A., & Schedl, T. (2004). Multi-pathway control of the proliferation versus meiotic development decision in the *Caenorhabditis elegans* germline. *Developmental Biology*, *268*(2), 342–57. doi:10.1016/j.ydbio.2003.12.023

Hardin, J., & King, R. S. (2008). The long and the short of Wnt signaling in *C. elegans. Current Opinion in Genetics & Development*, *18*(4), 362–7. doi:10.1016/j.gde.2008.06.006

Hargreaves, D. C., & Crabtree, G. R. (2011). ATP-dependent chromatin remodeling: genetics, genomics and mechanisms. *Cell Research*, *21*(3), 396–420. doi:10.1038/cr.2011.32

Hayes, G.D., Riedel, C.G., & Ruvkun, G. (2011). The *Caenorhabditis elegans* SOMI-1 zinc finger protein and SWI/SNF promote regulation of development by the *mir-84* microRNA. *Genes & Development*, *25*(19), 2079–92. doi:10.1101/gad.17153811

Hedgecock, E.M., & White, J.G. (1985). Polyploid tissues in the nematode Caenorhabditis elegans. *Developmental Biology*, *107*(1), 128–33.

Ho, L., & Crabtree, G.R. (2010). Chromatin remodelling during development. *Nature*, *463*(7280), 474–84. doi:10.1038/nature08911

Hohmann, A.F., & Vakoc, C.R. (2014). A rationale to target the SWI/SNF complex for cancer therapy. *Trends in Genetics : TIG*, *30*(8), 356–63. doi:10.1016/j.tig.2014.05.001

Hsiao, P.-W., Fryer, C.J., Trotter, K.W., Wang, W., & Archer, T.K. (2003). BAF60a mediates critical interactions between nuclear receptors and the BRG1 chromatin-remodeling complex for transactivation. *Molecular and Cellular Biology*, *23*(17), 6210–20. doi:10.1128/MCB.23.17.6210

Hu, P. (2014). Dauer. Wormbook. *WormBook*, ed. The *C. elegans* Research Community, WormBook, doi/10.1895/wormbook.1.144.1

Hubbard, E.J.A. (2007). *Caenorhabditis elegans* germ line: a model for stem cell biology. Dev Dyn. 2007 Dec;236(12):3343-57.

Hubbard, E.J., & Greenstein, D. (2000). The *Caenorhabditis elegans* gonad: a test tube for cell and developmental biology. Dev Dyn. 218(1):2-22.

Hubbard, E.J.A., & Greenstein, D. (2005). Introduction to the germ line. *WormBook : The Online Review of C. Elegans Biology*, 1–4. doi:10.1895/wormbook.1.18.1

I

Iwasaki, K., McCarter, J., Francis, R., & Schedl, T. (1996). *emo-1*, a *Caenorhabditis elegans* Sec61p gamma homologue, is required for oocyte development and ovulation. *The Journal of Cell Biology*, *134*(3), 699–714.

K

Kamath, R.S & Ahringer J. (2003) *Genome-wide RNAi screening in Caenorhabditis elegans*. Methods; 30(4):313-21.

Kiehl, T.R., Shibata, H., & Pulst, S.M. (2000) The ortholog of human ataxin-2 is essential for early embryonic development in *C. elegans*. *J Mol Neurosci15(3):231-41.*

Killian, D.J., & Hubbard, E.J.A. (2004). *C. elegans pro-1* activity is required for soma/germline interactions that influence proliferation and differentiation in the germ line. *Development (Cambridge, England)*, *131*(6), 1267–78. doi:10.1242/dev.01002

Kimble, J. & Crittenden, S.L. (2005) Germline proliferation and its control. Wormbook:1-14

Koreth, J., & van den Heuvel, S. (2005). Cell-cycle control in *Caenorhabditis elegans:* how the worm moves from G1 to S. *Oncogene*, *24*(17), 2756–64. doi:10.1038/sj.onc.1208607

Korta, D.Z. & Hubbard, E.J. (2010) Soma-germline interactions that influence germline proliferation in *Caenorhabditis elegans*. Dev Dyn. 239(5):1449-59. doi: 10.1002/dvdy.22268. Review.

Kostić, I., & Roy, R. (2002). Organ-specific cell division abnormalities caused by mutation in a general cell cycle regulator in *C. elegans. Development (Cambridge, England)*, *129*(9), 2155–65.

Kipreos, E.T. (2005) *C. elegans* cell cycles: invariance and stem cell divisions. Nat Rev Mol Cell Biol.;6(10):766-76.

Kumsta, C., & Hansen, M. (2012) *C. elegans rrf-1* mutations maintain RNAi efficiency in the soma in addition to the germline. PLoS One.;7(5):e35428. doi: 10.1371/journal.pone.0035428.

Kurz, C.L., & Tan, M-W. (2004). Regulation of aging and innate immunity in *C. elegans*. *Aging Cell*, *3*(4), 185–93. doi:10.1111/j.1474-9728.2004.00108.x

Kuzmanov, A., Karina, E.I., Kirienko, N.V, & Fay, D.S. (2014). The conserved PBAF nucleosome-remodeling complex mediates the response to stress in *Caenorhabditis elegans*. *Molecular and Cellular Biology*, *34*(6), 1121–35. doi:10.1128/MCB.01502-13

Kwon, C.S., & Wagner, D. (2007). Unwinding chromatin for development and growth: a few genes at a time. *Trends in Genetics : TIG*, *23*(8), 403–12. doi:10.1016/j.tig.2007.05.010

L

Lanerolle, P. & Serebryannyy, L. (2011) Nuclear actin and myosins: life without filaments. Nat Cell Biol.;13(11):1282-8. doi: 10.1038/ncb2364.

Lans, H., Marteijn, J. A., Schumacher, B., Hoeijmakers, J. H. J., Jansen, G., & Vermeulen, W. (2010). Involvement of global genome repair, transcription coupled repair, and chromatin remodeling in UV DNA damage response changes during development. *PLoS Genetics*, *6*(5), e1000941. doi:10.1371/journal.pgen.1000941

Large, E. E., & Mathies, L. D. (2014). *Caenorhabditis elegans* SWI/SNF subunits control sequential developmental stages in the somatic gonad. *G3 (Bethesda, Md.)*, *4*(3), 471–83. doi:10.1534/g3.113.009852

Lehner, B., Crombie, C., Tischler, J., Fortunato, A., & Fraser, A.G. (2006). Systematic mapping of genetic interactions in *Caenorhabditis elegans* identifies common modifiers of diverse signaling pathways. *Nature Genetics*, *38*(8), 896–903. doi:10.1038/ng1844

Leung, B., Hermann, G.J., & Priess, J.R. (1999). Organogenesis of the *Caenorhabditis elegans* intestine. *Developmental Biology*, *216*(1), 114–34. doi:10.1006/dbio.1999.9471

Lickert, H., Takeuchi, J.K., Von Both, I., Walls, J.R., McAuliffe, F., Adamson, S.L., Henkelmann R.M., Wrana J.L., Rossant J., & Bruneau, B. G. (2004). Baf60c is essential for function of BAF chromatin remodelling complexes in heart development. *Nature*, *432*(7013), 107–12. doi:10.1038/nature03071

Lints, R. & Hall, D.H. (2009) Reproductive system, germ line. In *WormAtlas*. doi:10.3908/wormatlas.1.23

Ljungman, M., & Hanawalt, P.C. (1992). Efficient protection against oxidative DNA damage in chromatin. *Molecular Carcinogenesis*, *5*(4), 264–9.

M

Maduro, M.F. (2010). Cell fate specification in the *C. elegans* embryo. *Developmental Dynamics : An Official Publication of the American Association of Anatomists*, *239*(5), 1315–29. doi:10.1002/dvdy.22233

Maine, E.M., Hansen, D., Springer, D., & Vought, V.E. (2004) *Caenorhabditis elegans atx-2* promotes germline proliferation and the oocyte fate. Genetics 168(2):817-30.

McCarter, J., Bartlett, B., Dang, T., & Schedl, T. (1997) Soma-germ cell interactions in *Caenorhabditis elegans*: multiple events of hermaphrodite germline development require the somatic sheath and spermathecal lineages. Dev Biol. 181(2):121-43.

McGhee James D. (2013) The *Caenorhabditis elegans* intestine. *WIREs Dev Biol*, 2: 347-367. doi: 10.1002/wdev.93

Miller, M.A., Nguyen, V.Q., Lee, M.H., Kosinski, M., Schedl, T., Caprioli, R.M., & Greenstein, D. (2001). A sperm cytoskeletal protein that signals oocyte meiotic maturation and ovulation. *Science (New York, N.Y.)*, *291*(5511), 2144–7. doi:10.1126/science.1057586

Mohrmann, L., Langenberg, K., Krijgsveld, J., Kal, A.J., Heck, A.J.R., & Verrijzer, C.P. (2004). Differential targeting of two distinct SWI/SNF-related *Drosophila* chromatin-remodeling complexes. *Molecular and Cellular Biology*, *24*(8), 3077–88.

Monahan, B.J., Villén, J., Marguerat, S., Bähler, J., Gygi, S.P., & Winston, F. (2008). Fission yeast SWI/SNF and RSC complexes show compositional and functional differences from budding yeast. *Nature Structural & Molecular Biology*, *15*(8), 873–80. doi:10.1038/nsmb.1452

Murphy, C.T., & Hu, P.J. (2013). Insulin/insulin-like growth factor signaling in *C. elegans*. *WormBook : The Online Review of C. Elegans Biology*, 1–43. doi:10.1895/wormbook.1.164.1

N

Narlikar, G.J., Sundaramoorthy, R., & Owen-Hughes, T. (2013). Mechanisms and functions of ATP-dependent chromatin-remodeling enzymes. *Cell*, *154*(3), 490–503. doi:10.1016/j.cell.2013.07.011

Neigeborn, L., & Carlson, M. (1984). Genes affecting the regulation of SUC2 gene expression by glucose repression in Saccharomyces cerevisiae. *Genetics*, *108*(4), 845–58.

Nie, Z., Xue, Y., Yang, D., Zhou, S., Deroo, B.J., Archer, T.K., & Wang, W. (2000). A specificity and targeting subunit of a human SWI/SNF family-related chromatin-remodeling complex. Mol Cell Biol.;20(23):8879-88.

O

Oh, J., Sohn, D.H., Ko, M., Chung, H., Jeon, S.H., & Seong, R.H. (2008). BAF60a interacts with p53 to recruit the SWI/SNF complex. *The Journal of Biological Chemistry*, *283*(18), 11924–34. doi:10.1074/jbc.M705401200

Oh, S.W., Mukhopadhyay, A., Dixit, B.L., Raha, T., Green, M.R., & Tissenbaum, H.A. (2006). Identification of direct DAF-16 targets controlling longevity, metabolism and diapause by chromatin immunoprecipitation. *Nature Genetics*, *38*(2), 251–7. doi:10.1038/ng1723

P

Petty, E., & Pillus, L. (2013). Balancing chromatin remodeling and histone modifications in transcription. *Trends in Genetics: TIG*, *29*(11), 621–9. doi:10.1016/j.tig.2013.06.006

Pinkston-Gosse, J. & Kenyon, C. (2007) DAF-16/FOXO targets genes that regulate tumor growth in *Caenorhabditis elegans*. Nat Genet ;39(11):1403-9. Epub 2007 Oct 14.

Porta-de-la-Riva, M., Fontrodona, L., Villanueva, A., & Cerón, J. (2012). Basic Caenorhabditis elegans methods: synchronization and observation. *Journal of Visualized Experiments : JoVE*, (64), e4019. doi:10.3791/4019

Priess, J. (2005). Notch signaling in the *C. elegans* embryo. *WormBook*, ed. The *C. elegans* Research Community, *WormBook,* doi/10.1895/wormbook.1.4.1

Puri, P.L., & Mercola, M. (2012). BAF60 A, B, and Cs of muscle determination and renewal. *Genes & Development*, *26*(24), 2673–83. doi:10.1101/gad.207415.112

R

Reisman, D., Glaros, S., & Thompson, E.A. (2009). The SWI/SNF complex and cancer. *Oncogene*, *28*(14), 1653–68. doi:10.1038/onc.2009.4

Riddle, D.L., Blumenthal, T., Meyer, B.J., & Priess, J.R. (1997). *C. elegans* II. Cold Spring Harbor Laboratory Press.

Riedel, C.G., Dowen, R.H., Lourenco, G.F., Kirienko, N.V, Heimbucher, T., West, J.A., Bowman, S.K., Kingston, R.E., Dilian, A.,Asara J.M., & Ruvkun, G. (2013). DAF-16 employs the chromatin remodeller SWI/SNF to promote stress resistance and longevity. *Nature Cell Biology*, *15*(5), 491–501. doi:10.1038/ncb2720

Rivera, C., Gurard-Levin, Z.A., Almouzni, G., & Loyola, A. (2014). Histone lysine methylation and chromatin replication. *Biochimica et Biophysica Acta*. doi:10.1016/j.bbagrm.2014.03.009

Roberts, C.W.M., & Orkin, S.H. (2004). The SWI/SNF complex-chromatin and cancer. *Nature Reviews. Cancer*, *4*(2), 133–42. doi:10.1038/nrc1273

Rocheleau, C.E., Downs, W.D., Lin, R., Wittmann, C., Bei, Y., Cha, Y.H., Ali, M., Priess J.R., & Mello, C. C. (1997). Wnt signaling and an APC-related gene specify endoderm in early *C. elegans* embryos. *Cell*, *90*(4), 707–16.

Rual, J.F., Cerón, J., Koreth, J., Hao, T., Nicot, A.S., Hirozane-Kishikawa, T., Vandenhaute, J., Orkin, S.H., Hill, D.E., van den Heuvel, S., Vidal, M. (2004) Toward improving *Caenorhabditis elegans* phenome mapping with an ORFeome-based RNAi library.Genome Res.;14(10B):2162-8.

S

Santen, G.W.E., Kriek, M., & van Attikum, H. (2012). SWI/SNF complex in disorder: SWItching from malignancies to intellectual disability. *Epigenetics : Official Journal of the DNA Methylation Society*, *7*(11), 1219–24. doi:10.4161/epi.22299

Sawa, H., Kouike, H., & Okano, H. (2000). Components of the SWI/SNF complex are required for asymmetric cell division in *C. elegans*. *Molecular Cell*, *6*(3), 617–24.

Schafer, W. R. (2005). Egg-laying. *WormBook : The Online Review of C. Elegans Biology*, 1–7. doi:10.1895/wormbook.1.38.1

Schindler, A. J., & Sherwood, D. R. (2013). Morphogenesis of the Caenorhabditis elegans vulva. *Wiley Interdisciplinary Reviews. Developmental Biology*, *2*(1), 75–95. doi:10.1002/wdev.87

Seydoux, G., Savage, C., & Greenwald, I. (1993). Isolation and characterization of mutations causing abnormal eversion of the vulva in *Caenorhabditis elegans*. *Developmental Biology*, *157*(2), 423–36.

Sgroi, D.C., Teng, S., Robinson, G., LeVangie, R., Hudson, J.R., & Elkahloun, A.G. (1999). In vivo gene expression profile analysis of human breast cancer progression. *Cancer Research*, *59*(22), 5656–61.

Shain, A.H., & Pollack J.R., (2013) The spectrum of SWI/SNF mutations, ubiquitous in human cancers. PLoS One. 2013;8(1):e55119. doi: 10.1371/journal.pone.0055119.

Sharma-Kishore, R., White, J.G., Southgate, E., & Podbilewicz, B. (1999). Formation of the vulva in *Caenorhabditis elegans*: a paradigm for organogenesis. *Development (Cambridge, England)*, *126*(4), 691–9.

Shibata, Y., Uchida, M., Takeshita, H., Nishiwaki, K., C., & Sawa, H. (2012). Multiple functions of PBRM-1/Polybromo- and LET-526/Osa-containing chromatin remodeling complexes in *C. elegans* development. *Developmental Biology*, *361*(2), 349–57. doi:10.1016/j.ydbio.2011.10.035

Stephens, P.J., Tarpey, P.S., Davies, H., Van Loo, P., Greenman, C., Wedge, D.C., Nik-Zainal, S., Martin, S., Varela, I., Bignell, G.R., Yates, L.R., Papaemmanuil, E., Beare, D., Butler, A., Cheverton, A., Gamble, J., Hinton, J., Jia, M., Jayakumar, A., Jones, D., Latimer, C., Lau, K.W., McLaren, S., McBride, D.J., Menzies, A., Mudie, L., Raine, K., Rad, R., Chapman, M.S., Teague, J., Easton, D., Langerød, A.; Oslo **Breast Cancer** Consortium (OSBREAC), Lee, M.T., Shen, C.Y., Tee, B.T., Huimin, B.W., Broeks, A., Vargas, A.C., Turashvili, G., Martens, J., Fatima, A., Miron, P., Chin, S.F., Thomas, G., Boyault, S., Mariani, O., Lakhani, S.R., van de Vijver, M., van 't Veer, L., Foekens, J., Desmedt, C., Sotiriou, C., Tutt, A., Caldas, C., Reis-Filho, J.S., Aparicio, S.A., Salomon, A.V., Børresen-Dale, A.L., Richardson, A.L., Campbell, P.J., Futreal, P.A., & Stratton, M.R.(2012). The landscape of cancer genes and mutational processes in breast cancer, *486*(7403), 400–404. doi:10.1038/nature11017. The Europe PMC Funders Group

Stern, M., Jensen, R., & Herskowitz, I. (1984). Five SWI genes are required for expression of the HO gene in yeast. *Journal of Molecular Biology*, *178*(4), 853–68.

Sternberg, P.W. (2005). Vulval development. *WormBook: The Online Review of C. elegans Biology*, 1–28. doi:10.1895/wormbook.1.6.1

Sulston, J. E., Schierenberg, E., White, J.G., & Thomson, J.N. (1983). The embryonic cell lineage of the nematode *Caenorhabditis elegans. Developmental Biology*, *100*(1), 64–119.

Sundaram, M. V. (2004). Vulval development: the battle between Ras and Notch. *Current Biology : CB*, *14*(8), R311–3. doi:10.1016/j.cub.2004.03.052

T

Takeuchi, J.K., Lickert, H., Bisgrove, B.M., Sun, X., Yamamoto, M., Chawengsaksophak, K., Hamada, H., Yost, H.J., Rossant, J., & Bruneau, B.G. (2007) Baf60c is a nuclear Notch signaling component required for the establishment of left-right asymmetry. Proc Natl Acad Sci USA;104(3):846-51.

Tang, L., Nogales, E., & Ciferri, C. (2010). Structure and function of SWI/SNF chromatin remodeling complexes and mechanistic implications for transcription. *Progress in Biophysics and Molecular Biology*, *102*(2-3), 122–8. doi:10.1016/j.pbiomolbio.2010.05.001

The *C. elegans* Sequencing Consortium. (1998). Genome Sequence of the Nematode *C. elegans*: A Platform for Investigating Biology. *Science*, *282*(5396), 2012–2018. doi:10.1126/science.282.5396.2012

Trent, C., Tsuing, N., & Horvitz, H.R. (1983). Egg-laying defective mutants of the nematode *Caenorhabditis elegans*. *Genetics*, *104*(4), 619–47.

V

van den Heuvel S. (2005) Cell-cycle regulation. In: WormBook: The Online Review of *C. elegans* Biology [Internet]. Pasadena (CA): *WormBook*

W

Walston, T., Tuskey, C., Edgar, L., Hawkins, N., Ellis, G., Bowerman, B., Wood, W., & Hardin, J. (2004). Multiple Wnt signaling pathways converge to orient the mitotic spindle in early *C. elegans* embryos. *Developmental Cell*, *7*(6), 831–41. doi:10.1016/j.devcel.2004.10.008

Walston, T.D., & Hardin, J. (2006). Wnt-dependent spindle polarization in the early *C. elegans* embryo. *Seminars in Cell & Developmental Biology*, *17*(2), 204–13. doi:10.1016/j.semcdb.2006.04.005

Wang, G.G., Allis, C.D., & Chi, P. (2007). Chromatin remodeling and cancer, Part II: ATP-dependent chromatin remodeling. *Trends in Molecular Medicine*, *13*(9), 373–80. doi:10.1016/j.molmed.2007.07.004

Wang, W., Xue, Y., Zhou, S., Kuo, a, Cairns, B.R., & Crabtree, G.R. (1996). Diversity and specialization of mammalian SWI/SNF complexes. *Genes & Development*, *10*(17), 2117–2130. doi:10.1101/gad.10.17.2117

Wang, Z., W. Zhai, J.A. Richardson, E.N. Olson, J.J. Meneses, Firpo, M.T., Chulho, K., Skarnes, W.C. & Tjian, R. (2004) Polybromo protein BAF180 functions in mammalian cardiac chamber maturation. Genes Dev. 18: 3106–3116.

Weinberg, P., Flames, N., Sawa, H., Garriga, G., & Hobert, O. (2013) The SWI/SNF chromatin remodeling complex selectively affects multiple aspects of serotonergic neuron differentiation. *Genetics*;194(1):189-98. doi: 10.1534/genetics.112.148742.

Weissman, B., & Knudsen, K. E. (2009). Hijacking the chromatin remodeling machinery: impact of SWI/SNF perturbations in cancer. *Cancer Research*, *69*(21), 8223–30. doi:10.1158/0008-5472.CAN-09-2166

White, J.G., Southgate, E., Thomson, J.N., & Brenner, S. (1986). The structure of the nervous system of the nematode *Caenorhabditis elegans. Philosophical Transactions of the Royal Society of London. Series B, Biological Sciences*, *314*(1165), 1–340.

Wilson, B.G., & Roberts, C.W.M. (2011). SWI/SNF nucleosome remodellers and cancer. *Nature Reviews. Cancer*, *11*(7), 481–92. doi:10.1038/nrc3068

Wong, M.-C., & Schwarzbauer, J.E. (2012). Gonad morphogenesis and distal tip cell migration in the *Caenorhabditis elegans* hermaphrodite. *Wiley Interdisciplinary Reviews. Developmental Biology*, *1*(4), 519–31. doi:10.1002/wdev.45

Y

Yan, Z., Cui, K., Murray, D.M., Ling, C., Xue, Y., Gerstein, A., Parson, R., Zhao, K., & Wang, W. (2005). PBAF chromatin-remodeling complex requires a novel specificity subunit, BAF200, to regulate expression of selective interferon-responsive genes. Genes Dev. 2005 Jul 15;19(14):1662-7.

Z

Zhang, Y., Ye, J., Chen, D., Zhao, X., Xiao, X., Tai, S., Yan, W., & Zhu, D. (2006). Differential expression profiling between the relative normal and dystrophic muscle tissues from the same LGMD patient. *Journal of Translational Medicine*, *4*(1), 53. doi:10.1186/1479-5876-4-53

Zipperlen, P., Fraser, A.G., Kamath, R.S., Martinez-Campos, M., & Ahringer, J. (2001). Roles for 147 embryonic lethal genes on *C.elegans* chromosome I identified by RNA interference and video microscopy. *The EMBO Journal*, *20*(15), 3984–92. doi:10.1093/emboj/20.15.3984